Cenozoic thick-skinned deformation and topography evolution of the Spanish Central System

G. de Vicente [a,*], R. Vegas [a], A. Muñoz Martín [a], P.G. Silva [b], P. Andriessen [c], S. Cloetingh [c], J.M. González Casado [d], J.D. Van Wees [c,e], J. Álvarez [a], A. Carbó [a], A. Olaiz [a]

[a] *Grupo de Investigación en Tectonofísica Aplicada, U.C.M. Depto. Geodinámica, Universidad Complutense, 28040 Madrid, Spain*
[b] *Depto. Geología, Universidad de Salamanca, Escuela Politécnica Superior de Ávila, 05003-Ávila, Spain*
[c] *Faculty of Earth and Life Sciences, Vrije Universiteit, Amsterdam, The Netherlands*
[d] *Laboratorio de Tectonofísica Aplicada, Dpto. de Geología y Geoquímica, Universidad Autónoma, Madrid, Spain*
[e] *TNO, Princetonlaan 6, 3584 CB Utrecht, The Netherlands*

Abstract

The Spanish Central System is a Cenozoic pop-up with an E W to NE SW orientation that affects all the crust (thick-skinned tectonics). It shows antiform geometry in the upper crust with thickening in the lower crust. Together with the Iberian Chain it constitutes the most prominent mountainous structure of the Pyrenean foreland.

The evolutionary patterns concerning the paleotopography of the interior of the Peninsula can be established by an analysis of the following data: gravimetric, topographical, macro and micro tectonic, sedimentological (infilling of the sedimentary basins of the relative foreland), P T t path from apatite fission tracks, paleoseismic and instrumental seismicity.

Deformation is clearly asymmetric in the Central System as evidenced by the existence of an unique, large (crustal-scale) thrust at its southern border, while in the northern one there is a normal sequence of north verging thrusts, towards the Duero Basin, whose activity ended during the Lower Miocene. This deformation was accomplished under triaxial compression, Oligocene Lower Miocene in age, marked by NW SE to NNW SSE shortening. Locally orientations of paleostresses deviate from that of the regional tensor, following a period of relative tectonic quiescence. During the Upper Miocene Pliocene, a reactivation of constrictive stress occurred and some structures underwent rejuvenation as a consequence of the action of tectonic stresses similar to those of today (uniaxial extension to strike slip with NW SE shortening direction). However, the westernmost areas show continuous activity throughout the whole of the Tertiary, with no apparent pulses. At the present time there is a moderate seismic activity in the Central System related to faults that were active during the Cenozoic, with the same kinematic characteristics.

Keywords: thick-skin tectonics; foreland tectonics; paleotopography; Cenozoic; Iberia

1. Introduction

The Spanish Central System constitutes the most prominent topographic elevation in the interior of the Iberian Peninsula (Fig. 1). It corresponds to the main

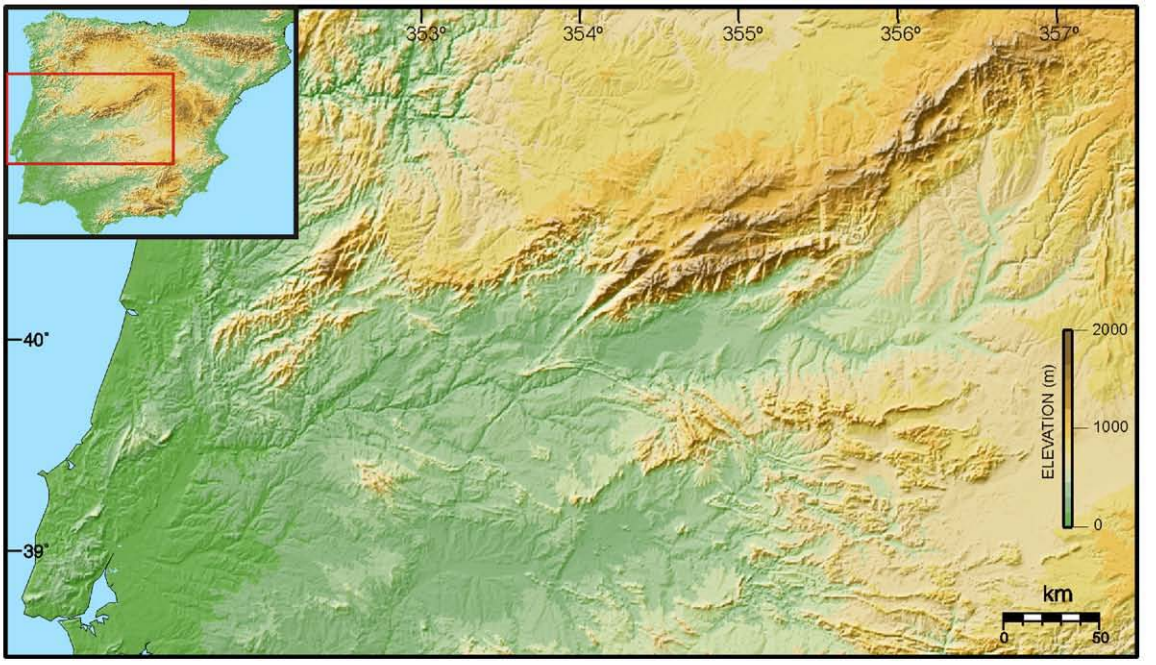

Fig. 1. Digital elevation model of the Central System and its location on a general map of the Iberian Peninsula (red square). (For interpretation of the references to colour in this figure legend, the reader is referred to the web version of this article.)

divide that separates two large Tertiary basins, the Duero Basin to the north and Tagus Basin to the south. It extends in a roughly ENE–WSW direction for more than 300 km with peaks reaching more than 2500 m. Together with the Sierra de Gata, near the Spanish–Portuguese border, and the Estrela and Montejunto mountain ranges in Portugal, it forms a stepped ("en echelon") system of NE–SW basement elevations, producing a topographic high that

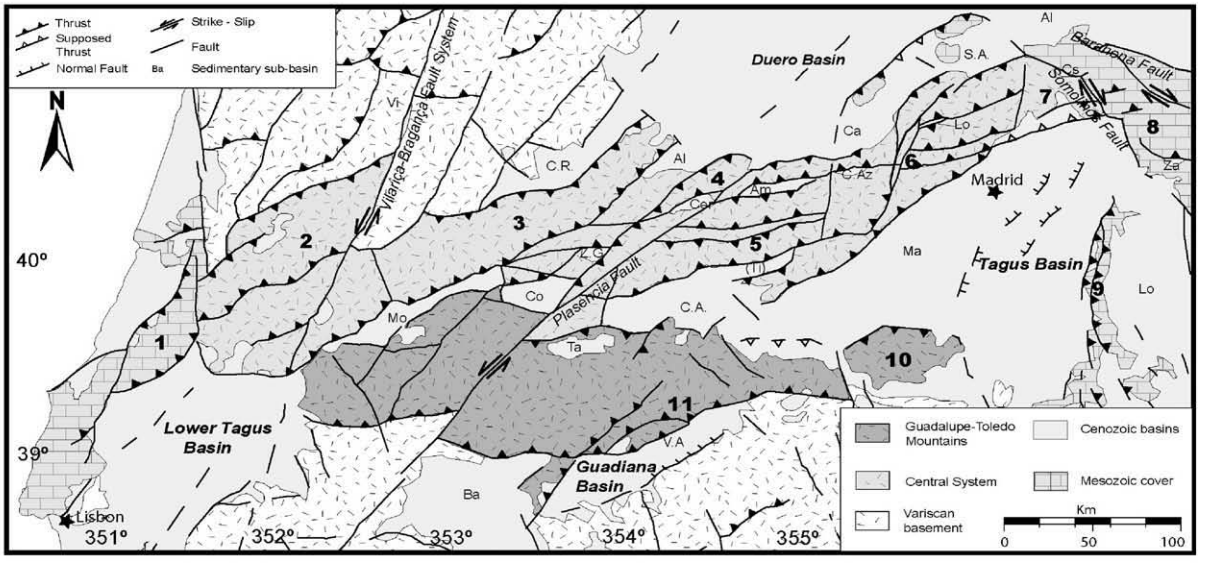

Fig. 2. Tectonic map of the Cenozoic Central Ranges of Western Iberia: 1—Montejunto Range. 2—Serra da Estrela. 3—Gata-Peña de Francia. 4—Sierra de Avila. 5—Gredos. 6—Somosierra and Guadarrama. 7—Transition zone (Tamajon thrusts). 8—Iberian Chain. 9—Altomira Range. 10—Toledo Mountains. 11—Guadalupe Ramp. Minor Basins: Vi—Vilariça. Mo—Moraleja. Co—Coria. CR—Ciudad Rodrigo. Ba—Badajoz. VA—Vegas Altas. CA—Campo Arañuelo. Am—Ambles. Caz—Campo de Azalvaro. Lo—Lozoya. SA—Sepulveda—Ayllon. AL—Almazan. Za—Zaorejas. Lo—Loranca. Ma—Madrid. Ti—Tietar.

runs for more than 700 km, from the Atlantic Ocean to the western border of the Iberian Chain, where ENE–WSW morphostructures interfere with the main NW–SE striking structures of the chain (Figs. 1 and 2).

The range, in pre-Plate Tectonics times, was described as a sort of giant vault or horst standing between two subsiding "interior" basins (Bergamín and Carbó, 1986). Thereafter it was assumed to be bounded by two main crustal-scale normal faults, despite evidence of some thrust faulting at its borders (e.g. Birot and Solé-Sabaris, 1954). Later a relationship with far-field stresses was established in the context of the Alpine compressive deformation in the interior of the so-called Iberian Plate (Vegas and Banda, 1982). In recent literature there is general agreement that this basement uplift is a thick-skinned double-vergence (pop-up) intraplate range built as a result of polyphase evolution (Vegas et al., 1990; Ribeiro et al., 1990; De Vicente et al., 1996, 2004) (Figs. 2 and 3). The deformation partitioning of the basement in the intraplate convergence setting of Iberia has had a profound influence on the development of Topography. There is geological evidence of intense neotectonic (Plio-Quaternary) activity, although instrumental seismicity is currently low and nucleated on Cenozoic structures. The active tectonic setting, good surface exposure and availablility of extensive geological and geophysical datasets render central Iberia an excellent setting for studying the interaction of deep crustal deformation dyamics and surface processes. This topic is the main focus of this paper in which the tectonic origin and evolution of the relief of the chain will be discussed. For this purpose all data have been compiled in a multidisciplinary context, covering crustal geophysics, structural and sedimentary basin geology, stress and strain reconstruction, denudation history from AFT, source–fill relations based on sedimentology.

2. Tectonic setting

The topographic elevation of the Central System emerges above two high *plateaux* developed indistinctly on the Tertiary continental sediments of the Duero and

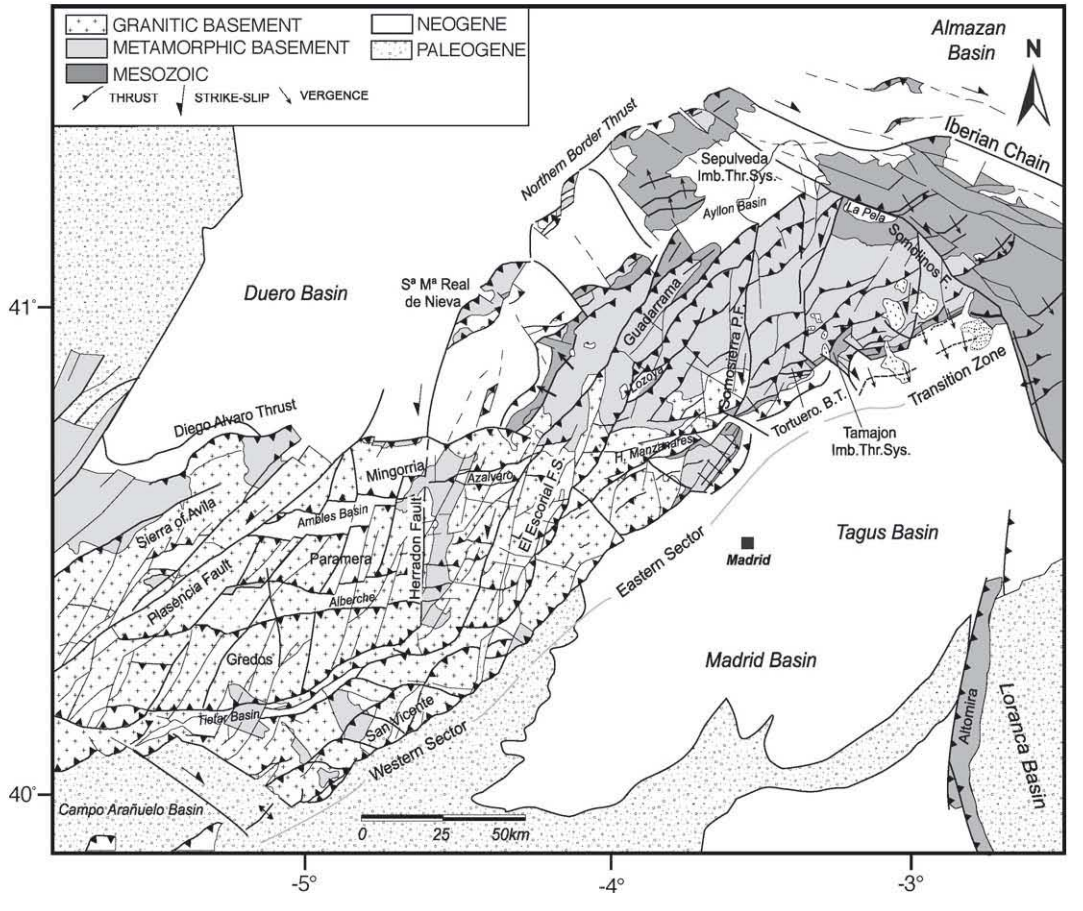

Fig. 3. Geological map of the studied area. Tectonically homogeneous areas: Western sector. Eastern sector. Transition zone.

Tagus Basins and on the Palaeozoic rocks of the Iberian Massif (Figs. 2 and 3). The contact with these plateaux is always a major thrust fault (Variscan basement over Cenozoic sediments), currently defined as the Northern and Southern Border Faults, which clearly indicates the compressive origin of this range (Fig. 4).

Several morphostructural differences support the idea of a tectonic-based division of this interior chain into two segments or sectors that broadly correspond to the Gredos and Paramera sierras to the west and the Guadarrama and Somosierra ranges to the east (De Vicente, 2004) (Fig. 3).

The Gredos–Paramera sector, or *western sector* (Fig. 3), is formed by three E–W mountain alignments, the Mingorría sierra to the north, the above-mentioned sierras of Paramera in the centre, and Gredos to the south, corresponding to sort of pop-ups, with a minor wavelength, in the interior of the main basement uplift. The three ranges are flanked by three associated narrow E–W intramontane depressions (pop-downs), Amblés, Alberche and Tietar, partially filled by Tertiary and Quaternary sediments. This western sector contains the highest peak (Almanzor, 2592 m) in the southern Gredos pop-up and is separated from the Sierra de

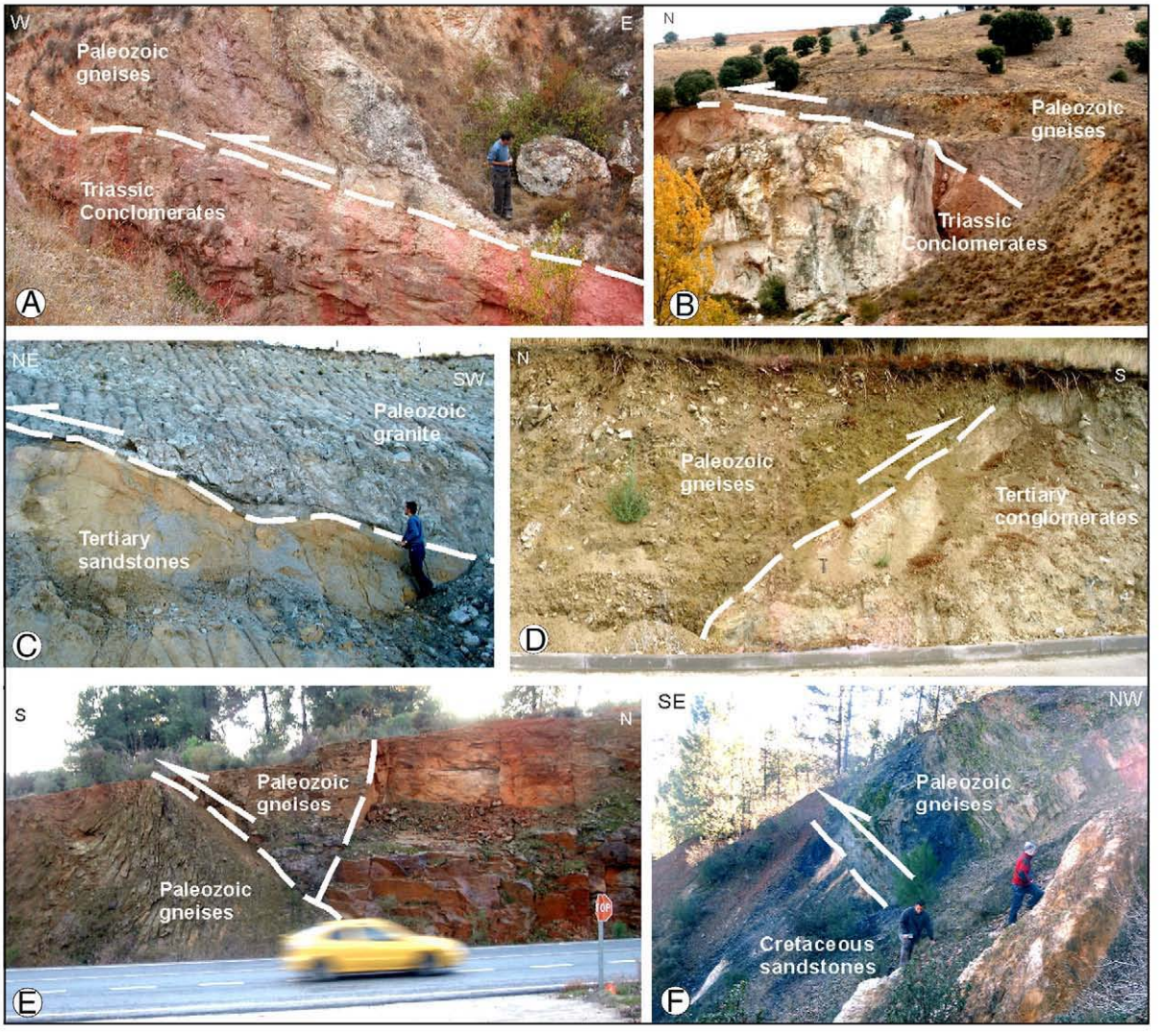

Fig. 4. Some field examples of basement thrusts in the Central System. A), B) The Northern Border Thrust at Sepulveda massif (Variscan gneises over Triassic conglomerates) Honrubia area. C) Next southern imbricate thrust (Villacastin): Variscan granite over Cenozoic sandstone facies. D) The Southern Border Thrust (Variscan gneises over Cenozoic proximal alluvial fan facies) Villanueva del Pardillo area. E) The Southern Border Thrust at Gredos (Navalmoral). Hangingwall and footwall are both Paleozoic gneises. F) Southeastern thrust at Tamajon area (Beleña). Paleozoic gneises over Cretaceous sandstones.

Gata by a NNE–SWW tectonic depression along which a tributary of the Tagus (the Alagon) penetrates the northern meseta (plain), which is drained by the Duero river. The eastern border of this depression constitutes a series of elongated sierras aligned NNE–SSW (Sierra de Avila) against which the main pop-ups terminate. In its turn, the topographic boundary between this sector and the *eastern* one constitutes a narrow NNE–SSW transpressive corridor (Sierra de El Escorial) that offsets the main divide highs to the NE (Fig. 3). Taken as a whole, this western sector has the form of a parallelogram that extends in an E–W direction. The uplifted basement in this area mainly consists of Variscan homogeneous (non-pervasive-deformed) granites with minor high-grade metamorphic inlets. The lack of Mesozoic sedimentary cover is traditionally attributed to non-sedimentation rather than erosion (Querol, 1989).

The Guadarrama–Somosierra sector, or *eastern sector* (Fig. 3), is also formed by two ENE–WSW alignments, the Guadarrama–Somosierra sierra to the north and the Miraflores–Canencia sierra to the south. Both alignments can be considered as basement pop-ups separated by a tectonic depression or *pop-down* (Lozoya) containing preserved Upper Cretaceous sediments. To the south of the Miraflores–Canencia range, a broad platform, with minor residual crests (Manzanares, San Pedro) and a small depression (Guadalix), has developed over the basement. This sector shows a clear dissymmetry with the higher altitudes in the northern pop-up (Peñalara, 2200 m) and a broad ramp-like surface on the southern face. This southern border is delimited by a clear thrust fault, the so-called *Southern Border Thrust* (Figs. 3 and 4D, E, F), that extends south of the Gredos range. Taken as a whole, this sector has a general NE–SW strike and is limited by the above-mentioned NNE–SSW El Escorial transpressive range and the NW–SE structures corresponding to the Castilian Branch of the Iberian Chain, where NE–SW and E–W folds are also ubiquitous. In contrast to the western sector, the uplifted basement corresponds to high-grade gneisses probably of Upper Precambrian age and Variscan granites in the western part, and to low-grade Lower Palaeozoic metasediments in the eastern part (Fernández Casals, 1976). No sedimentary ruptures appear between Upper Cretaceous and Paleocene sediments on both the northern and southern borders.

Besides these two main tectonic zones or sectors, it is worth mentioning, from a tectonic point of view, the zone where the structures of the Spanish Central System give way to the Iberian Chain. In certain respects this zone has a peculiar tectonic style, with some Iberian Chain structures, typically NW–SE oriented folds, which interfere with the general pattern of the Spanish Central System. Conversely, Central System-type basement-and-cover thrust and ramp folds seem to be well-developed inside the Iberian Chain, forming a general right-lateral transpressive area. As a result of this, a sort of *transition zone* (Fig. 3) can be differentiated, which encompasses the two main tectonic domains that accommodate the internal deformation of the Iberian Peninsula.

3. Gravity and isostatic analysis

Owing to the scarcity of deep seismic information for the region, gravity and isostatic analysis has been carried out in the Iberian interior in order to constrain the crustal structure of the Spanish Central System (Fig. 5). The seismic available data consists of a deep seismic profile (Suriñach and Vegas, 1988) and some "old" multichannel seismic sections carried out by different oil companies in the Tagus and Duero basins (Racero, 1988; Querol, 1989). However, plenty of data is available from gravity studies, as well as from rheological models (Mezcua et al., 1996; Tejero et al., 1996; Tejero and Ruiz, 2002; Gómez-Ortíz et al., 2005) allowing study of the crustal structure of the Iberian Block to be approached by integrating gravity maps (Bouguer and isostatic residual gravity) with rheological models.

In the following sections we will describe the gravity and topographic data used in this study. The crustal density distribution of the Iberian interior is inferred from the Bouguer gravity anomaly, because of the strong reverse correlation of Bouguer gravity and topography an isostatic analysis is required to remove the gravity effects of the Central System mountain roots. Our isostatic analysis includes a crustal thickness map based on the Airy model of isostatic compensation and an isostatic residual gravity map of the same model.

Finally two cross-sections of 2 and 1/2D gravity models of the Central System have been made to quantitatively constrain the crustal density structure of this intraplate range.

3.1. Gravity data analysis

The Bouguer gravity field (Fig. 5B) used for density modelling and isostatic analysis were obtained by combining sets of data, provided by the Instituto Geográfico Nacional (IGN) and the Bureau Gravimetrique International (Toulouse). Additional measurements come from unpublished works by ENRESA. There are now about 12,000 gravity stations available in the study area. Details on the

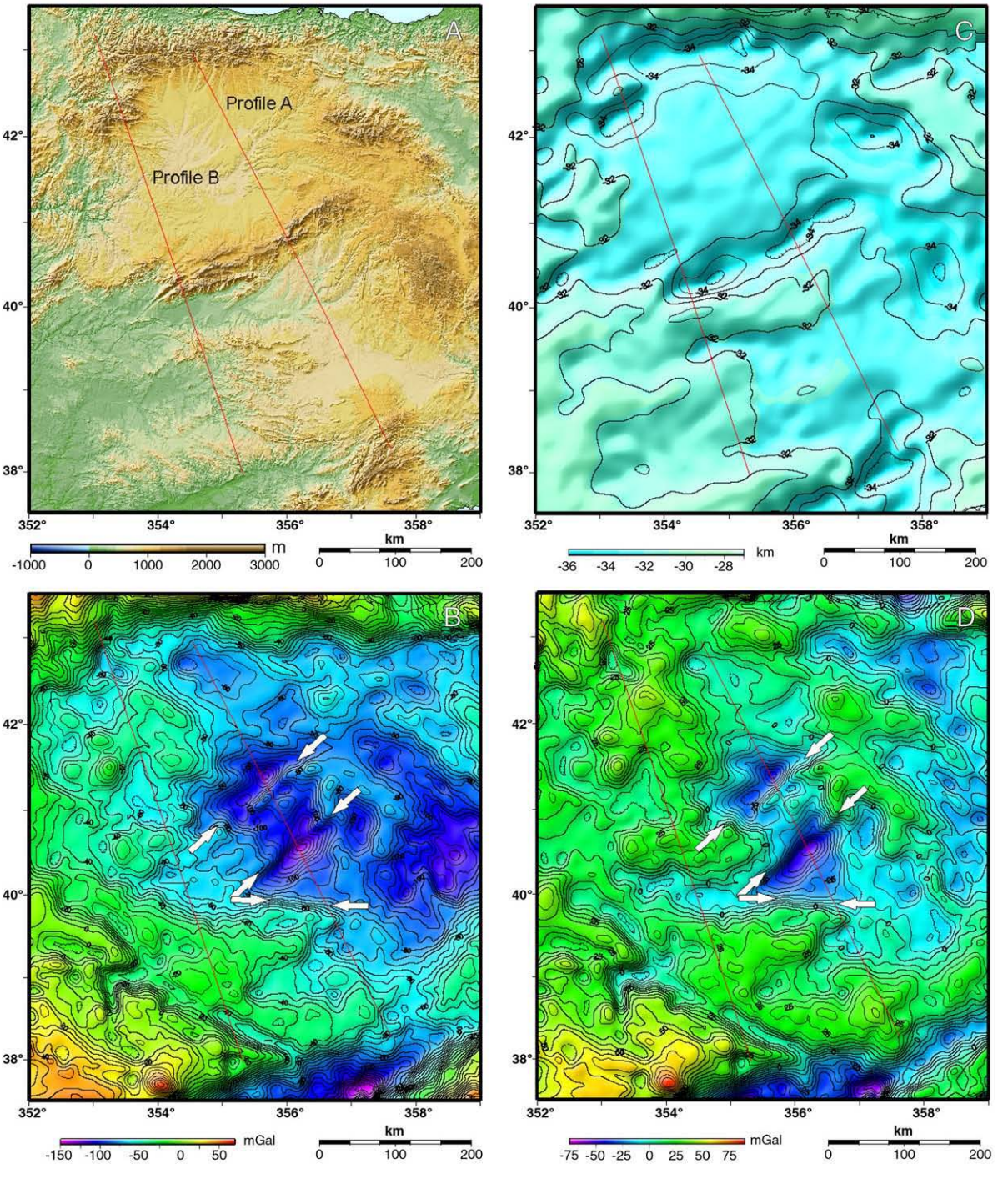

Fig. 5. A) Digital elevation model for central Iberia. B) Bouguer anomaly map (mGal). C) crustal thickness calculated from topography assuming local isostatic compensation. D) Isostatic Residual anomaly map for the same parameters than B). Arrows show the gradients associated with the main Alpine thrusts in the Central System and Toledo Mountains. Gravity data are from IGN (Mezcua et al., 1996) and ENRESA. Location of modelled gravity profiles of Figs. 6 and 7 are also shown.

processing and topographic reduction of the gravity field can be found in the final report of the PRIOR project (De Vicente et al., 2005a,b).

The density used for the station complete-Bouguer reduction was 2670 kg/m^3 The data were homogenized and linked to the ISGN 71 gravity datum. Topographic

reduction was achieved by approximating topographic masses with polyhedrons within a radius of 167 km. Data errors were assumed to be less than 2.10 ^{5} m/s^{2} (2 mGal) (Table 1).

The topographic data (Fig. 5A) used for gravity reductions and isostatic investigations are based on the GTOPO30 data (U.S. Geological Survey, 2000), with additional data from the SRTM topography mission from NASA.

3.1.1. Bouguer anomaly map

The Bouguer gravity field of the Iberian interior varies between −132 and +34 mGal. This difference of 166 mGal indicates large-scale variations in the crustal structures within the area. It should be emphasized that negative values of the Bouguer anomaly are distributed over almost all the surface of the Iberian interior, except in the southwest zone where high-density igneous and metamorphic rocks crop out. Some of the gravity anomalies shown on this map can be assimilated with mapped geological bodies at surface; nevertheless, in other zones this relation is no longer so clear, as it is masked by the distribution in depth of the isostatic roots supporting the topography.

In contrast to clearly marked Variscan trends, the main Alpine characteristics of the Bouguer anomaly map (Fig. 5B) are a series of NE to SW trending gravity highs and lows, separated from each other by high gradient zones along the same direction, that correspond geologically to major Alpine thrusts (Muñoz-Martín et al., 2004). From those which have a pronounced amplitude and extension, it is possible to identify the northern and southern borders of the Spanish Central System, as well as the northern thrust of the Toledo Mountains (arrows on Fig. 5B).

3.2. Isostatic analysis

In order to explain the isostatic behaviour of the central Iberian lithosphere, we have considered the three main models of isostatic compensation. In two of them, the Pratt–Hayford model (Hayford and Bowie, 1912) and the Airy–Heiskanen model (Heiskanen and Moritz, 1967), the compensation mechanism is local, whereas Vening Meinesz (1939) proposed a model taking into account a regional mechanism of compensation. As the main objective of this study is to characterize the Iberian interior geologically, rather than to investigate the most appropriate model of isostatic compensation, we have selected the Airy–Heiskanen model for its ease of calculation and the good results obtained in continental areas (Simpson et al., 1986; Álvarez et al., 2002).

Table 1
Used parameters in the gravity forward modelling

	Layer geological units	Density (g/cm3)
1	2.3	Tertiary and Quaternary Rocks
2	2.55	Jurassic and Cretaceous Rocks
3	2.8	Triassic Rocks
4	2.6	Granitic Rocks
5	2.8	Metamorphic Rocks
6	2.67	Upper Crust
7	2.9	Lower Crust
8	3.4	Mantle

Previous studies dealing with the Airy isostasy of the central Iberian Peninsula already indicate that the Spanish Central System is in local isostatic equilibrium (Stapel, 1999). Evidence for this is that some of the greatest elevations correspond to the observed Bouguer gravity minimum values across the Alpine range (Fig. 5B). For this study, a more detailed database of gravity stations and topographic height data was available, which makes a re-evaluation of the isostatic state of central Iberia possible.

3.2.1. Airy Moho map

The Airy Moho map shown in Fig. 5C has been calculated for the known topography. The Airy root, $T_{(x)}$, was calculated using the formula:

$$T_{(x)} - h_{(x)} \frac{\rho_t}{\Delta\rho} + T_C \tag{1}$$

where T_C is the normal crustal thickness, ρ_t the density of topography, $\Delta\rho$ the density contrast between the lower crust and the mantle, and $h_{(x)}$ the topographic height. A description of the most appropriate values for these parameters can be found in Muñoz-Martín et al. (2004). These values are consistent with previous seismic crustal studies of Iberia (ILIHA DSS Group, 1993).

The Airy Moho map shows crustal thicknesses ranging from 30 km to 34 km in the Iberian Block, with the greater crustal thicknesses occurring in the Central System and the Leon Mountains. It also fits well with the values proposed for the Central Iberian zone (Bergamín and Carbó, 1986). These two chains, as well as other minor ranges (Serra da Estrela, Guadalupe range, Sierra Morena) present an anisotropic character, with a clear elongation aligned in a NE–SW direction, perpendicular to the present active tectonic stress field (Cloetingh and Burov, 1996). These crustal thickening zones present a high relationship between amplitude and wavelength, unlike other thickened inner zones, like the Iberian Mountain

range, which present a more circular character and greater wavelength (Salas and Casas, 1993).

3.2.2. Isostatic residual anomaly map

The isostatic residual anomaly map in Fig. 5D is obtained by removing the isostatic correction from the Bouguer anomaly. The isostatic correction reflects the gravitational attraction of a crustal root under a topographic load. This isostatic correction or isostatic regional field (Jachens et al., 1989) has been calculated following the method of Simpson et al. (1986), which is based on the "Parker algorithm" (Parker, 1973).

The Airy isostatic residual anomaly map (Fig. 5D) shows the differences between the measured Bouguer anomaly and the isostatic gravity field. The main residual anomalies have maximum amplitudes with a range of between −55 and 62 mGal. This map contains long wavelength anomalies that can be related to the absence of isostatic balance, or to the existence of other mechanisms of non-local compensation (regional compensation). The greatest gravity gradient is located along the Southern Border Fault of the Spanish Central System. There are also two long wavelength negative anomalies that can be clearly seen at the edges of the range. These negative anomalies correspond to the Duero and Tagus sedimentary basins and can be associated with high sediment thickness, the flexural behaviour of the lithosphere through topographic loading and the presence of horizontal tectonic stresses (Van Wees et al., 1996; Andeweg et al., 1999; Stapel, 1999). The negative anomaly of the Duero basin presents a smaller amplitude, probably due to the greater strength of the crust in this zone, as suggested by rheological models (Tejero and Ruiz, 2002).

The shorter wavelengths are not related to the compensation mechanisms, but to geological bodies with density contrast located in the uppermost kilometres of the upper crust (Van Wees et al., 1996). The good correlation between short wavelength isostatic residual anomalies and geological bodies suggest that the upper crust is the origin of additional masses that cause deviations from isostatic equilibrium and possibly trigger subsidence and uplift processes. This is probably the case, for example, in the central sector (Guadarrama) of the Central System, where negative values suggest uplift, this being in agreement with previous geological data (De Vicente et al., 1996) and thermocronological studies (De Bruijne and Andriessen, 2002; Ter Voorde et al., 2004).

Within the Iberian foreland there is an interference pattern of gravity anomalies related to NW–SE to E–W-trending Variscan structures and the NE–SW-trending anomalies related to Alpine contractional structures.

3.3. Spectral analysis of gravity and topography

Results from spectral analysis of gravity and topography indicate the existence of a dominant wavelength of 200 (±50) km in both the topographic and gravity undulations along profiles A and B (Fig. 6). The gravity power spectra also show a large wavelength of at least 500 km, which probably reflects the high average base level elevation of Iberia, with a steep contrast at its borders. These characteristics of the signal spectra have been interpreted as a process of lithospheric folding in response to Alpine tectonics. The presence of different wavelengths in the gravity and topographic signal may be related to mechanical decoupling of the lithosphere. Short wavelengths are related to crustal folding controlled by the elastic thickness of the lithosphere and previous mechanical discontinuities (Cloetingh et al., 2002).

3.4. Gravity modelling

To analyse the Alpine crust structure of central Iberia, and especially that of the Central System, two gravity models were developed in 2+1/2D cross sections (Talwani and Heirtzler, 1964; Won and Bevis, 1987), perpendicular to the main structures and subparallel one to each other (see Fig. 5 for location):

a) Profile A. (Fig. 7A) This profile crosses, from S to N, the front of the Alcaraz thrust (the northern limit of

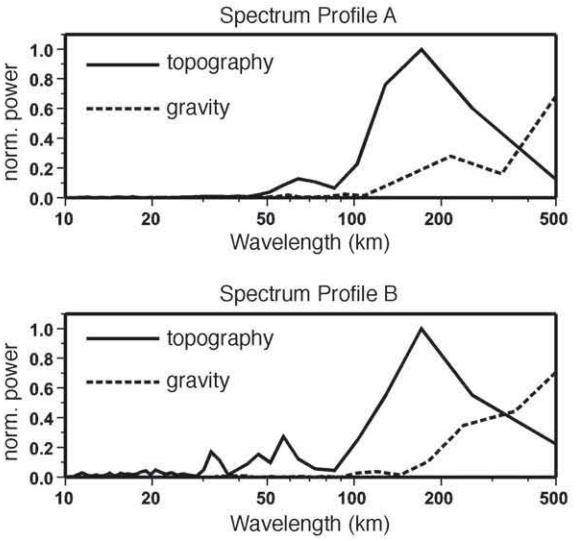

Fig. 6. Normalized power spectra of the topography (solid lines) and bouguer gravity anomaly (dash lines) of the profiles shown in Fig. 5. See Cloetingh et al. (2002) for details.

the Betic Mountain chain), the Toledo Mountains, the Tagus Tertiary Basin, the Central System (Guadarrama), the Duero Basin and the S edge of the Cantabrian Mountains, and the two main zones of high gradient bordering the Central System, as well as both absolute gravity lows in the interior of the peninsula.

b) Profile B: (Fig. 7B) It begins to the S of the limit between Sierra Morena and the Guadalquivir Basin. It then crosses the Guadalupe range, the Central System (Gredos), the Gata range, the Duero Basin, the Leon Mountains, the Bierzo Cenozoic basin and the Ancares range.

Both models have been adjusted, using the abundance of geological and structural information (Vera, 2004), seismic and borehole information (Racero, 1988; Suriñach and Vegas, 1988; Querol, 1989), as well as the crustal thickness deduced from the isostatic analysis previously described. Abundant seismic information

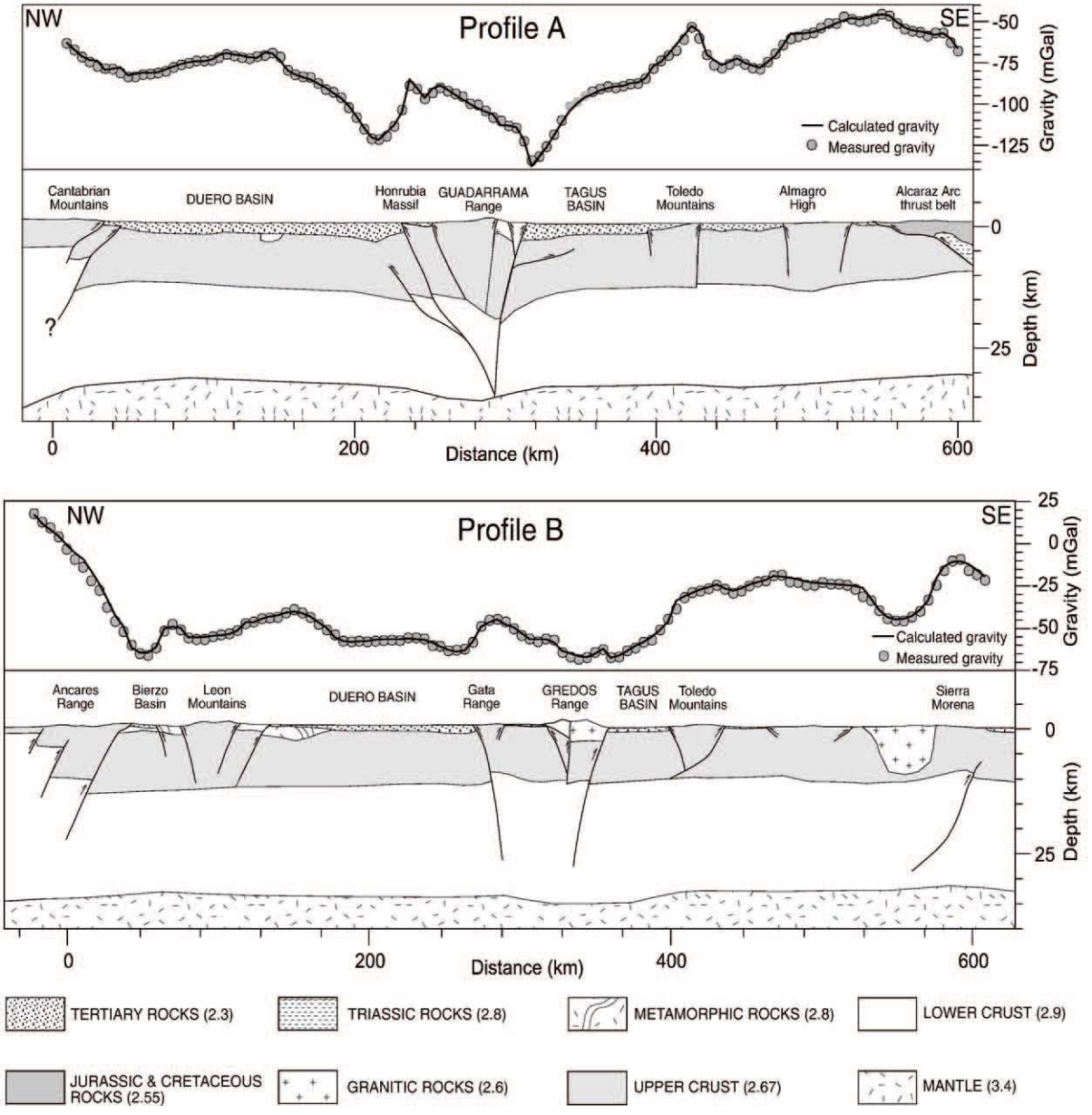

Fig. 7. 2+1/2D gravity models for central Iberia. The location of profiles is shown on Fig. 5.

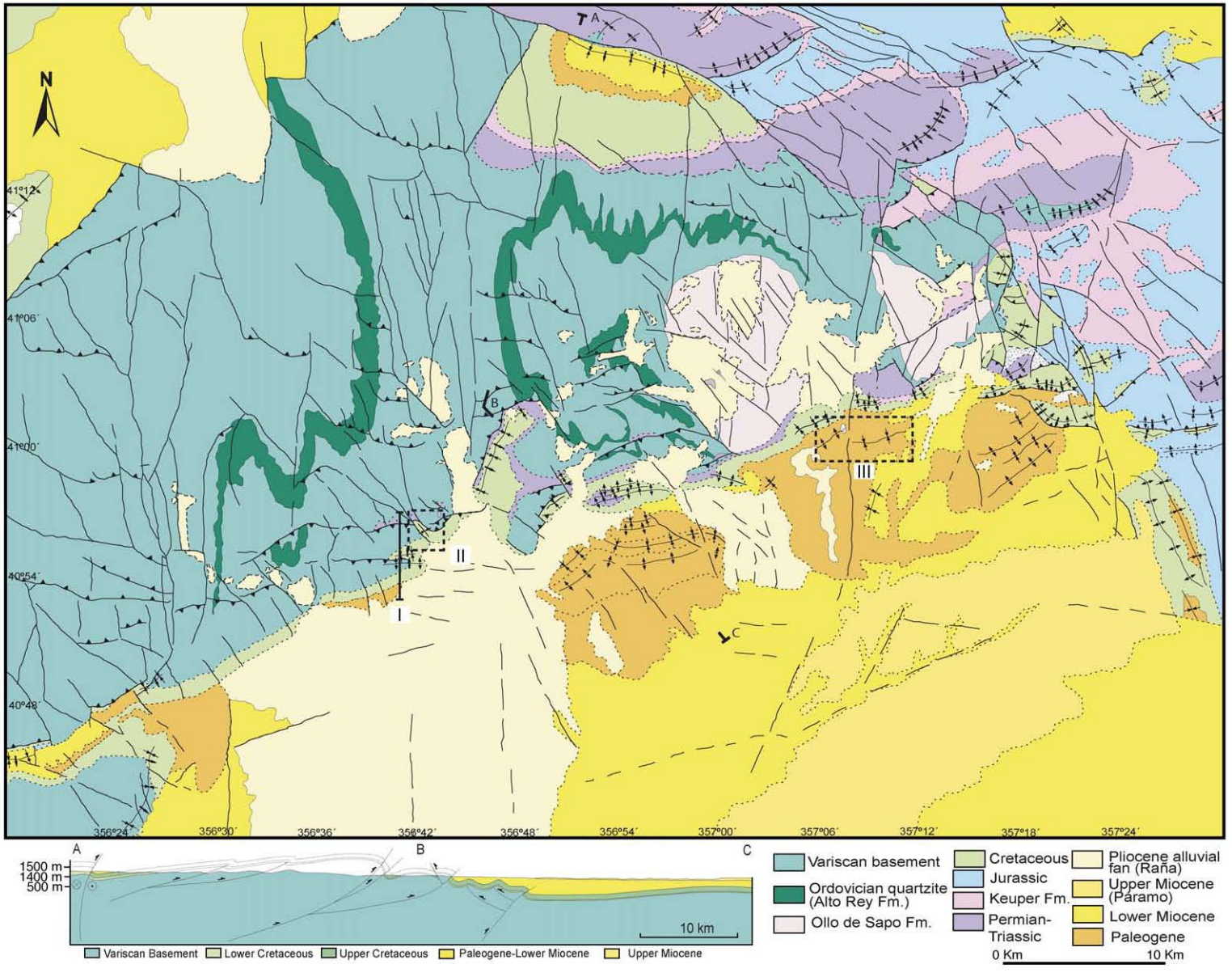
N
A
B
C
I
II
III
41°12´
41°06´
41°00´
40°54´
40°48´
356°24´
356°30´
356°36´
356°42´
356°48´
356°54´
357°00´
357°06´
357°12´
357°18´
357°24´
A
B
C
1500 m
1400 m
500 m
10 km
Variscan Basement
Lower Cretaceous
Upper Cretaceous
Paleogene-Lower Miocene
Upper Miocene
Variscan basement
Ordovician quartzite (Alto Rey Fm.)
Ollo de Sapo Fm.
Cretaceous
Jurassic
Keuper Fm.
Permian-Triassic
Pliocene alluvial fan (Raña)
Upper Miocene (Páramo)
Lower Miocene
Paleogene
0 Km
10 Km

(ILHIA, IBerseis) that exists for the areas bordering central Iberia allows us to further constrain the crustal structure. Regarding the regional character and the extension of the models, lithologies have been simplified and grouped into 8 principal units. The density values used appears in Table 1. The accumulated error is 1.50 mGal for model A and 1.77 for model B.

Both models show a series of large wavelength undulations in the Moho surface, indicating a synform under the Central System, and two descents towards the S (Betic Mountain chains) and the N (Cantabrian Mountains). Minor folds appear over these undulations in the upper crust, and their flanks are usually cut by large thrusts. The most important upper crust antiforms are: the Central System, the Toledo Mountains, the Guadalupe Ramp, the Leon Mountains, the Ancares and the Sierra Morena. In the upper crust synclines, tertiary and quaternary basins have developed.

3.5. Discussion of the gravity models of the Central System

The Central System is clearly defined by a gravimetric minimum of large wavelength that presents a relative asymmetric maximum in its central part. This feature is more accentuated in model A (Eastern Sector) than in B (Western Sector). These are associated with two added effects: On one hand, with a Moho downwarping that leads to an increase in upper crust thicknesses of up to 3–4 km, and on the other, with the close presence of the main Duero and Tagus depocentres, where there are more than 3000 m of Tertiary sediments. The Central System nucleus is an asymmetric maximum that suggests an elevation of the upper crust by means of crustal-scale faults, and a ductile thickening of the lower crust. This block of raised upper crust presents a ramp geometry converging to the N with two principal steps on its N edge, and another two at the S edge. Thrust offset at the S edge is greater than in the N. In model B, though the structural style is maintained, both the number of steps and the vertical offset change, are lower than those at the S edge of model A. This is in agreement with a relatively low volume of sediments in the basins. The gravimetric reflex has a smaller minimum extent and shows a few gradients of lower magnitude.

The Toledo Mountains (Fig. 2) present a significant low angle thrust at their N edge, with a decreasing offset towards the W (Model B). In Model B, the equivalent structure of the Toledo Mountains S edge is the Guadalupe Ramp. Both systems form the axis of a smooth crustal-scale antiform with a large wavelength over a small area that mimics that of the Central System towards the S (Fig. 2). This series of structures appears in continuity with the "bulge" of the Tagus Basin (towards the W), and in general terms can be related to the S border thrust of the Central System and to an increase in the thickness of Cenozoic sedimentation towards the E.

An interesting point is the occurrence of consistently lower values for the crustal thickness (excluding Cenozoic sediments) of ca 30 km in Profile A compared to crustal thickness values of ca 33 km in Profile B.

4. Macrostructural description

4.1. Central System Range

As previously stated, the Central System can be divided into the following tectonic units (De Vicente, 2004): From East to West, the Iberian Chain link area (*Transition Zone*); Somosierra and Guadarrama (*Eastern Sector*); Gredos and Paramera (*Western Sector*) (Fig. 3).

4.1.1. Transition Zone (The Iberian Chain link area) (Fig. 8)

The northwestern end of the Castilian–Valencian Branch of the Iberian Chain is characterized by the presence of a series of folds with similar NE–SW axis trend to those of the Central System, with an "en echelon" pattern and a wavelength of less than 10 km. Southerly vergence (Riba de Santiuste, Sigüenza, NE corner of Fig. 8), related to basement thrusts in the southern flanks (fault propagation folds), are also visible. These compressive structures appear to be limited by the Barahona Faults System to the north and by the Somolinos Fault System to the south, both with Iberian trends (NW–SE) and with a clear right-lateral strike–slip movement (Fig. 3). The latter has traditionally been considered to be the limit between the Iberian Chain and the Central System. Taken as a whole, these structures define a transpressive shear zone that seems to end against the Northern thrust of the Central System in the Sepúlveda–Honrubia uplift (Fig. 3). The Somolinos Fault also shows a clear reverse component, especially where it runs in a more ESE–WNW direction, as in the restraining step-over of Sierra de la Pela (Fig. 3), where

Fig. 8. A) Tectonic map of the transition zone of the Central System; link area with the Iberian Chain. Note the triangular zone described in the text: The Southern border corresponds to the Tamajon Imbricate Thrusts area. The Eastern transpressive zone is the Tortuero Backthrusts area. B) Simplified cross section of the area. Dashed boxes corresponds to maps of Figs. 11, 12 and 17. See also Fig. 22.

a small tertiary basin appears, separated from that of Almazán by a N block thrust showing incomplete tectonic inversion, with no relation to the actual relief.

In addition this transpressive zone (Barahona–Somolinos faults system) also borders a triangular zone within the Central System that is limited to the west by another transpressive zone (Tortuero backthrusts), in this case with an N–S trend and left-lateral strike–slip movement up to the Somosierra Pass Fault (Figs. 3 and 8. see also Fig. 11). The intersection of both transpressive zones constitutes the N vertex of this triangular zone, the S side of which corresponds to the northeastern edge of the Tagus Cenozoic Basin. This limit is formed from a series of imbricate basement thrusts (Tamajón Imbricate Thrusts) and fault propagation folds that affect the Mesozoic–Paleogene cover of the Basin edge, showing clear tectonic transport towards the SE (Fig. 8). This triangular zone has a deformation gradient with increasing shortening from the N vertex to the S border, giving the tightest structures of the whole Central System, with wavelengths around 5 Km. This seems to indicate the presence of a shallow detachement in this S basement sector, probably favoured by the Variscan structure. In the Hiendelaencína Massif, the main Variscan schistosity is subhorizontal. These dips in the schistosity appear forming a type 1 fold interference that is reflected in the general dome structure of the massif within which strike–slip faults predominate. Later folds have a NE–SW orientation and produce interferences of similar wavelengths to those of the Alpine pop-ups and imbricate thrusts of the S edge, which are clearly related (Rodríguez-Fernandez, 1990). Thrust orientation (N80E) is somewhat different from that of the rest of the S edge (N60E), and appears as a continuation of the ENE band, that extends up to the Amblés Basin towards the west (Fig. 3). Laterally, thrusts progressively become oriented N–S in the western limit (Tamajón zone), and ENE–WSW in the area of contact with the Iberian Chain, reducing its vertical displacement at the same time.

In the northeastern corner of the Central System, the imbricated thrust systems of Tamajón in the S and Sepúlveda in the N present very similar structural characteristics and tectonic tertiary evolution (Figs. 8 and 9), though in the latter case tectonic transport is towards the NW and does not show Pliocene activity, as it does to the S. The Sepúlveda imbricate thrust zone (Fig. 9A), a Mesozoic cover folded zone, ends towards the NW, close to the Honrubia massif, along the Northern Border thrust of the Central System, where the basement outcrops again. The basal detachement surface of the imbricated structure should be located in the upper crust (De Vicente et al., 1996; Van Wees et al., 1996). The gravimetric gradient along the Northern Border thrust of the Central System is similar to that of the S, indicating that this more shallow thrust system joins another deeper structure as in the NW (Fig. 9B). The vertical offset of these thrusts increases towards the S, up to the Northern Border of the Somosierra Thrust, with about 1000 m of minimum vertical displacement. The major topographic gradient is located N of Somosierra and related to this fault which, because of its length, must be probably rooted deep in the upper crust. The undetached cover folds present a smooth plunge towards the NE, before disappearing under the tertiary sediments of the Almazán Basin (Fig. 3), which can be considered as thick-skinned piggy-back basin of the Cameros–Demanda N Thrust (Guimerá, 2004).

This area shows clear strain partitioning and can be considered as the NW end of the Somolinos–Barahona right-lateral fault system (Fig. 3) along which pure strike–slip and thrust faults (Fig. 9A, B, C, D) arranged in a series of restraining bends develop.

On both sides of the Somosierra Pass Fault (Fig. 3), N–S shortening predominates. In the Variscan basement, a later deformation stage, D5, is defined (Gil Toja et al., 1985; IGME, 1990), which folds all the earlier structures, without schistosity development, by means of large E–W folds. In many cases, it is the cause of regional immersion changes in the N–S Variscan folds, as in the Majaelrayo syncline and produces a type 1 interference pattern. Given the intensity of Cenozoic deformation, it is probable that this D5 stage is indeed of Tertiary age (Fig. 10).

4.1.2. Eastern Sector (Somosierra and Guadarrama)

The intermediate sector of the Central System includes the Guadarrama and Somosierra sierras, as well as other series of minor reliefs associated with the thrusts along the N and S edges (Fig. 3). The Somosierra consists of a pop-up that loses height where it makes contact with the Somolinos Fault. In this sector the major vertical offset corresponds to the N thrust of the Somosierra pop-up, opposite to what occurs with the Sepúlveda imbricate thrust system (no morphological offset), and constitutes the morphological limit of the Central System. Towards the S, the Somosierra Pass Fault delimits two different zones: to the E, the already-mentioned Tortuero backthrusts transpressive zone, and to the W, a relatively depressed area with fewer topographic contrasts (Fig. 11. see also Fig. 8).

The Tortuero area, on the S edge, is particularly representative of Alpine deformation style and basement accommodation. The S border thrust does not reach the surface, and a large N60E fold propagation fault can be

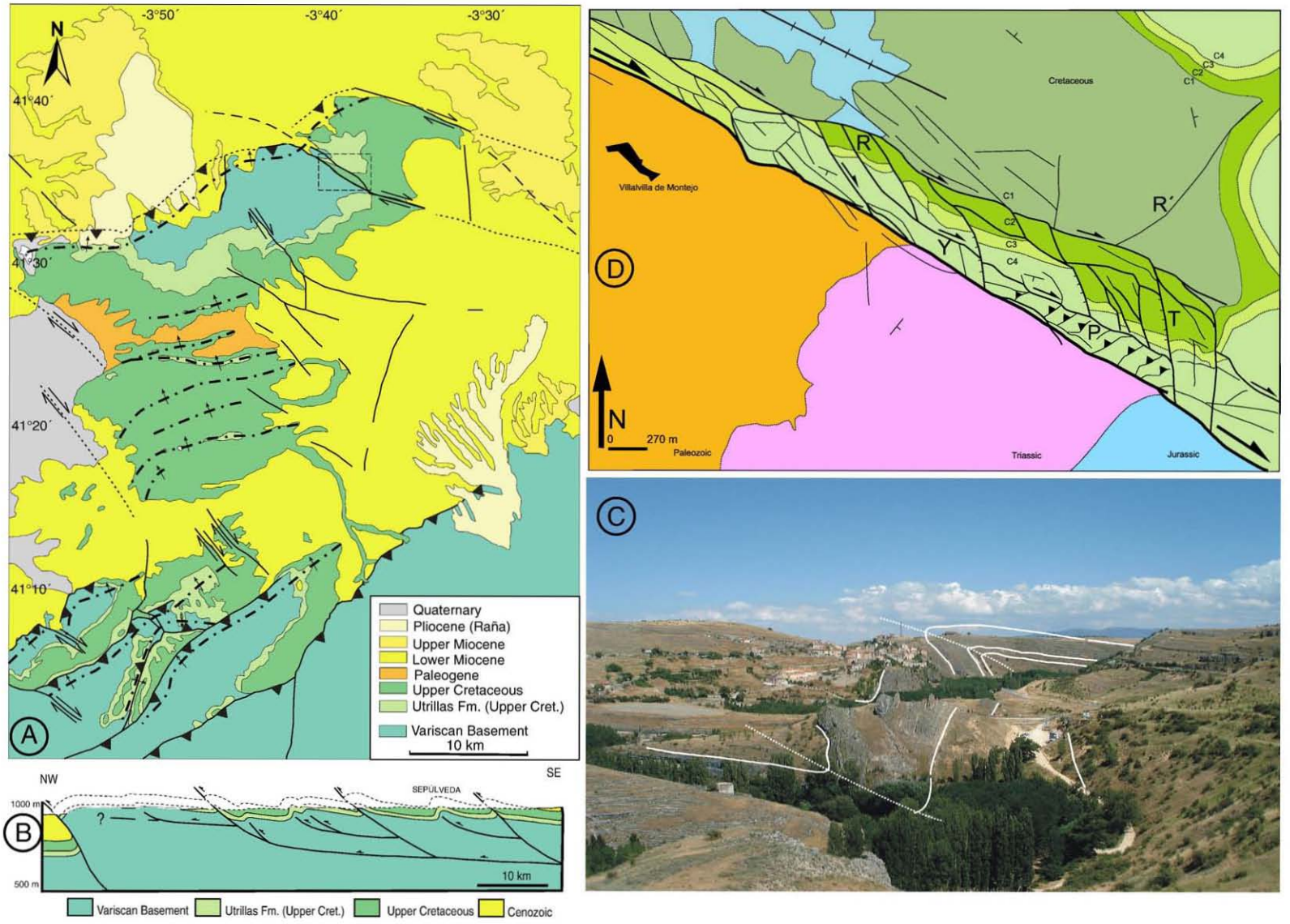

Fig. 9. A) Tectonic map of the Sepulveda Imbricate Thrusts area (NE Central System). Strain partitioning: B) Schematic cross section of the imbricate thrust system (1–1′ on A). C) Right lateral Transpressive zone (square C in A). D) Sepúlveda fold (located in B as D).

established from land-cover cartography (Fig. 8). This structure is cut by two Northward verging backthrusts (Fig. 11). Its orientation progressively changes to N–S, constituting the southern end of the Somosierra Pass Fault. From this geometry and from inversions of fault slip data, tectonic transport towards N150E can be deduced. However, to the N of Tortuero, a series of thrusts with N vergence appear to end at the N Somosierra thrust. The horizontal separation between these structures decreases from N to S. The Atazar backthrust, which appears immediately to the N of that of Tortuero, duplicates the periclinal termination of the Variscan anticline of El Cardoso (IGME, 1990), enabling its reverse offset to be estimated at 1750 m (Fernández-Casals and Capote, 1970) (Figs. 3, 8A, 11). This vergence pattern indicates a main concentration of SE tectonic transport on the Southern Border thrust, and a much more dispersed deformation in NW tectonic transport structures, which developed close to a S thrust. The distribution of this deformation is in agreement with the deep structure deduced from gravimetric profiles (Fig. 7A) and from sedimentary infilling of the Duero Basin (see below). In the eastern termination of the S border Permian conglomerates crop out along its trace (Sopeña, 1979), leading the idea of the post-Variscan origin of this fault. The evident relation between the topography and the geometry of this backthrust system (and that of the Somosierra pop-up), makes cartography possible, even where it cuts into two homogeneous and slightly competent basements (Fig. 12B). On the other hand, the accommodation of the Alpine deformation in the basement is more appreciable, as in the Valdesotos area (Figs. 8 and 12) that can be used as a key to interpret the Cenozoic dynamics of the whole Central System (see Fig. 12A, B, C, D, E and paleostress discussion below) (Olaiz et al., 2004). In the cases of the Sepúlveda and Tamajón imbricated thrusts, the subhorizontal schistosity operates mechanically in a very similar way to the cover. Nevertheless, here the Variscan schistosity is subvertical, which facilitates the left-lateral strike–slip movement, but not the development of fault propagation folds. In this case only reorientations and metric kink folds are appreciated, with the same vergence close to that of Alpine thrusts (Fig. 12B, E).

Towards the west, at its contact with the Guadarrama, the Somosierra pop-up gives way to a more complex structure consisting of two pop-ups separated by the Lozoya pop-down which contain the major topographic highs in the intermediate and eastern sectors of the Central System. To the south N70–80E structures appear. The pop-down of the Upper Manzanares is one of the most noticeable (Fig. 3).

The S border, west of the Somosierra Pass Fault, presents the most characteristic trend of the Central System: N60E. The contact with the Tagus Basin is very clear and almost straight at higher levels. It extends as far as the Sierra de San Vicente in the southern part of Gredos (Fig. 13A), and corresponds to one of the most important gravity gradients in the whole Iberian Peninsula (Fig. 5B). A seismic profile shows a reverse fault geometry with a vertical offset of more than 3000 m (Querol, 1989; Fig. 16). The scanty relief of the

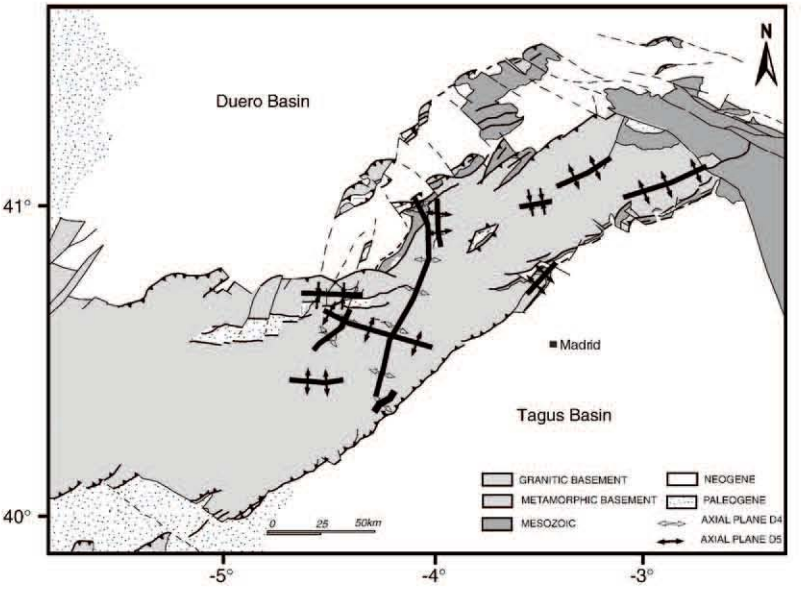

Fig. 10. Large radius (smooth) folds in the Variscan structure (Gil Toja et al., 1985; IGME, 1990), that are here interpreted as formed during Cenozoic times.

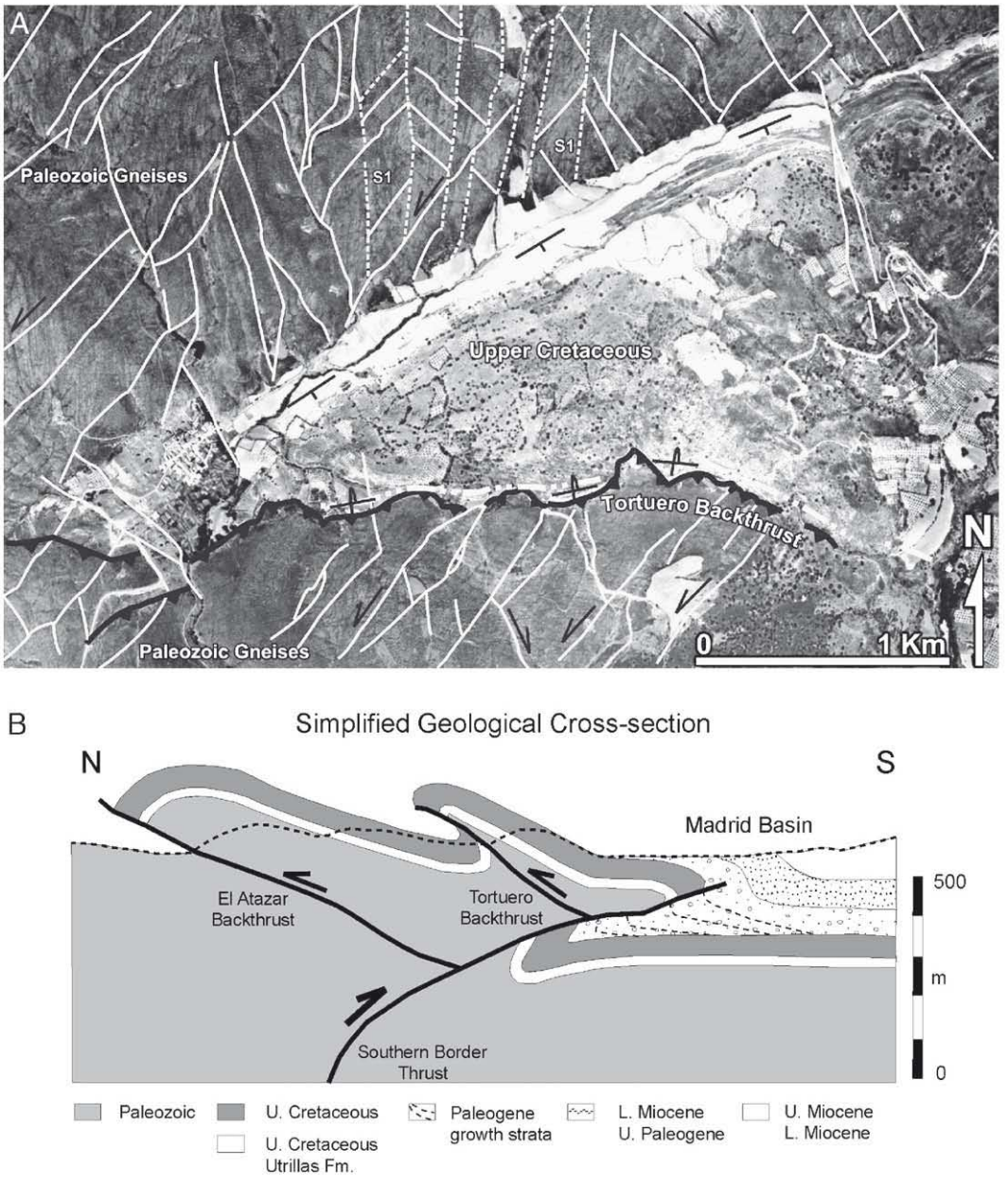

Fig. 11. A) Photo-interpretation of the Tortuero backthrust (black). Note the inversion of the Mesozoic stratification in the thrust footwall and the shallow dip of the main fault. Related strike–slip faults (white) are NW–SE (right-lateral) and NE–SW (left-lateral). S_1 (main Variscan schistosity). B) Simplified cross section of the Tortuero backthrusts system. Location on Fig. 8A (I–I′).

roof block of this fault may indicate mainly Paleogene activity in the context of a more or less constant rising throughout the Tertiary (Martín Serrano, 1991; Alonso-Zarza et al., 2004).

To the N of the S border fault there is a backthrust that forms a 10 km wide pop-up, which also continues to the Sierra de San Vicente, though here the topography is slightly more pronounced. This structure is segmented by N110E right-lateral and N20 left-lateral faults, that progressively change their orientation into the pop-up edges, to connect with the N60E thrusts, resulting in a zigzag appearance from where a very constant shortening direction can be deduced: N150E (Fig. 13).

The most important topographic step of the southern border is located to the east of the Upper Manzanares in the Guadarrama, N of the El Escorial Fault. It constitutes

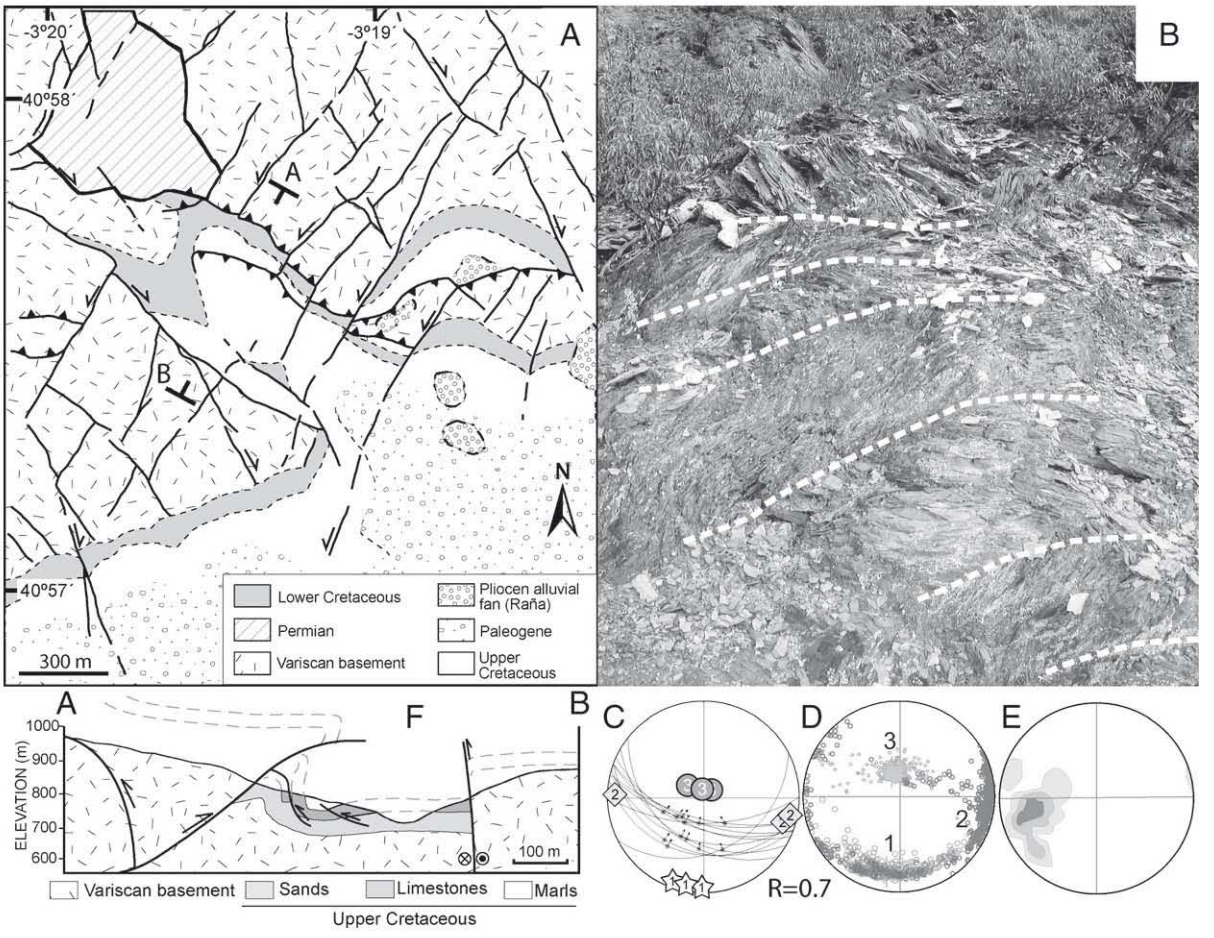

Fig. 12. A) Geological map of the Valdesotos thrust area (see Fig. 8A for location). B) E–W kink folds developed on the Variscan basement in the footwall of the main thrust. Microstructural analysis: C) Stress inversion of the footwall reverse faults. D) Bootsrap of C). E) Density diagram of the kink axis in the hanging wall (B).

the limit of a N30E left-lateral transpressive pop-up, formed by Variscan contacts between the granitic intrusions and the metamorphic massifs. This set of NNE faults continues N–S towards the west as far as the El Herradón Fault, one of the most spectacular in the whole Central System (Fig. 3).

The N edge of the intermediate sector, west of Sepúlveda, continues to the pop-up of Santa Maria la Real de Nieva across a series of unconnected outcrops. As a whole, the N edge forms an arch that indicates a NW tectonic transport direction (also deduced from inversion of fault slip data) (Fig. 3). Its morphology is much less marked than that of the S edge, developing an erosive surface towards the Duero Basin, which has levelled much of the tectonic structure of this edge. However, it is also a clear gravity limit, similar, though slightly less so, to that of the S edge. The relief does not recover up to the Guadarrama pop-up. As in the Sepúlveda area, a series of imbricated thrusts characterize this edge. It is segmented by N140E and NNE strike–slip faults.

4.1.3. Western Sector (Gredos)

The name Gredos is used to define the western segment of the Spanish Central System, though, strictly speaking, it corresponds to one of the ranges of mountains in this geographical division. Its general structure is simpler than that of the intermediate and eastern sectors, which is probably due to more homogeneous basement materials, consisting of granites (Figs. 3 and 13). As a whole, it forms an 80 km wide pop-up, which is subdivided into four secondary pop-ups (San Vicente, Gredos, La Paramera and Mingorría) with a width of 10–20 km that limit three straight pop-downs (Tietar, Upper Alberche and Amblés). These mountainous high plateaus are aligned in an E–W trend,

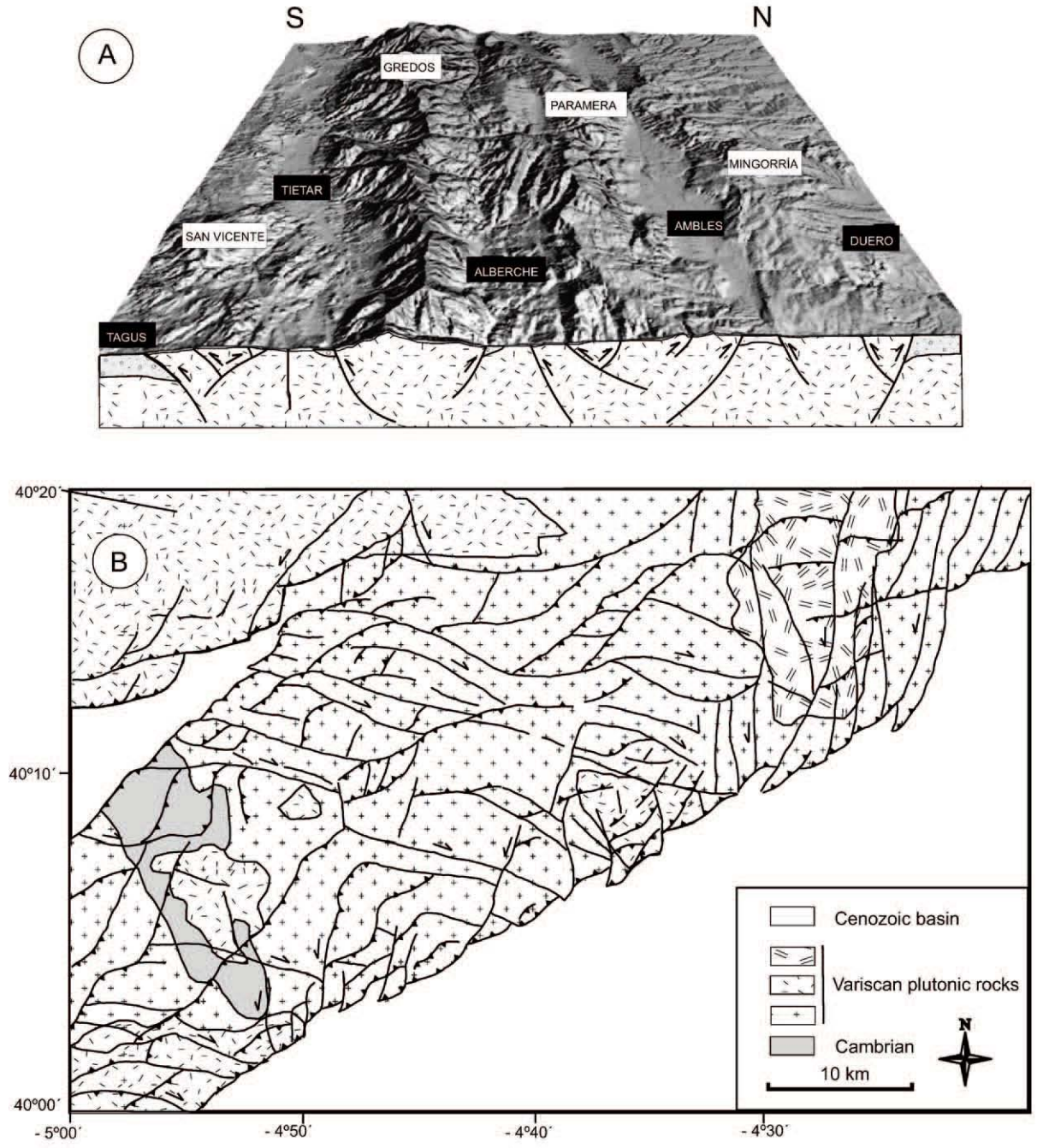

Fig. 13. A) Schematic cross section of the Western sector of the Central System (Gredos). Pop-ups: San Vicente. Gredos. Paramera. Mingorria. Pop-downs: Tietar. Alberche. Ambles. B) Main faults of the San Vicente pop-up area (S Gredos zone).

except on the S edge of San Vicente, which presents a NE–SW direction. Laterally, the Gredos pop-up is limited to the east by a NE–SW alignment of the El Escorial Sierra Faults system, and to the west by another NE–SW Sierra (the Sierra de Avila), which contains the large Plasencia dike that forms the depressed alignment of the Jerte valley (NE of Plasencia Fault) (Fig. 3). It can be considered a long restraining bend of the Plasencia left-lateral fault. This strike–slip fault is orientated in the same direction as the Southern Central System Thrust, and it constitutes a clear example of strain partitioning, probably developed under constrictive stresses (see

below). As a whole, the NE–SW and E–W edges of this western sector of Gredos form a parallelogram that extends in a close E–W trend with the relief increasing in height towards the S. This gives an unsymmetrical relief with an almost imperceptible N edge (only 100 m at its contact with the Duero Basin), whereas the southern limit includes the major topographic step (2100 m) on the south wall of Gredos.

On the southeastern slope the vertex of the parallelogram is a lower pop-up: the Sierra de San Vicente (1300 m) (Fig. 13A). This narrow pop-up breaks up into two relief alignments separated by the depression of the River Guadyerbas. Both of these lose height towards the SW to disappear where the Tietar and Tagus Basins join. The northern alignment limits the Tietar pop-down and is oriented E–W, parallel to the edge of Gredos, whereas the southern alignment has a NE–SW direction and represents the continuity of the southern edge of Guadarrama, that is, of the main thrust that connects the Tagus Basin with the Central System. In contrast, the N edge of the latter relief corresponds to a N vergence thrust which can be traced up to the western Toledo Mountains. Looked at in this way, the southern edge of the Central System appears to form part of a large fracture line, from the Eastern Sector to the Guadalupe Sierra relief (Fig. 3).

In summary, deformation appears to consist mainly of very segmented E–W structures associated with parallel and massive reliefs, and, in the case of NE–SW structures, narrower and discontinuous Sierras. Strike slip faults displace the E–W faults segments, generally with left-lateral movements, which results in a more N70–80E general trend.

4.2. Gata and Estrella Sierras

The mountain ranges of Gata (1.367 m) and Peña de Francia (1.723 m) constitute the most western relief of the E–W alignment of central Iberia in Spanish territory (Fig. 1). They correspond to a basement elevation with two NE–SW thrusts of opposite vergences (Fig. 2). The northern thrust breaks down into two staggered segments that separate the basement of the Ciudad Rodrigo Paleogene basin (SW Duero Basin). Both segments appear to be part of structures that extend between Salamanca and the Portuguese frontier, with a relatively large compressive deformation. The more southern E–W thrust belongs to a fault system that produces a more complex relief when it crosses more depressed areas containing discontinuous Neogene basins (Coria, Zarza de Granadilla, Castelo Branco) that form some kind of continuity with the Gredos segment and are related to NE–SW left lateral strike–slip faults restraining bends. In contrast there is a northern thrust that, with smaller displacements, appears to be a continuation into Spanish territory of the Ponsul Thrust (Northen Moraleja Basin (Mo), see Fig. 2), defined in Portugal as a reverse fault with neotectonic activity (Cabral and Ribeiro, 1989).

This basement elevation is conditioned by E–W structures that interfere with the dominant NE–SW faults. Standing out among these E–W structures is the thrust that limits the Sierra de Gata relief from the smaller topographical area (SE corner of Fig. 2). In some ways this fracture line has a longer trace, since it can be continued through the Alberche pop down as far as the eastern border of Gredos (Fig. 2).

To the west of Gredos, the basement deformation pattern is evidently simpler and very different from that of the easternmost segments. The Cenozoic contraction is mainly taken up by NE–SW thrusts that define a series of pop-ups of the same orientation, while the E–W thrusts appear as a subordinate fault system, although some of them are part of large alignments, which nowadays are very segmented. This pattern seems to continue towards the west up to the Serra da Estrela. Its northern border (1.993 m) corresponds to the Lousâ NE–SW thrust, with a large vertical displacement and a better morphological expression of the whole Central Iberian Ranges (Fig. 2).

4.3. Guadalupe ramp

The Guadalupe and Montánchez Mountains, with a NW–SE trend, are the result of a single NE–SW and E–W thrust. Related alluvial fans points out to a clear Pliocene activity (Figs. 2 and 14).

It has less than 1000 m of vertical displacement, with a 80 km trace that connects in the SW with the E–W thrust that forms the northern border N of the Badajoz Cenozoic basin (Ba on Fig. 2), and in the NE with the southern thrust of the Toledo Mountains, both with a S tectonic transport (Fig. 14A). The alternation in orientation of these thrusts mimics that of the Central System. This Sierra system represents one of the areas of the interior of the Iberian Peninsula where Alpine rejuvenation relief from the previous Variscan basement is clearly evident. The highest peak of this system is the 1600 m high "La Villuerca".

In the Iberian foreland ranges, these mountains have a relatively simple structure: a single thrust that raises the hanging-wall block and that, given its length, appears to cross much of the upper crust, defining a thick-skin tectonic style without cover (Fig. 14B). A series of isolated syntectonic alluvial fans (known as

"rañas") appears on the depressed SE limb that merge towards the east. The deformation is very recent (Rodríguez-Vidal and Díaz del Olmo, 1994), which would also explain why it is one of the most spectacular Alpine structures of the centre of the peninsula in satellite images and digital elevation models. In topographical profiles, running in a perpendicular trend to the main thrust, the typical geometry associated with a NW dipping monocline ramp is observed. Although very asymmetric it actually constitutes the watershed of the Guadiana and Tagus river basins.

The associated stresses (Álvarez et al., 2004) show NW–SE horizontal compression, that were able to displace not only N60E reverse faults, but also the N30E faults with more strike–slip component that segment the main thrust. In the northern border of the Badajoz basin, a N–S Cenozoic shortening occurs (Pérez-Estaún et al., 2002). The recent deformation nucleation of these structures appears to have muffled those to the NW such as the Plasencia fault (Capote et al., 1996).

4.4. The Duero Basin structure

Together with the Ebro Basin, to which it is connected, this represents the Pyrenees foreland basin. It also corresponds to the foreland of the N border of the Central System. In its eastern part a series of thick-skinned piggy-back basins appear (Almazán, Ayllón) (De Vicente, 2004). It shows a progressive increase in basement depth and structural complexity from west to east, with more recent Cenozoic sediments also appearing in its eastern area. It is affected by basement thrusting along its borders, except the westernmost one, where Variscan rocks, at the western end of the transpressive zone of the Vilariça-Bragança faults, onlap (Fig. 2). Locally, this system of faults affects Tertiary sediments in the interior of the basin (Antón, 2003). At its southwestern end, the Paleogene basin of Ciudad Rodrigo shows thrusting by the Sierra de Gata pop-up along faults with very similar trends to those appearing both in the Central System and in the Serra da Estrela in Portugal (Vegas, 2004).

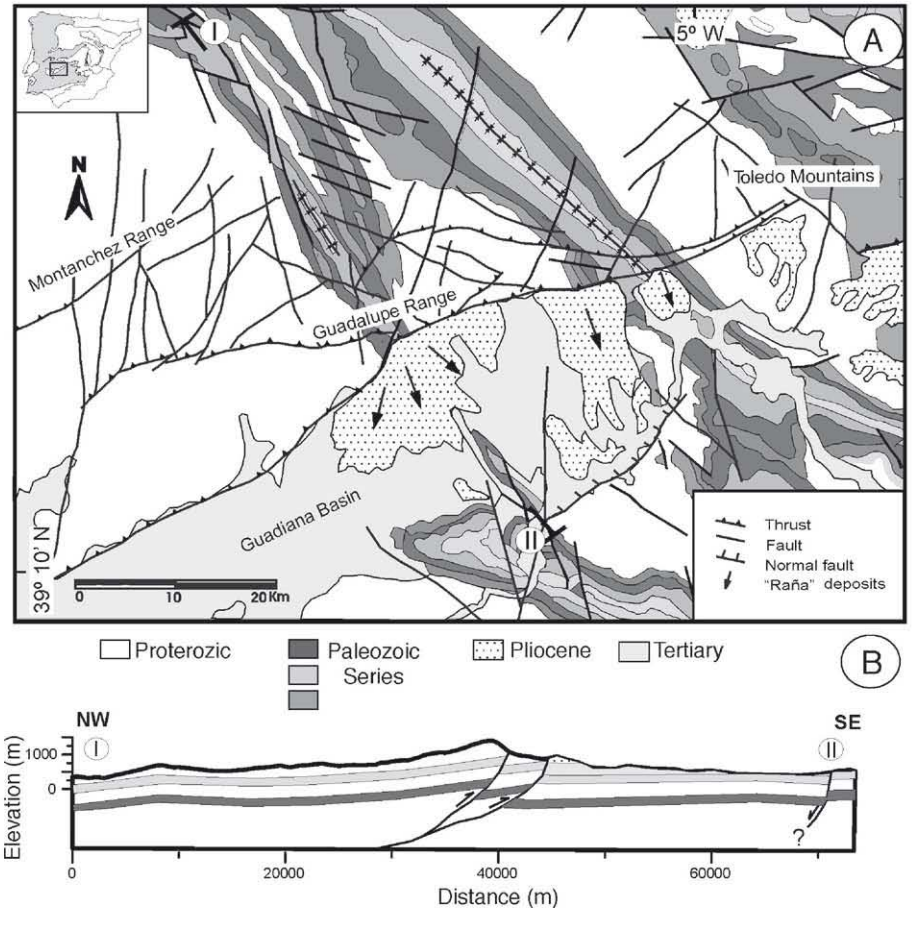

Fig. 14. A) Tectonic map of the Guadalupe ramp. B) Schematic cross section.

Narrow synclines are present in front of the main thrusts to the south of the Cantabrian Mountains and to the north of the Central System (Fig. 15). The latter are aligned with the Diego Alvaro thrust (prolongation of the Northern Border Thrust west of the Plasencia fault) (Figs. 2 and 3), in front of the Santa María la Real de Nieva Massif that extends up to Honrubia-Sepúlveda. It has a pronounced gravity signature (Fig. 5B, D). The largest basin basement depths have their exact location to the north of Honrubia-Sepúlveda, where they reach a depth of more than 2800 m. A structure interference appears in the Palencia highlands. Basement gaps smooth out towards the west (Fig. 15).

At its eastern end, the N edge of the Almazán Basin shows deformations in the basement roof with a similar formation to that appearing on the S edge of the Cameros Unit (Fig. 15), where it links up with the Iberian Chain. The Cenozoic sediments decrease in thickness towards the S, where they are involved in the transpressive limit between the Almazan Basin and the Iberian Chain (Fig. 3) (Bond, 1996).

The origin of these structures is of Paleogene age, as is demonstrated by the disposition of the lacustrine sediments of the Neogene infilling in the Duero Basin (Alonso-Zarza et al., 2004), which overlaps, or is close to, the S edge of the Cameros Unit, the N front of the Honrubia-Sepúlveda imbricate thrusts and the N border of the Castilian Branch of the Iberian Chain.

4.5. The Tagus Basin structure

The Tagus Basin subdivides into a central sector (the Madrid Basin), and an eastern one, to the E of the Altomira Sierra (Loranca or Intermediate basin) (Figs. 2 and 3). In the western area, to the S of Gredos, a narrow E–W sub-basin can also be differentiated (Campo

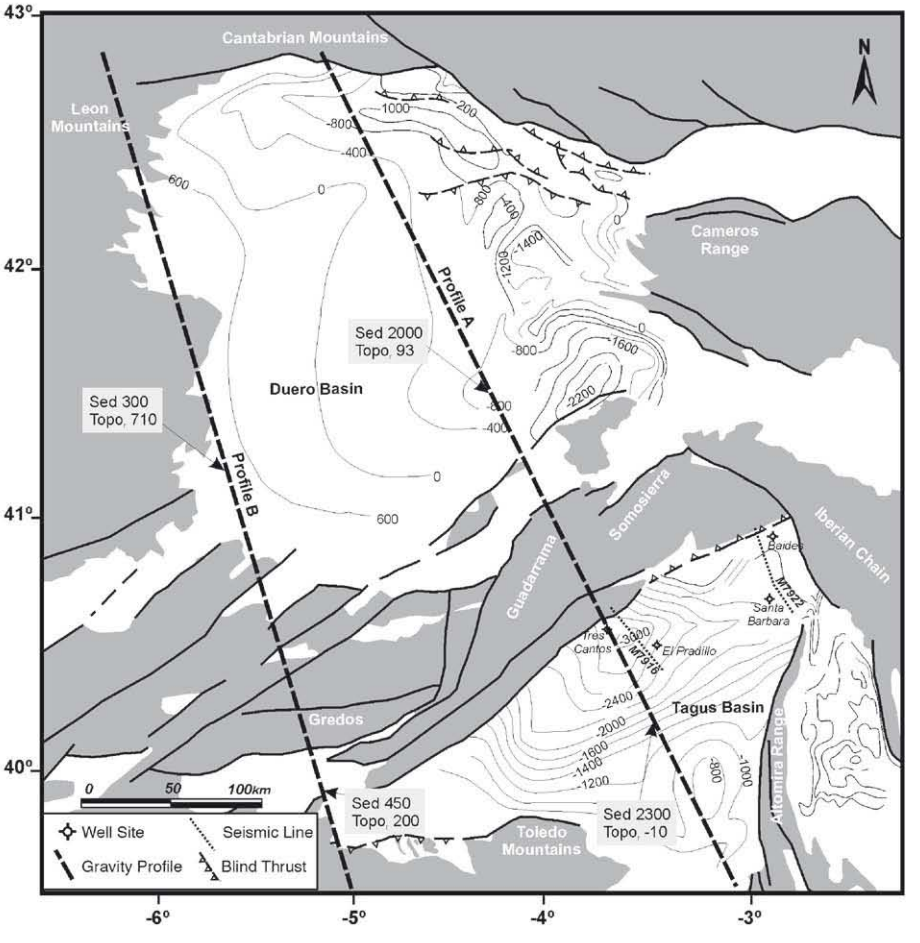

Fig. 15. Isobaths map of the cenozoic infilling of the Duero (N) and Tagus (S) Cenozoic Basins.At 4 locations, Tertairy isobath values and Tertiary sediment thickness (Sed) and have been used to calculate paleo-topography at the end of Cretaceous (Topo). See Section 8 in text for further explanation.

Arañuelo). Towards the S this is connected with the Neogene deposits of the plain of La Mancha (SE corner of Fig. 15), which furthermore appear to be thrusted to the S by the Betic front.

All the limits of the basin show thrusting, with some centripetal directions of tectonic transport: towards the SE and S in the Central System, towards the N in the Toledo Mountains, towards the W in the Altomira Sierra and towards the SW in the Castilian-Valencian Branch of the Iberian Chain.

In general, the basement depth displays narrow synclines adjacent to the chains, the most significant being the one in the eastern sector of the Central System, where Cenozoic infill reaches over 3000 m (Fig. 16). This is most pronounced in the Madrid and Campo Arañuelo areas. The structure of the westernmost sector of the Tagus Basin consists of an E–W pop-down between the S Gredos thrust and that of the N Toledo Mountains, though its present morphological appearance is highly unsymmetrical, with a large topographic step in the western sector. It can be considered as the southern prolongation of the general Gredos structure, though its width is considerably more than that of the rest of the pop-downs situated more to the N (Tietar, Alberche, Amblés). Information on the distribution, thickness and age of the Cenozoic infilling, which is arkosic, is scanty, though a Paleogene age is given. The general E–W structure of this sector appears locally interrupted by others oriented NE–SW: the San Vicente pop-up in the S Central System and the monocline ramps at Lagartera and Almaraz in the Toledo Mountains. The latter two show tectonic transport towards the NW. The S edge thrust of the Central System is interrupted by a series of right-lateral strike slip faults that separate this sector from the Tagus Basin and change the vergence of the thrust. The present drainage of the river Tagus appears to be affected by a SW threshold continuation of the San Vicente pop-up, which shows some neotectonic activity (Tagus river course is forced to erode the basement rocks of the W Toledo Mountains).

The Madrid Basin shows a general increase in basement depth towards the E, though at its centre there is a NE–SW threshold. This can be interpreted as a polyphase "bulge" developed before the Middle Miocene, since the isopachs of this unit show a different infilling geometry. The threshold appears as a continuation of the Toledo Mountains, and, as a whole, forms a subparallel structure to the Central System.

In the NE corner of the basin, the Paleogene sediments have been affected by folding similar to that of the south eastern end of the Central System (the area of the Tamajón imbricated thrusts), which constitute a continuation of structure overlap towards the relative foreland, with

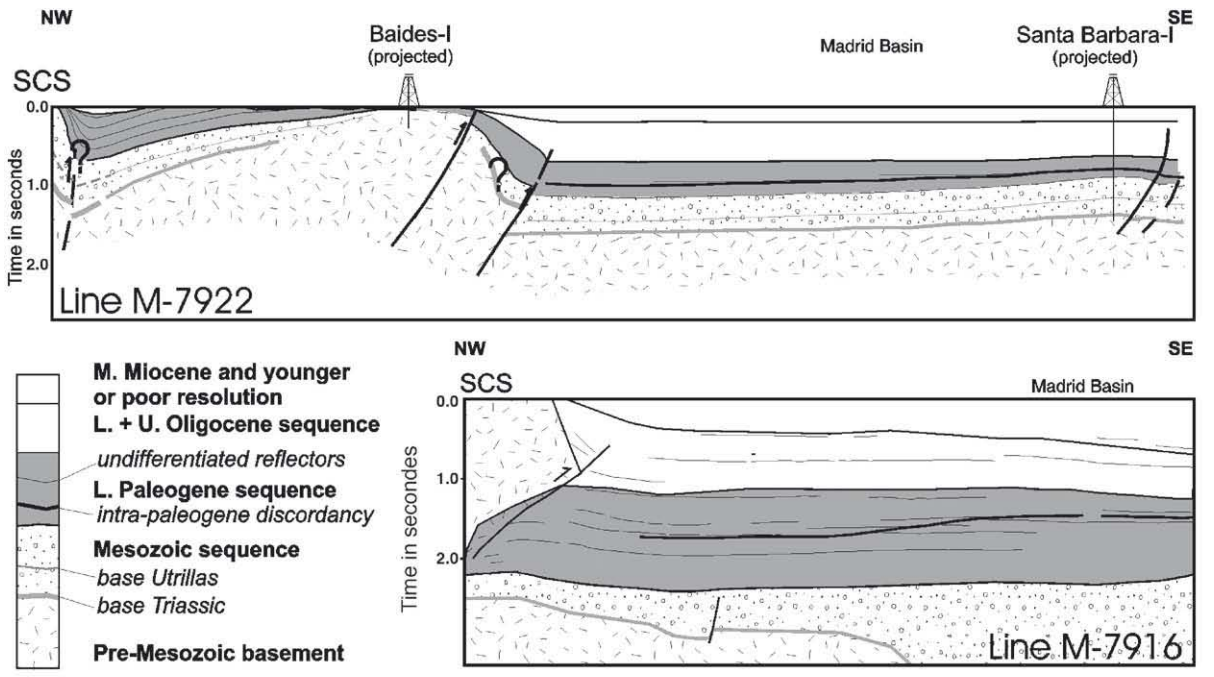

Fig. 16. Interpretation of the two available seismic sections crossing the Southern Thrust and the Northern Tagus Basin (Line M-7922, S Transition zone. Line M-7916, S Eastern area) (After Querol, 1983; Andeweg, 2000).

tectonic transport towards the SE. As a whole, these are rooted in a shallow detachment, inside the Variscan basement (Fig. 8). The western completion of these thrusts constitutes a NW–SE right-lateral shear zone, which shows up very well on the isopach maps.

At present, the Madrid Basin is tilted towards the SW with a 0.5% hanging average along more than 130 km, affecting Upper Miocene lacustrine sediments. The tilting age is therefore Plio-Quaternary.

Paleoseismic structures in Quaternary terraces are abundant in the bulge area (see before). This situation seems to continue to the present day. Seismicity is relatively frequent in the central basin area, and increases towards the E and S.

5. Cenozoic deformation dating

5.1. Sedimentary Cenozoic infilling at the Spanish Central System borders

The nature and assemblage of the different sedimentary sequences at both margins of the Spanish Central System have classically been used to establish the erosive history of the range, as well as the evolution of its relative uplift (Alonso-Zarza et al., 1993, 2004) (see Figs. 25–27 and discussion below for general background).

5.1.1. Paleogene infilling: Duero Basin

In the Duero Basin, Cenozoic sediments typically appear conformable on the underlying Upper Cretaceous materials, at eastern locations. They are unconformable over the Variscan basement in the western segment of the Central System (i.e., Salamanca sandstones Fm). These materials represent the alluvial fan progradation towards the pristine NE trending axial fluvial system of the basin during the Cretaceous–Paleocene (Alonso-Gavilán, 1989, 1996, 2003; Alonso Gavilán and Armenteros, 2004).

In contrast, the northern border of the basin was still undefined at that time, since subtidal environments appear in stratigraphic continuity with the Cretaceous sediments (i.e., the upper part of the Boñar Fm; Corrochano, 1989). Over these Cretaceous sediments, conformable fluvio-lacustrine sediments were deposited (Aparicio et al., 1982). A similar situation is also recorded at the Iberian Chain margin of the basin. In the eastern sector of the Central System, the correlation of evaporitic facies between the Tagus and Duero Basins indicate that at the Cretaceous–Paleogene boundary the Iberian Range had still not been emerged (Alonso-Gavilán and Armenteros, 2004).

There is evidence of activity in the NNE–SSW faults at the western border of the Duero during the Middle Eocene (Rhenanien), which gave rise to elongated thresholds and basins characteristic of strike–slip faults. At this time tectonic activity also began at the northern border of the basin (the Cantabrian Mountains range), marked by the development of basinwards prograding alluvial fan systems. The landscape shows that the southwards propagation of deformation from the southern Cantabrian thrust was very quickly. In contrast, at most eastern locations in the Basque–Cantabrian Basin the prevailing shallow marine environments continued. This is the sector to where basin drainage was directed (eastwards drainage), (Alonso Gavilán and Armenteros, 2004). Within the Central System a lengthened threshold limited by the North-edge fault has been recorded, which may be evidence of the initial left-lateral strike–slip movements preceding the global pop-up deformation of the whole range.

In the Amblés Basin, within the Gredos range (Figs. 3 and 13A), two coarsing upwards sedimentary sequences of Eocene–Middle Oligocene age can be differentiated (Martín-Serrano et al., 1996). Both sequences record the development of prograding alluvial fans, so, the activity of the northern Amblés thrusts seem to have been a later feature.

During the Upper Eocene (Headonien), the activity of the Vilariça fault system increased (western limit of the Duero Basin), since at the western sector of the basin alluvial fans prograded over earlier marly lacustrine facies (Alonso Gavilán and Armenteros, 2004), while at the northwestern edge, alluvial fan facies became more proximal, indicating the southward migration (relative foreland) of the Pyrenean deformation in the Cantabrian Mountain range. The overall flux of sediments within the basin continued towards the NE, where lacustrine sediments had already appeared. In the Central System, the elongated threshold related to the northern border fault disappeared, while north-facing thick alluvial wedges started to develop (e.g. the aforementioned Amblés Basin), giving rise to the generation of an associated relief along the southern Central System border, this being earlier than the emplacement of the northern-edge thrusts in the Central System.

Though not well dated, in the Ciudad Rodrigo and Alba basins (Western Duero Basin), sedimentation during the Oligocene is characterized by the progradation of arkosic fans, supplied by large braided systems oriented to the NE (Corrochano, 1980), which may indicate a propagation of the deformation throughout the Oligocene. On this northern edge of the Central System alluvial fans had more proximal facies than

those deposited during the Eocene, indicating the shifting of the deformation towards the NW, though still not affecting the northern border fault (Alonso Gavilán and Armenteros, 2004). On the north edge of the Duero Basin, deformation shifted towards the east, with an intense activity in the Cameros Unit of the Iberian Chain that had already started during the Eocene.

5.1.2. Paleogene infilling: Tagus Basin

In the Madrid Basin, Amoco, Shell and Teneco Oil companies carried out seismic reflection profiling in the late seventies and early eighties. The seismic lines (Querol, 1989) give a limited resolution with depth, and as a result information on crustal structures is restricted or absent. However, the lines show in detail the sedimentary sequences that filled the basin and their interrelation. Tectonic activity on the edge of the basin can be inferred from the internal architecture in the sedimentary sequence. Two interpreted profiles (Line M-7922 and Line M-7916) that run in a SSE direction through part of the basin from its northern border (Central System) are shown on Fig. 16.

Line M-7922 shows important constraints on episodes of fault activity. With the use of surface information (Fig. 17), growth strata dipping steeply southward can be inferred at the extreme NNW of the line. The southern flank of this growth syncline is characterized by north-dipping Paleogene reflectors. These reflectors run parallel, showing that tilting of this block occurred after the deposition of this sequence.

The Mesozoic sequence shows a significant reduction in thickness towards the Baides well (Figs. 15 and 16) while in the Madrid Basin the Mesozoic sequence is thick and evenly distributed (0.5s TWT). This shows that the zone around Baides was an active high during Mesozoic sedimentation. The superficial S Border Fault interpreted by Querol (1989) could not have behaved like a normal fault, because of the low dip towards the north. Most likely, the interpreted thrust is the near-surface expression of motion along a deeper crustal fault, which might have been a normal fault during earlier stages. This thrust fault is the Southern Border Fault of the Central System in this area, marked by a vertical offset of the basement of about 2.5 km. In the Santa Barbara well an intra-Paleogene unconformity is observed that can be traced northwestwards (Fig. 16).

M-7916 seismic profile runs from the Central System basement just north of Madrid into the Madrid Basin. The Southern Thrust of the Central System can be observed in the extreme NNW of the profile. One of the most interesting features of the profile is a similar intra-Paleogene unconformity (Fig. 16). Upper Paleogene sediments onlap truncated Lower Paleogene sediments, clearly indicating an intra-Paleogene tectonic activity. This unconformity is linked to the Oligocene in the nearby El Pradillo well (Fig. 15). At this location drilling has taken place in Late Oligocene to Lower Miocene deposits to a depth of 1450 m, but to the east (Santa Barbara), this is reduced to around 800 m. Paleogene sediments are lacustrine-evaporitic deposits and represent distal foreland basin sediments and do not have a terrigenous nature. The Upper–Middle Miocene sediments are coarse sediments, indicating a more proximal position to the thrust belt.

The Paleogene succession in the Tagus Basin is composed of lacustrine and marshy deposits. Towards the margins of the basin, and upwards, these facies progressively grade into siliciclastic materials belonging to the main marginal fan systems. Their thickness reaches 2500 m in the zone close to the eastern sector of the Central System (Figs. 15 and 16). There is a lower evaporitic unit of Middle Eocene age and an upper one, locally unconformable (Querol, 1989), of lacustrine carbonates and siliciclastics (Arribas and Arribas, 1991). The evaporitic unit is ca. 800 m thick and is well exposed in the north eastern zone of the Madrid Basin (IGME, 1990 486.). The upper unit is covered by Eocene to Lower Oligocene fan sediments dominated by N–S trending sediment fluxes. Deposits of Eocene to Oligocene age in the Cogolludo–Jadraque–Pinilla area (southern border of the Transition Zone) show growth strata (De Bruijne, 2001) (Fig. 17). Fan architecture and stacking patterns, as well as synsedimentary deformation structures indicate that at least the northeastern part of the Central System has been tectonically active from the Early Paleogene onwards. The first appearance of erosion products in the Central System occurs in Upper Eocene–Lower Oligocene sands containing fragments of schist (up to 5% of the grains) (IGME, 1990). Even Upper Eocene to Oligocene conglomerates contain over 40% of clasts >2 cm of quartzite and schist, which clearly shows provenance from the eastern Central System. While Paleocene to Middle Eocene sand contains up to 15% fragments of dolomitic rocks (IGME, 1990) (erosion of Mesozoic cover), Upper Eocene to Oligocene sand shows deeper erosion into the Central System: 30% dolomite and limestone fragments and 5% schist fragments. Increased tectonic activity of the range is shown by the increasing size of erosion products: the Oligocene sediments consist of a coarsening sequence of up to 660m of mud, sand and conglomerate. The fraction of pebbles larger than 2 cm shows an average of −55% Mesozoic provenance (15–35% limestone, 25–40% dolomites) and −45%

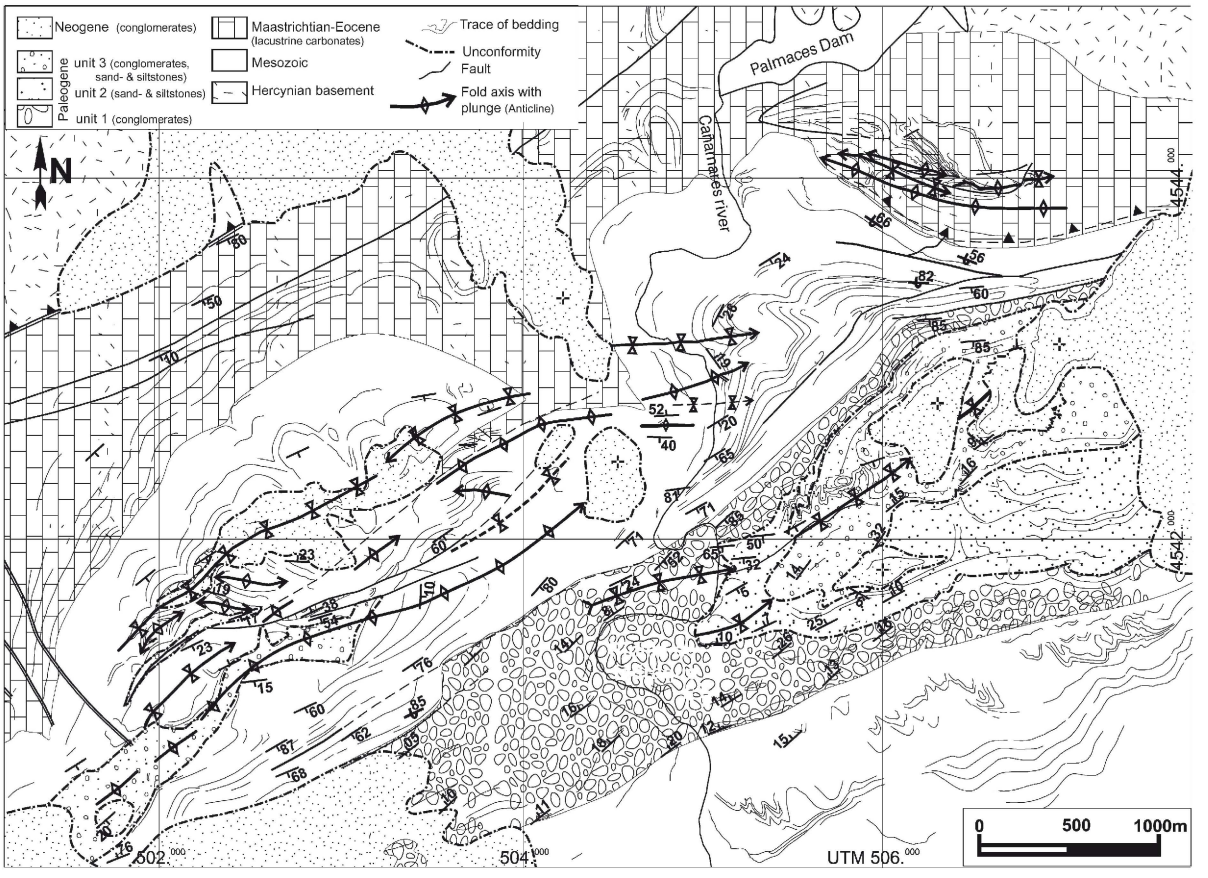

Fig. 17. Detailed geological map of the Pinilla de Jadraque area (S Transition zone. See Fig. 8A for location) showing sintectonic deformation of the Eocene–Oligocene sediments (Andeweg, 1999; De Bruijne, 2001).

basement (35–45% quartzite, 0–7% slate and schist). However, the higher levels have a higher slate and schist content and therefore show ongoing unroofing of the Central System. These sediments are clearly synorogenic.

These alluvial deposits are evidence of the onset of the earliest erosion of metamorphic materials in the Central System from the Lower Oligocene. The whole Paleogene sequence is deformed by similar tectonic structures to those operating at the southern border of the range and the adjacent Iberian Chain.

The Neogene infilling of the Tagus Basin has classically been subdivided into three main megasequences and/or tectosedimentary units: Lower, Intermediate and Upper Miocene Units (Garrido-Megías, 1982; Hoyos et al., 1986), in addition to a complicated set of Pliocene alluvial and fluvial sequences topped by complex red-soils and laminar calcretes predating the basin dissection and inversion (Alonso-Zarza et al., 2004). The Miocene units are composites of marginal siliciclastic wedges (of an arkosic nature at the range margin) grading to evaporitic (lower), carbonatic (upper) and mixed (intermediate) lacustrine deposits which define clear climatic and tectonic trends during this period. Middle Miocene sediments (Intermediate Unit) are unconformable deposited over earlier ones and are marked by relatively low degree of deformation. Nevertheless, the facies are more proximal than those of the Paleogene units, indicating a closer active tectonic edge, which seems to indicate the migration of active deformation towards the relative foreland of the Madrid Basin (De Bruijne, 2001) (Fig. 17). From this point of view, the Miocene Lower Unit seems to be more related to the Paleogene evolution than to the more recent deposits.

Left-lateral activity along the southern edge of the Central System during the Paleogene (De Bruijne, 2001) is suggested by the occurrence of “en echelon” folding and thrusting involving Mesozoic and Paleogene materials. However, thrusts are bent, delineating arched NE–SW to N–S structures. Apparent bending can be related to the presence of oblique ramps: NW–SE right-lateral and N–S left-lateral, though this geometry

invalidates any possible right-lateral displacement (Fig. 12). The reduction of vertical displacement of both structures towards the South, where trending becomes NNE–SSW, seems to indicate a tectonic style more related to broad N60–80E pure thrusting than to transpression. Bent folds affecting Paleogene materials in the NE corner of the basin (South of the Transition Zone) display two main orientations: N60E and E–W, otherwise characteristic of the whole Central System. They present asymmetric synclines and tapered strata with increasing thickness towards the fold-axes, which is evidence of synsedimentary active folding. Three unconformable Upper Eocene–Oligocene units that are weakly affected by Paleogene tectonics have been differentiated in this NE sector of the basin (De Bruijne, 2001). However, increasing upward deformation within this sedimentary sequence gave rise to an angular unconformity that can be traced through the entire Madrid Basin (intrapaleogene sedimentary rupture) (Fig. 16).

This evolution of the Madrid Basin from the Eocene to the Middle Miocene seems to be simplistic, with a mainly aggradational history. During this earlier period, sedimentation was dominated by the development of large alluvial fan systems prograding over large-scale inland lacustrine zones of mostly evaporitic character (salts and gypsums). Only at the end of the Intermediate Miocene Unit did fresh-water carbonate deposition dominate in the central zone of the basin, though it was accompanied by complex diagenetic phenomena of dolomitization and silicification (Cañaveras et al., 2003). In this first scenario, sedimentation was mainly controlled by Central System uplift due to the Pyrenean compressive stress field (Eocene–Oligocene), which was punctuated by intervening deformation and uplift of the Iberian Chain and related thin-skinned Altomira thrusts (that separates the Madrid and Loranca Basins) to the east during the Early Miocene (Capote et al., 1990; De Vicente et al., 1996; Muñoz Martín et al., 1996; Andeweg et al., 1999) and the eventual onset of the NW–SE Betic compression. Thus, from the Lower Miocene Unit, alluvial fan systems became dominant in the Neogene filling of the Madrid Basin as active systems along its borderland zones, but also as controlling sedimentary environments at basin centre locations through continual progradation–retrogadation inputs.

5.1.3. Neogene infilling

At this time, earlier Oligocene uplift of the Central System provided the first extensive (and effective) source area. It produced the development of large drainage basins, necessary for the evolution of the huge arkosic alluvial fan systems, that characterize the Miocene infilling, not only of the Tagus Basin, but also of the Duero (Alonso-Gavilán et al., 2004). Nearly pure evaporitic sedimentation lasted in both basins until the Middle Miocene (i.e. Vallesian), but in the Duero Basin it began to be substituted by carbonate deposition (i.e. Aragonian). In the Madrid Basin, most of the arkosic material originating from the denudation of the Central System was deposited in a growing NE–SW syncline subparallel to the front of the range. This growing syncline nucleated along the lithospheric flexure reactivated by the NW–SE "Betic" compression (Andeweg et al., 1999). In this way, increasing loading by fan deposition triggered the progressive uplift and amplification of the peripheral foreland bulge south of the Central System, which has continued from the Lower–Middle Miocene to the present. Alluvial fan deposition took place also along the Iberian margin of the Tagus Basin (Alonso-Zarza et al., 1993), and included sedimentation at the front of the Altomira thrust range and in the Loranca piggy-back basin (Alonso-Zarza et al., 2004). In the Duero Basin, foreland arkosic fan sedimentation during this period was mainly concentrated on the narrow synclines that developed over the frontal zones of the main thrust faults of the northern border of the Central System (Armenteros et al., 2004), and only clayey distal fan facies surpass these intervening tectonic reliefs (e.g.. the Sta. María de Nieva massif). Markedly, sedimentation in the Duero Basin shifted to the east while in the Tagus Basin it became more extensive.

In the Madrid Basin the transition between the Middle and Upper Miocene units is characterized by the development of a widespread erosive and fairly angular unconformity within the basin. In contrast, this sedimentary discontinuity is hardly defined at locations on the basin margins (Alonso-Zarza et al., 2004), which may imply that range activity was not really involved in the event. At the basin centre the unconformable horizon is clearly defined by a relevant paleokarstic surface affecting the carbonate facies (lacustrine deposits) that developed at the top of the Middle Miocene Unit (Cañaveras et al., 1996). This intra-Vallesian paleokarst largely implies the occurrence of a notable lowering of the regional base level, calculated to be between 10 and 35 m for north and south basin locations respectively (Cañaveras et al., 2003). In the transitional zones, ancient lacustrine centres to the western fan systems formed, and pseudokarstic processes (type-piping) substituted typical karstic processes (Pozo et al., 2004). In this sector, some of the cavities generated during this episode now constitute the Late Vallesian

mammalian fossil sites, currently the only remnants of Late Neogene sedimentation in this sector of the basin.

This new geomorphological context can be related to the onset of regional flexure linked to the far-field NW–SE Betic compression (De Vicente et al., 1996; Andeweg et al., 1999; De Bruijne and Andriessen, 2002) or to a general isostatic rebound of all of the area that was affected by shortening in the previous stage. This complex foreland bulging allowed the generation of emergent intrabasinal reliefs subparallel to the Central System, initially nucleated along the limit between the central chemical deposits and marginal fans SW of the city of Madrid. This process led to the initiation of basin inversion since from this period the typical quasi-concentric closed basin scheme was never repeated, and dissection became more and more relevant west of the Jarama–Tagus river valley lines. This relief was later the scene of relevant large-scale collapse structures (e.g.. Los Gozquez-Valle de las Cuevas "Syncline", Capote and Carro, 1968; Vegas et al., 1975) controlling the drainage patterns within the basin (Pérez-Gonzalez et al., 2004).

Collapse structures, together with the so-called intra-Vallesian paleokarstic surface, developed as a consequence of the uplift (up-bending) of evaporitic materials in the Intermediate and Lower Miocene units above the regional base level. From then on, the presence of internal topography within the basin conditioned the subsequent sedimentary environments during the Late Miocene and Pliocene. Thus, sedimentation (Upper Miocene Unit) restarted with the development of extensive fluvial systems, which crossed the entire basin from NE to SW–SSW locations, the so-called "Intra-Miocene Fluvial System" (Capote and Carro, 1968; Cañaveras et al., 1996) (with westward drainage, as opposed to the initial Eocene pattern). Classic intramiocene fluvial facies (red clays with sands and quartzite gravels) come mainly from the extensive denudation of the metamorphic rocks in the NE sector of the Central System (Eastern Sector–Transition Zone) which follow NE–SW paths sculpted during previous paleokarstic crises throughout the eastern sector of the basin. Recently, intramiocene fluvial deposits of an arkosic nature have been identified along the NE–SW collapse structure of Los Gozquez-Valle de las Cuevas (Pérez-Gonzalez et al., 2004; Montes and Silva, in press) in the western sector of the basin. In fact, the karstic collapse of the ancient axis of the foreland bulge of the Central System led to the development of a linear tectonic paleovalley type (Pérez-Gonzalez et al., 2004).

The connection between this early drainage network and a primitive Atlantic drainage system (to the west), or with a pre-existing Mediterranean outlet through the ancient Betic Strait (to the South), is still an open debate (Alonso Zarza, 2004). However, recent data on the Portuguese outlet of the Tagus (Proença-Cunha et al., 2004) does not suggest any Atlantic paleo-drainage line before the Pliocene s.s. Whatever the case, Upper Miocene sedimentation continued with fluvio-lacustrine and palustrine environments. This was extensive in the eastern and southern sectors of the basin, where freshwater carbonates, clays and sands filled and levelled the previous topography, giving rise to the "Páramo limestone" Fm. (Alonso-Zarza et al., 2004). But these facies were not deposited in the western sector of the basin beyond the foreland bulge, where dissection by collapse structures persisted (Pérez-Gonzalez et al., 2004). In fact, this sector of the basin has been subject to dissection up till present day, and is characterized by the presence of Plio-Pleistocene piedmont ramps of an arkosic nature adjacent to the Central System, and relics of structural relief showing evidence of the ancient collapse structure (Pérez-Gonzalez et al., 2004).

5.1.4. Recent sedimentary-erosion evolution

During the Pliocene s.s. AFT data (see below) indicate that accelerated uplift occurred in the Central System (De Bruijne and Andriessen, 2002), while within the basin deformation continued, generating large-scale gentle surface folding into the "Paramo surface s.l." (Top of the Upper Miocene Unit). NW–SE shortening-related strike–slip faults clearly cut this unit (Giner, 1996). Deformation took place in response to the amplification and eastward propagation of the initial forebulge, which also facilitated the occurrence of repeated karstic processes at the deformed surface. Strike–slip faults appear at the E border of the basin, restricting the bulge-related deformation which is not reproduced in the Iberian Chain. In this scenario the NE–SW Tagus and Tajuña synclines developed during the Lower Pliocene (Fernández and Garzón-Heydth, 1994; Andeweg et al., 1999), related to NE–SW normal faulting that has been interpreted as a lateral extension of the bulge (Giner, 1996). Along these structures a new subsequent fluvial system developed, burying once more the paleokarst generated on the "Paramo surface s.s.". Incision was limited and most of the gently folded "Paramo surface" was subject to repetitive and intensive calcrete development, which also covered the Pliocene fluvial deposits in some eastern and southern locations (Pérez-González, 1982; Sanz, 1996). In central basin locations (e.g. at the junction of the Jarama–Tajo–Tajuña river valleys) Early Quaternary fluvial deposits overlapped the Pliocene deposits giving rise to considerable thickening of the

fluvial series. Fluvial thickening occurred here as a complex feedback process in which deep-seated karstic subsidence, collapse, and repeated tectonic faulting generated a wide range of deformational structures, including sand dikes in the uppermost fluvial terraces (see before), which clearly indicate paleoseismic events (Silva et al., 2003; Giner et al., 1994). At the basin margins Pliocene and Early Pleistocene sedimentation is characterized by the deposition of coarse-grained alluvial fan systems along the northern and southern (Toledo Mountains.) borders of the basin. These alluvial formations (rañas), which are fed by metamorphics, formed extensive alluvial platforms (Pérez-González, 1982; Pérez-González and Gallardo, 1987) in the piedmont zone of Somosierra. To the SW (Guadarrama) the gravel formations of the "rañas" were substituted by extensive arkosic piedmonts, fed by granites, such as the ramps of Madrid, Griñon-Las Rozas and Navalcarnero (Vaudour, 1979; Silva, 1988). Finally, at the southern end of Gredos, large subsequent rivers (e.g. the Alberche and Tietar) developed subparallel to the southern border of the range, which dissected the western sector of the basin. These alluvial piedmonts were connected with, and fed by, the axial fluvial lines at basin centre locations nucleated around the main fluvial axis (Henares–Jarama–Tagus). This was also subparallel to the Central System and was captured by the primitive Atlantic drainage system (Martín Serrano, 1991).

This situation continued up to around the Late–Middle Pleistocene boundary, and eventually came to an end following a major collapse event at the centre of the basin, which led to the incision of all the fluvial valleys and the generation of lineal marginal cliffs up to 60–80 m high (Silva et al., 1988a). In all cases, these valley cliffs are carved on evaporitic (mainly gypsums) Miocene facies and it is common to observe strata bending, collapse and faulting. This event, probably caused by uplift and amplification of the Central System "foreland bulge", promoted river valley underfit (i.e. deep vertical incision and capture) due to the competitive development of the rivers within the uplifted intrabasinal sectors (Lazaro-Ochaitia and Asensio-Amor, 1980; Silva et al., 1988a,b, 1999). The most significant example is that of the Manzanares river valley (south of the city of Madrid) which was captured by the Jarama Valley, leaving its ancient valley (the Prados–Guaten Depression) abandoned at the centre of the basin since the Middle Pleistocene (Silva et al., 1988b, 1999, Silva, 2003). During this period, fluvial capture processes were also important along the southern border of the Central System, related to fault activity (Vidal Box, 1944). The evolution of Middle Pleistocene to Holocene valleys within the basin was determined by the generation of overlapped fluvial terraces at its centre, where thickened fluvial deposits, some more than 20 m thick, are found in the linear valleys of the Jarama, Manzanares, Tajuña and Tagus. This shows a variety of soft-sediment deformation structures that are similar to those observed in the upper terrace levels and are once more interpreted as paleoseimites (Silva, 1988; Giner et al., 1996; Silva et al., 1997, 2003; Silva, 2003). In contrast, fluvial terraces developed on the marginal Miocene and/or Pliocene detritic facies have the typical staircased arrangement of repeated strath terraces. This data suggests that terrace thickening, lineal valley development, and in general all the neotectonic features reported for the Madrid Basin originated as a response to the eastward propagation of the polyphase forebulge of the Central System, locally amplified by the collapse of evaporitic materials.

Paleoseismic structures in Quaternary terraces are abundant in the "bulge" area. This situation seems to continue up to the present day. Instrumentally registered seismicity is relatively frequent (see before).

The Late Miocene to Pliocene evolution of the Duero Basin is not as well documented as the Tagus Basin, but similar Middle lacustrine and Upper fluvio-lacustrine Miocene units also developed in this basin (Armenteros et a1., 2004). However, the basin infilling does not record relevant unconformities or paleokarstic surfaces and its recent evolution seems to be more simplistic and with less neotectonic activity. Sedimentation from the Vallesian (Late Miocene) is concentrated in the easternmost sector of the basin (Somosierra) overlapping the Northern Border Thrust (Sepúlveda area), while that of the western sector remains obscure. Some authors (Mediavilla et al., 1996) relate the fluvio-lacustrine Upper Miocene Unit with the initial stages of dissection within the basin 10 to 5 Ma ago. At the same time, "raña-type" piedmonts from the Pliocene s.l. are also abundant in the western sector of the basin (Molina and Armenteros, 1986; Martín Serrano, 1991), but further fluvial development and dissection has clearly taken place. In relation to the Northern Thrust west of the Plasencia Fault (Figs. 2 and 3) and the Honrubia–Sepulveda area only limited processes of fluvial piracy and active gorging occurred (Fernández and Garzón-Heydth, 1994). As Atlantic drainage seems to have started earlier in the Duero Basin than in the Tagus Basin (Antón, 2003), the result of this different erosive pattern is that almost all rivers in the Variscan basement of the Central System drain towards the S (Tagus). The explanation for this must be either a very different distribution of external climate-erosive processes or more intense recent tectonic activity in the S.

5.2. Apatite Fission Track (AFT) analysis

Spontaneous fission of ^{238}U creates damaged zones in the crystal lattice (Fleischer et al., 1975) of apatite with an initial length of 15.9 to 16.5 μm (e.g. Green et al., 1985). The resultant fission tracks are shortened in a process called annealing (e.g. Naeser, 1979) at a rate dependent on the ambient temperature, the composition of the apatite and to a lesser extent on time. At temperatures of −110 to 120 °C, tracks anneal completely over geological time. In the temperature range −110 to 60 (+−10) °C, referred to as the partial annealing zone (PAZ; Wagner et al., 1979; Gleadow and Fitzgerald, 1987), track lengths are shortened and, as a result, fission track ages are reduced. Fast cooling through the PAZ results in a narrow track length distribution with a mean track length >=14 μm (Gleadow et al., 1986). A broad track length distribution with a mean track length <14 μm is indicative of a slow or complex cooling history. The thermal history of a sample can be modelled using an optimisation procedure that uses a "genetic algorithm" (Gallagher and Sambridge, 1994), with the fission track age and length distribution as constraints.

Applications of fission track analysis in different geological settings have been summarized, for example, by Brown et al. (1994) and Gallagher et al. (1998). Here we use AFT analysis to elucidate the denudation history and behaviour of the different tectonic blocks in the Central System, where mean confined track lengths are all <14 μm and broad and complex track length distributions are common. Therefore, the AFT ages alone do not represent the timing of exhumation accompanying rock uplift that led to the formation of the Central System. Rather, they record a thermal history, indicative of residence at temperatures within the apatite PAZ, alternating with periods of abrupt acceleration in the cooling rate. These accelerated cooling events indicate a sudden change in denudation and/or tectonic activity. Simultaneous accelerated cooling events across the entire region reveal periods of tectonic activity or dramatic changes in drainage-organisation or climate. Application of the "accelerated cooling" approach, obtained from thermal modelling of distinct track length distributions and AFT age data along with geological information on some of the samples, allows the timing and magnitude of denudation of the area to be established.

The obtained AFT ages of the Variscan basement rocks are all younger than the crystallisation age of the granitoids. AFT ages range from 214+−28 to 10.6+−1.5 Ma, with mean track lengths between 10.6 um to 13.9 μm. In the entire data set, there is only one sample with a mean track length above 14 μm, indicative of a single fast cooling event through PAZ. All sampled sediments yield AFT ages younger than or similar to their stratigraphic age with a low mean track length, indicating a thermal overprint after deposition. There is no simple relation between mean track length and AFT age, just as there is no general correlation between elevation and AFT age. The lack of a straightforward correlation is not unique and may be the result of multiple denudation events as discussed in detail by Fitzgerald and Stump (1997). However, the complete lack of any correlation in the Central System between age, length and elevation, suggests differential movement and denudation of individual tectonic blocks.

To obtain information on the denudation history of the range, three profiles with an elevation difference of 1020 to 1980 m were sampled (De Bruijne and Andrieessen, 2002) (Fig. 18). The advantage of the "elevation-profile approach" is that it allows tighter constraints to be placed on the timing of onset and rate of exhumation. However, to be able to date tectonic or denudational events, the rack column that moves through the PAZ during a single event has to be sufficient to uplift and/or freeze at least an entire PAZ. Another requirement is that a profile has to be sampled in a single tectonic unit. Unfortunately, this was probably not the case in the sampling of the Central System.

Two of the three analysed elevation profiles show considerable disturbance (De Bruijne and Andriessen, 2002) because discrete denudation events were too small to expose or freeze an entire PAZ, in order to reveal its age or deduce proper denudation rates. In any case, uplift of the southern Gredos pop-up amounts to more than the present day elevation difference, indicating that the vertical movement along the southern border thrusts would amount to about 2.6 km. The age of this uplift must be younger than 20 Ma (the youngest apparent AFT), as evidenced by the mean track length of the youngest samples which reveals residence within the PAZ before being uplifted. Therefore, the age of the rock uplift cannot be determined from these elevation profiles, because the magnitude of denudation was not enough to expose rocks that could date the vertical movements of the tectonic units, i.e. rocks from below the partially exhumed paleo-PAZ. To reveal the age of this uplift and the apparent complex cooling history involved, modelling of AFT data from individual samples is the best approach.

Modelling thermal histories from AFT data and interpreting the results demands a somewhat cautious

approach. A statistically well-fitting modelled history is never unique. Episodes of cooling prior to reheating are not well recorded by fission track data for those temperatures lying below the maximum temperature of the reheating event. This is because the fission tracks formed during the period of cooling are partially or totally annealed during the reheating period. As a consequence, no distinction can be made between residence at a certain temperature and cooling followed by reheating, when modelling a thermal history, except when geological information is available.

Modelled thermal histories from AFT data results of single samples might vary considerably within one area and therefore differ from the elevation-profile approach which is usually confined to a discrete tectonic block. To prevent over-interpretation of the modelling results and to discern regional trends, modelled accelerated cooling events were grouped by time, since they are indicative of a sudden change in denudation and/or tectonic activity. In order to distinguish between slow cooling and periods of accelerated cooling, a boundary was arbitrarily placed at 2 °C Ma $^{-1}$. Although this is not an especially rapid cooling rate, the emphasis here is on the sudden acceleration of the cooling ratio. Possibly, in other study areas, this boundary should be assigned to a different ratio. Cooling rates of the modelled accelerated

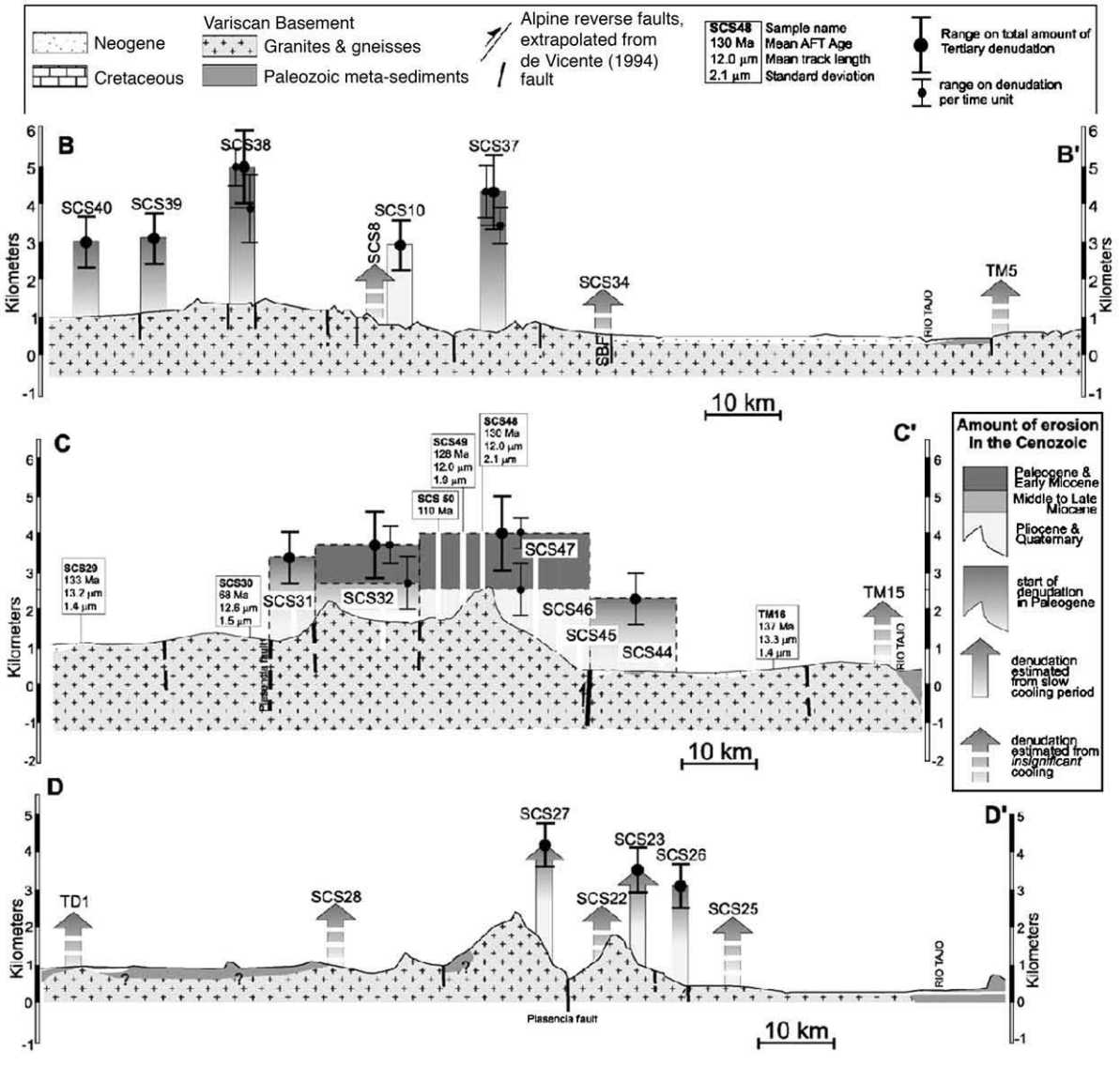

Fig. 18. Denudation profiles across the Central System (De Bruijne and Andriessen, 2002) B) Guadarrama (Eastern area) C) and D) Gredos (Western area).

cooling events range from 2 to 59 °C Ma $^{-1}$, with an average of 16 °C Ma $^{-1}$ and an estimated error of about 20%. In the Central System most accelerated cooling events can be grouped in four periods (De Bruijne and Andriessen, 2002):

1. Middle to early Late Eocene 43±7 Ma
2. Early to early Late Oligocene 30±4 Ma
3. Early Miocene 19±3 Ma
4. Late Miocene to present day 5±5 Ma

This last very recent cooling event is revealed by all samples from the Eastern Sector, except the northern and southernmost ones. Most of this cooling occurs in the Pliocene to the present day. In the Western Sector, only the two lowermost samples reveal this Pliocene to present day cooling event.

The two youngest samples from the Guadarrama show a Middle Miocene accelerated cooling event before the youngest cooling, something that is also detected along the NE–SW trending Plasencia fault (Figs. 2 and 3). The Southwestern Gredos and San Vicente pop-ups show more or less continuous cooling (0.5–1.3 C Ma $^{-1}$) throughout the Tertiary. The only sample from the western Gredos that reveals accelerated cooling in the Tertiary is the lowermost sample in this area, sampled close to the southern thrust of the Gredos (Fig. 13).

6. Paleostress analysis

Cenozoic Paleostress characteristics in the Central System, deduced from fault populations and brittle microstructures analysis, can be explained by a single tectonic event with NNE (N155E) oriented maximum shortening direction (De Vicente et al., 1996), although westernmost and easternmost parts of the considered area show solutions closer to N–S compression (Rodríguez Pascua and De Vicente, 1998; Elorza et al., 1999) (Fig. 19).

This paleostress field was thought to be Middle Miocene (De Vicente et al., 1996), but taking into

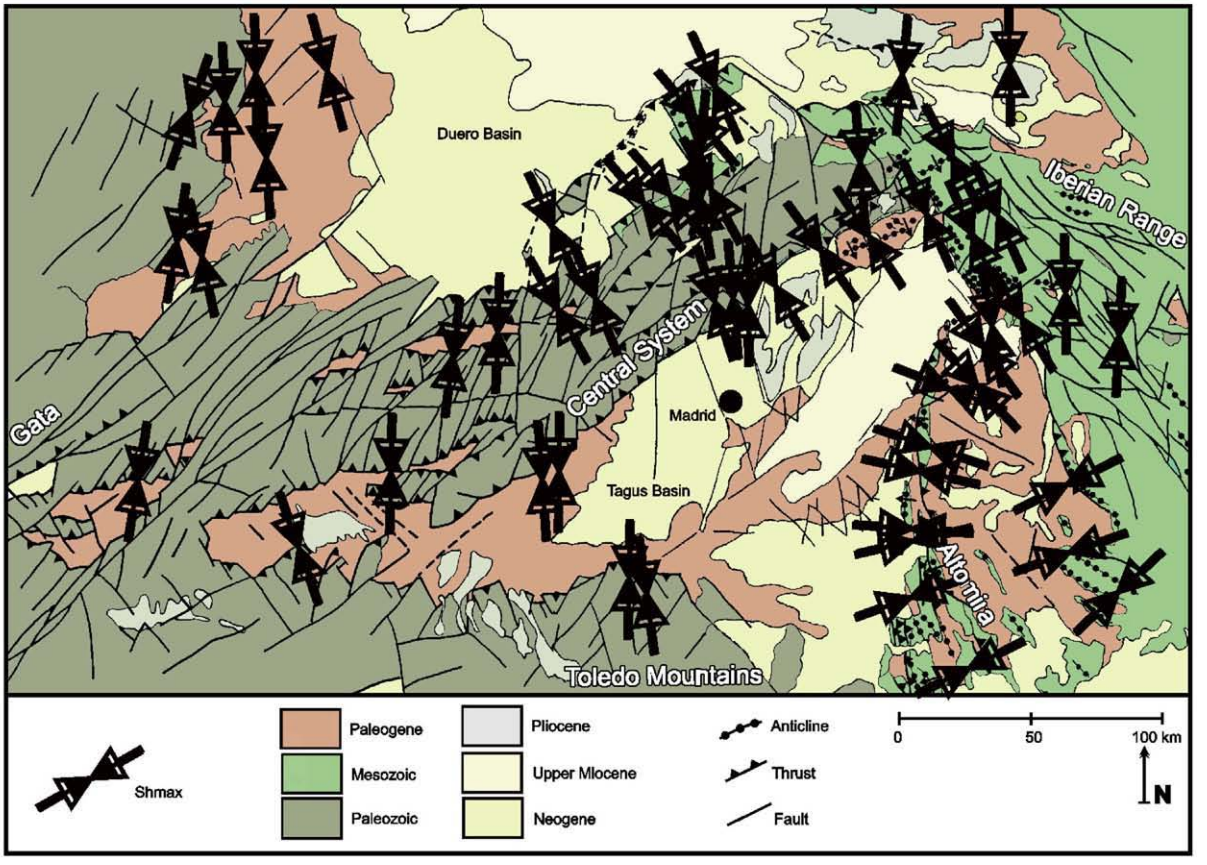

Fig. 19. Principal orientation inversion for Oligocene–Lower Miocene Times in the Central System. Double arrows shows principal horizontal maximum shortening directions (De Vicente et al., 1996; Antón, 2003).

account the new dating of deformation from the previous section, it has become clear that during the Oligocene–Lower Miocene, NE–SW striking thrusts structures of the Central System were also active (Segovia, St ª M ª la Real de Nieva, Honrubia, Sepúlveda, Sierra de la Pela). In a more general frame of far-field paleostress reconstruction during the main Pyrenean collision event throughout central Iberia (Oligocene–Lower Miocene), important curvatures can be deduced in paleostress trajectories (Figs. 19 and 20), since the Altomira Range was thrusting to the W (in this case, with a related E–W compression) (Muñoz Martín et al., 1998). This stress pattern has been interpreted as the result of constrictive conditions related to a neutral stress point situated on the Iberia interior (De Vicente et al., 2005a,b), with Africa–Iberia plates mechanically coupled (Vegas et al., 2005).

Taking into account the stress inversion solutions, the appearance of strain–stress partitioning inidicative for uniaxial compression is evident and is related to pure thrusting and pure strike–slip with the same σ_1 direction, which is also clear on a macrostructural scale (Figs. 2 and 3). This is shown in many cases as intermediate tensorial solutions (Fig. 21), analysed with sample replacement techniques (Reches et al., 1992), which have an interchange tendency between σ_3 and σ_2 (Fig. 21, B, D). These tensors, together with triaxial compression and pure strike–slip solutions with σ_1 orientated NNW–SSE, are the most characteristic of the Central System. Nevertheless, partitioning with normal NNW–SSE faults, related to extensive stresses, also occurs (Fig. 21A).

Constrictive deformation conditions can be also deduced from tensorial paleostress solutions, with horizontal interchanges between σ_1 and σ_2 (Fig. 21C). In this situation, local NE–SW compression can be recorded. These solutions can be attributed to conditions of local deformation (see Fig. 12 for the key area).

These stress trajectory bends are obvious at the SE edge where a large arched structure occurs, indicating tectonic transport towards the SSE (Figs. 3 and 8A). With this configuration, constrictive conditions appear at the intersections between the thrusts and the lateral ramps, giving rise to triaxial compressions that can locally present a NE–SW oriented σ_1 (Fig. 22) (Olaiz et al., 2004).

This does not necessarily imply the interference with an "Iberian" NE–SW paleostress field as has been suggested for the Iberian Chain (Simón-Gómez, 1989). In these more constrictive areas, the deformation in the basement metamorphic rocks is very intense with the development of metric folds (Fig. 12B). At the axis of the arched structures, tensorial solutions are usually close to NE–SW uniaxial extension. This favours the development of small depressions (perpendicular to the main thrusts) where post- or syntectonic alluvial fan apexes are rooted (Fig. 8). The location of these thrusting arched faults is determined by the Variscan

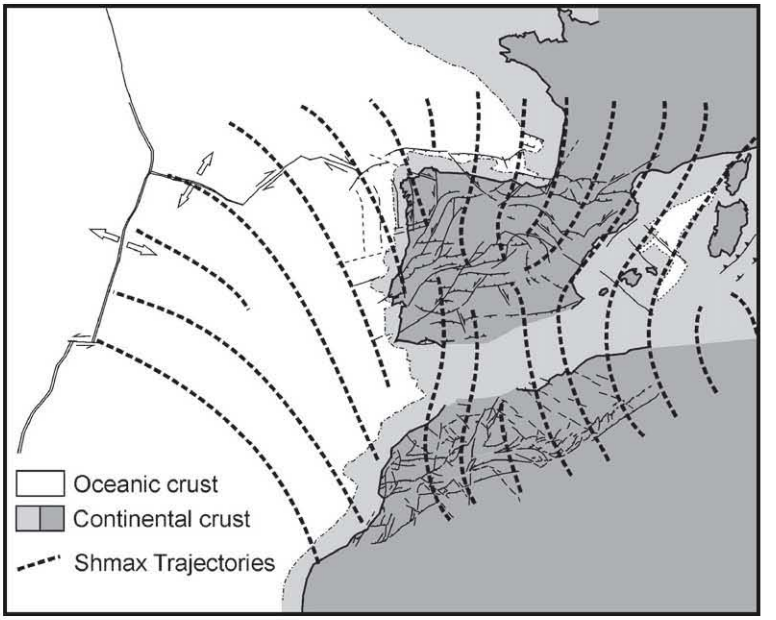

Fig. 20. Plate reconstruction and maximum horizontal shortening trajectories during Oligocene–Lower Miocene. Iberia is mechanically coupled to Africa. A neutral point of stresses appears on Iberia interior (De Vicente et al., 2005a,b; Vegas et al., 2005).

mechanical structure. This way, the presence of granites surrounded by metamorphic rocks in the trace of an important fault produces a structure such as the one described (see Diego Alvaro Thrust in Fig. 3). In these more homogeneous rocks, thrusts usually nucleate at the borders, while in the interior, strike–slip faults and shear stresses develop. This rheology-induced partitioning also occurs in Variscan anticlines, where there are outcrops of Precambrian ortogneisses enclosed by slate materials (Fig. 8). NE–SW and NW–SE extensions are also very common in granites at the hanging wall of main thrusts (Gutiérrez Elorza, 2005). In these situations it is normal to record simultaneous stress tensor solutions in the same station analysis, like those described in Fig. 21A, B.

This last type of uniaxial extension, with NW–SE horizontal σ_3, is mechanically incompatible with NW–SE compression. It can be interpreted as a lateral extension in of the NE–SW compressive structures. This situation is clear in the Tagus Basin "bulge" today, as described before. Though some authors have proposed left-lateral strike slip movements in the S Central System border during the Paleogene (De Bruijne, 2001), there is no clear record of paleostress during this episode. Though the deformation seems to have begun earlier in the Western Sector in relation to the Pyrenean foreland, the N80E striking thrust that connects the S Gredos edge with the Tietar pop-down shows Pliocene movements (De Bruijne, 2001) (Fig. 13B).

During Upper Miocene–Pliocene "betic" rejuvenation, a more general (with no local bends) NW–SE compression developed. Related paleostress can be deduced from fault populations on Upper Miocene sediments (De Vicente, 1996). This stress field can be directly related to present-day active tectonic stresses. Associated deformation conditions were less constrictive while present day stresses show uniaxial extension that activates mainly strike–slip and normal faults (De Vicente et al., 1996; CSN, 1998; Herraiz et al., 2000).

In any case, there is a risk of oversimplifying the evolution of the tertiary deformations in the Central System by concentrating on thrust orientation and related tectonic transport (Pyrenean E–W, and Betic NE–SW) as mentioned. Constrictive conditions in the stress tensor can be enough to activate thrusts striking in a large span of directions as mentioned above. It is also true for main structures that cut the whole upper crust.

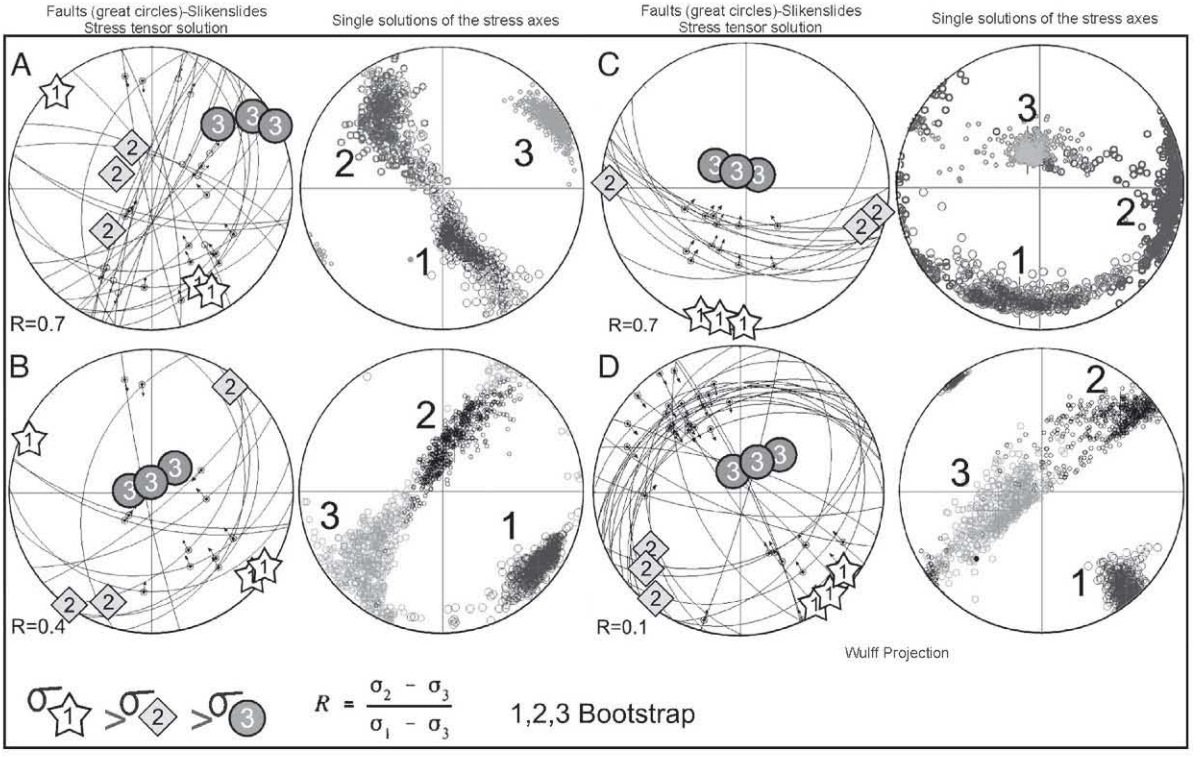

Fig. 21. Tensorial paleostress solutions of the Central System with main stresses interchanges. A) S_1 and S_2 (horizontal to vertical) B) S_3 and S_2 (horizontal to vertical) C) S_1 and S_2 (horizontal, constrictive stress) D) S_2 and S_3 (horizontal to vertical) with R close to 0 (partitioning) (After De Vicente et al., 1996; Elorza et al., 2005).

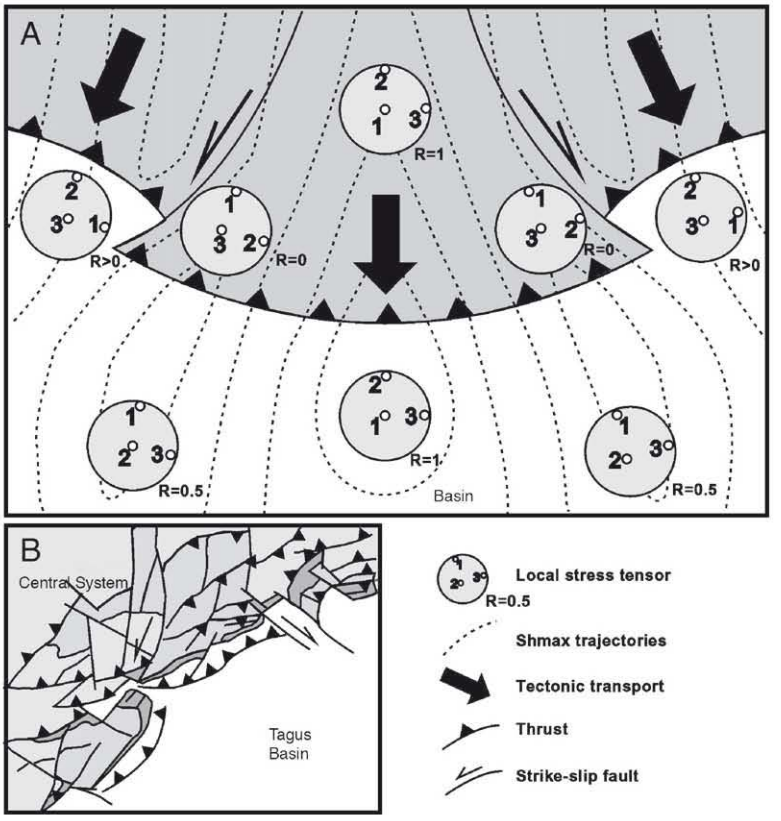

Fig. 22. A) Conceptual model of stress trajectory bends, fitted from field data, at the intersections between main thrusts and lateral ramps giving rise to triaxial compressions. Different "tectonic Phases" are not needed to explain different paleostress solutions. B) Southern Border Thrust between Tamajon area and Somosierra Pass Fault (see Fig. 3). See also Fig. 8 and 12 for detailed structure and paleostress results.

This appears to have been the case in the Central System during most of the Cenozoic.

7. Instrumental seismicity

Between N41.85–38.75 latitude and E2.03–6.82 longitude, that is, the Central System (Somosierra–Guadarrama–Gredos), the S Duero Basin and the entire Tagus Basin, 463 earthquakes have been registered (instrumentally) since 1961. Most of these (442) have been registered since 1986, when there was a notable increase in detectability by the Spanish National Seismic Network. Between 1996 and December 2004, 347 earthquakes occurred (70 during 2004) (Fig. 23).

On the whole, seismicity can be considered as low to medium. The highest measured magnitude was 5.2 (2-10-1961) in the SW of the Duero Basin, and there are frequent earthquakes with a magnitude of around 4. The b parameter of the seismicity has a value of 1.7, while the distribution of the barycentre of Cenozoic faults has a similar fractal dimension Do, 1.63 (De Vicente et al., 2005a,b).

Although the registered magnitudes are relatively low, it should be noticed that seismicity not only has taken place throughout the whole period under consideration, but also there have been small seismic "crises" nucleated on tectonic structures that were active throughout the Cenozoic. Seisms of this type (103 earthquakes) regularly take place in the Tagus Basin "forebulge". The first instrumental record was registered in 1954 (M 4.0) and the most recent one almost coincides with the end of the period under consideration (12-25-2004, M 1.7). Two earthquakes with a magnitude of 4.1 stand out (6-30-1979 and 2-23-1982). Seismic crises with activity that lasts for periods of several days (less than one month) are relatively frequent: there were 10 earthquakes between August 9th and 16th 2001 with a maximum magnitude of 3.6, and 12 earthquakes between April 9th and 25th 2002 including two magnitude 3.2 earthquakes. There were also shorter crises such as the eight earthquakes, the highest with a magnitude of 2.8, that occurred on March 21st 1999. The range of depth is wide, reaching up to 20 km (6-4-1969). There is evident concentration, limited by the

Henares and Tagus rivers valleys, coinciding with the Páramo marl Fm outcrop (Upper Miocene), although the most evident epicentral alignments are located in accordance with NW–SE trends. In the Loranca (or Intermediate) Basin one of these alignments seems to limit the bulge activity toward the east, with relatively large earthquakes at depths of around 15 km. To the N of the Henares river valley a shadow area, reaching the Central System Southern Thrust, can be detected, coinciding with the northern flank of the bulge, which would support the idea of a Plio-Quaternary reactivation of this structure (deformation is concentrated on the hinge) (Andeweg et al., 1996). Paleoseismic evidence is abundant in the Quaternary terraces of the Jarama, Tajuña and Tajo rivers, where injections of sand dikes are observed (Fig. 24) (Giner et al., 1996), indicating important seismic tremors ($M>5.5$). At surface level, and coinciding with the axis of the forebulge, numerous normal NE–SW faults appear, affecting the Upper Miocene materials which may account for the current NE–SW grabens morphology of the area. The related strain has been interpreted as an extension upwards of the non-longitudinal finite deformation surface of the bulge (De Vicente et al., 1996). This idea seems to be confirmed by the calculated focal mechanisms of the area; even though they do not present a high quality in the solution determination, they show the simultaneous presence of pure NE–SW (NW–SE extension) trending normal and reverse (NW–SE compression) mechanisms (Fig. 23).

Between 1984 and 2004 seven epicentres were located along the S border thrust of the Central System, with magnitudes of around 3 and shallower depths than those of the previous structure (9 km maximum, 17-11-1995) and an apparent W–E migration during the registration period. Similar earthquakes have been registered on the S border of Gredos since 2001. Given the size of the fault, which cuts into the whole upper crust, seismic activity is clearly scarce. Paleoseismic evidence is less than in the previous structure, although locally there are tilted Paleocene materials and faulted Pliocene alluvial fans.

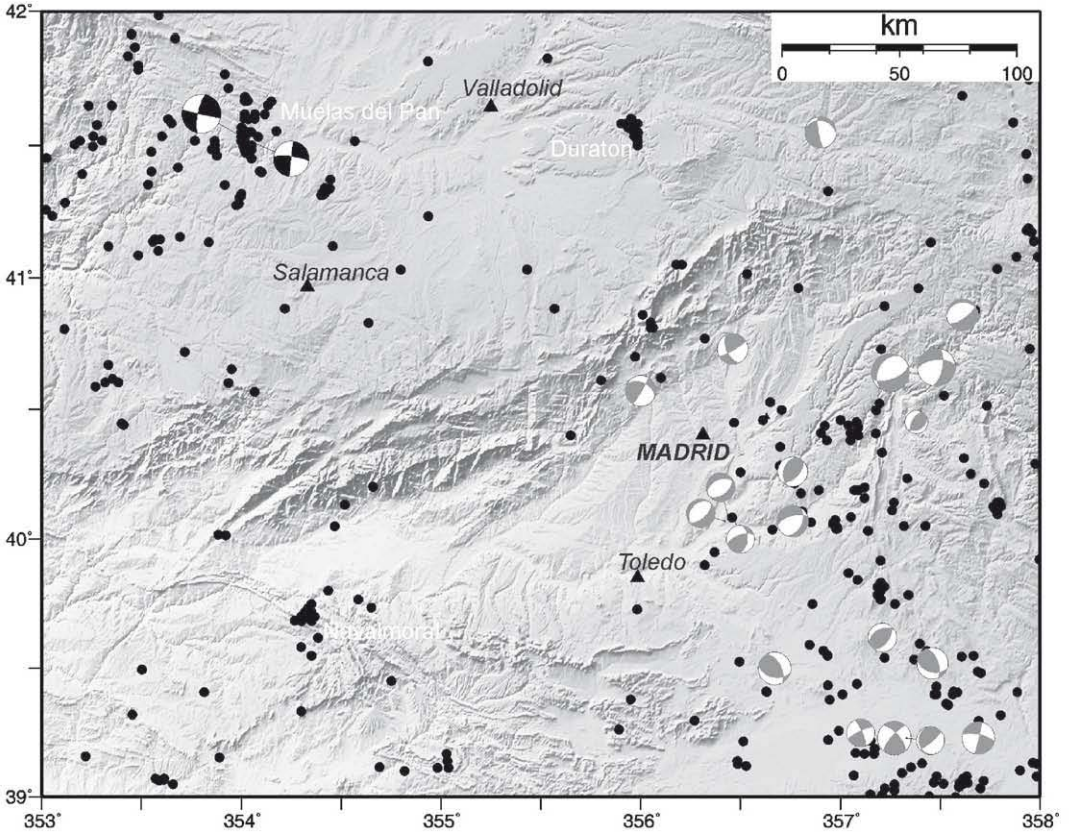

Fig. 23. Distribution of earthquakes (1961–2005) and focal mechanisms in central Iberia. Epicentres data are from I.G.N. (Instituto Geográfico Nacional) catalogue, and focal mechanism are from the Tensor Moment Catalogue (I.G.N. in black), De Vicente et al. (1996), and Rueda and Mezcua (2005). (in gray).

The El Escorial fault system (Fig. 3) presents similar activity, with earthquakes of $M<3$ and depths less than 9 km. The western part of the Lozoya pop-down registered four earthquakes during 1999 (1–12, 4–18, 9–17 and 9–18) with the same order of magnitude as the ones registered in the El Escorial fault system. The N Somosierra border also registered two very shallow earthquakes on 10-13-2000 (M 2.1 and 2.3).

The seismic series of the Duratón River and of Navalmoral de la Mata during 2003–2004 are more interesting. The first series appears to be rooted on the lateral ramp of the Sepúlveda-Honrubia imbricate thrusts system, with a NW–SE trend (although N–S epicentral alignments can also be traced) along the course of the Duratón river. The series consists of 19 earthquakes that began 1-18-2003 and appeared to finish on 6-19-2004. The largest earthquake in the series took place almost at the end, on 1-30-2004 (M 3.3) with a depth of 6 km. The Navalmoral de la Mata series, in the SW structural continuation of the San Vicente pop-up in the Toledo Mountains (Fig. 2), consists of 18 earthquakes between 3-5-2003 and 5-31-2004. Although the magnitudes were relatively low (around 2, the highest being the first one at M 2.2), nucleation was clearly on the Navalmoral monoclyne ramp, with a NE–SW trend, and on the N lateral ramp, oriented NW–SE , that constitutes the limit with the Campo Arañuelo subbasin. The close proximity of some important dams in both areas does not exclude the possibility that these series were induced by a relatively rapid rise in water level in the close reservoirs.

The Guadalupe Ramp (Figs. 2 and 14) mimics the layout of the S border of the Central System, and the same thing seems to happen with the distribution of seismicity. Nine earthquakes have occurred along the thrust, similarly spaced to those located on the S edge of the Central System, the largest with M 3.5 (12-17-1993), and concentrated mainly during 2002, so they precede the Navalmoral series just to the N. In the relative bulge (Vegas Bajas del Guadiana) (Álvarez et al., 2004) earthquakes deeper than those in the main thrust (up to 13 km) have taken place, with magnitudes close to 2.5, one in 1988, another in 2003 and the rest (4) during a small crisis between August and October, 1996.

However, the best example of instrumental seismicity nucleation on a "very" active fault system during the

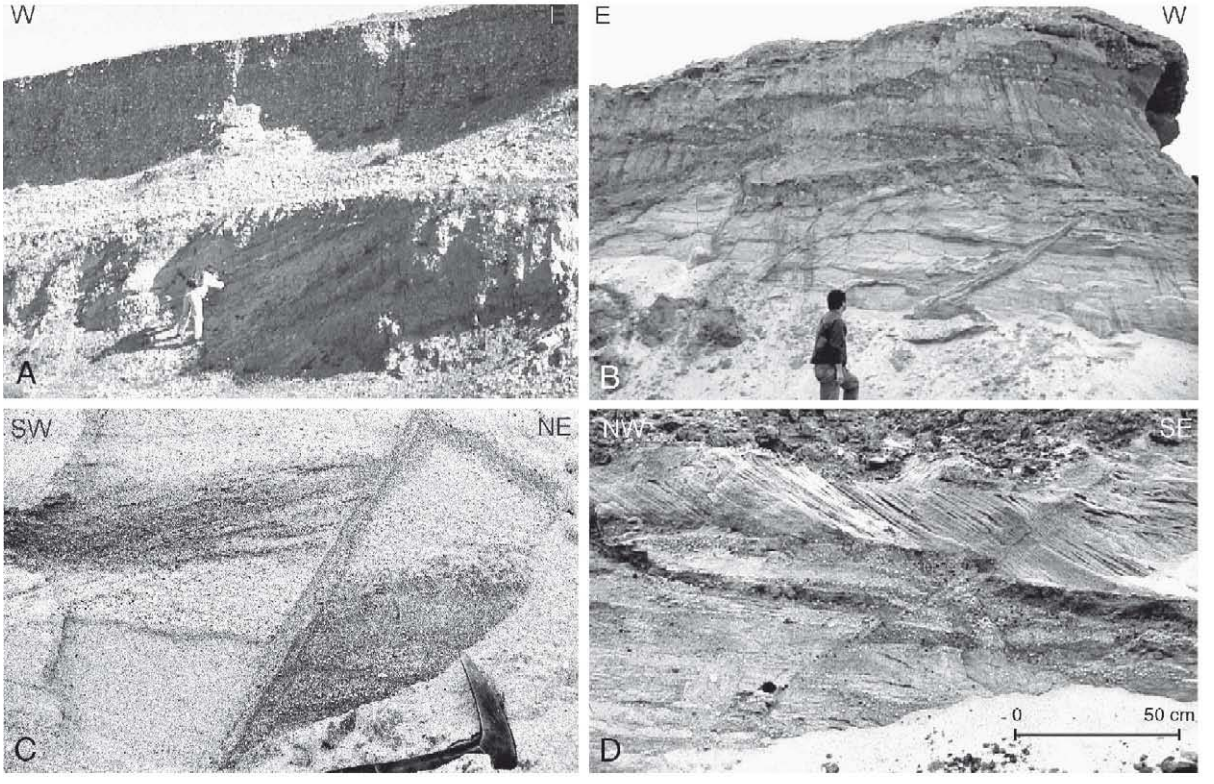

Fig. 24. Paleoseismological evidences in the Madrid Basin. Deformed materials are sandstones of the Jarama river terraces and are Middle Pleistocene in age. A) Enhanced uncomformity of two Jarama River terraces. B) Domino normal faulting and sand dikes. C) Sand dike. D) Reverse faulting.

Cenozoic, is the Muelas del Pan series (Antón, 2003) on the SW border of the Duero Basin (Fig. 23). Although a M 4.5 earthquake was recorded at the beginning of the registry period (12-22-1961) 99 earthquakes have been registered since January 2003 (up to 27-1-2005), four with $M>3.5$ (M 4.3, 1-12-2003, the first of the series; M 3.7, also on 1-12-2003; M 4.4 on 1-23-2003 and M 3.6 on 7-27-2003). The epicentres join at the easternmost end of the Vilariça–Braganza fault system, which has a N10–20E trend, and is considered as active in the Portuguese Neotectonic map (Cabral and Ribeiro, 1990). Seismicity was concentrated between January and March, 2003, on the N15E Muelas del Pan fault, but later on it affected other similar structures, including the Duero fault near the Portuguese frontier, and even reached the borders of the Sierra de Gata.

This fault system allowed the transfer towards the S of the deformation from the western end of the Pyrenees (Cantabrian Mountain range) to the Central System (Vegas et al., 2004) with a strike–slip left-lateral movement. The implementation of the IAG focal mechanism calculation of seismic moment tensor solution from 1997 (Stich et al., 2003), for $M>4$ earthquakes allows the focal mechanism of the largest two earthquakes to be calculated: These are almost pure strike–slip faults with one nodal plane oriented NNE (with left-lateral movement). The neotectonic evidence from the area (Peñausende fault) (Antón, 2003), as well as that from Portugal, leads us to consider the entire Vilariça–Braganza fault system as moderately active within the Duero Basin, from the Atlantic coast as far as the Zamora longitude (N Portuguese–Galician Fault System) (De Vicente and Álvarez, 2005).

To the W of the area described in detail, the continuation of the Central System, the Estrela and Montejunto ranges (Fig. 2) as far as the Atlantic coast, already shows some instrumental seismicity characteristics that are similar to those already analysed. The absence of earthquakes related to the Ponsul thrust (N Moraleja Basin, Mo in Fig. 2), where there is evidence of Quaternary activity should be pointed out. In the Serra da Estrela, seismicity distribution seems to indicate a higher relationship with the Vilariça–Braganza fault system, not with its NE–SE thrust faults. The Montejunto range, however, presents a greater earthquake concentration.

As a conclusion, instrumental seismicity is being nucleated on faults that have moved during the Cenozoic in relation to far-field "betic" stresses. Because of the size of some of those faults, and from paleoseismological evidences, large earthquakes cannot be excluded around the Central System.

8. Discussion and conclusions

8.1. Record of intraplate deformations

In the context of plate convergence, the main cause of shortening in the Central System, one can compare the erosion–sedimentation and apatite fission-track data with the nature of the stress-transmissions from the plate boundary. Precisely for this reason the idea of Iberia as an almost ideal Natural Tectonic Laboratory can be explored (Fig. 20).

During the first stage–from initiation of deformation up to the building of the mountainous range–relatively fast N–S convergence is accommodated in the inherited (Mesozoic or earlier) faults or crustal weakness-zones (Variscan discontinuities) probably by means of limited transcurrent movements with subordinate vertical displacements (Figs. 25 and 28). As the lithospheric coupling between Eurasia and Iberia increases at the plate boundary, strain appears to be more concentrated in the favourable and conspicuous N30–40 and N60 faults delineating the future main blocks of the chain. This stage culminates in the Pyrenean collision and subsequent blocking of convergence at the N plate boundary. As a result of this collision, a reduction in the rate of convergence, as well an intraplate concentration of the deformation, can be predicted (Cloetingh and Burov, 1996). In this context, the deformation is concentrated on the southern part of the Central System, probably due to the existence of a weaker zone in the crust related to the present-day southern main border thrust of the Central System. This "slow" convergence continues until the onset of a new stage of deformation in the Upper Miocene–Pliocene (Figs. 26–28).

During this second stage, the N130 convergence causes the renewal of activity in fault zones that do not exactly coincided with those of the previous stage. The concentration of deformation along these fault zones can be tentatively ascribed to the size of the crustal structures and to a corner effect in the zone of interference between the Iberian Chain and the Central System (Fig. 27).

Cenozoic topography evolution of central Iberia appears to be the result of far-field tectonics. Every single deformation event nucleates on faults inherited from previous stages, producing multiple reactivation–rejuvenation of faults which are also seismically active nowadays.

8.2. Lithospheric folding

The formation of this striking foreland range can be described as the evolution of a *small-radius* lithospheric

fold having a marked effect on both the brittle and ductile parts of the crust (Cloetingh et al., 2002). This lithospheric fold forms part of a wide region that extends from the Pyrenees to the Anti-Atlas of Morocco, and outlines a sort of *soft* interface between the more *rigid* Eurasian and African crusts. Within this intermediate zone, the Tertiary Africa–Eurasia convergence, and hence the crustal, lithospheric shortening, is accommodated by means of: a) inversion of Mesozoic extensional structures, b) basement uplifts or c) a combination of both tectonic processes. The Central System corresponds to type b) and, as stated above, it is a crustal fold that can be considered as a lithospheric fold whose surface expression is a basement uplift (CSN, in press) (However geophysical data has not enough resolution to demonstrate this interpretation) (Fig. 29).

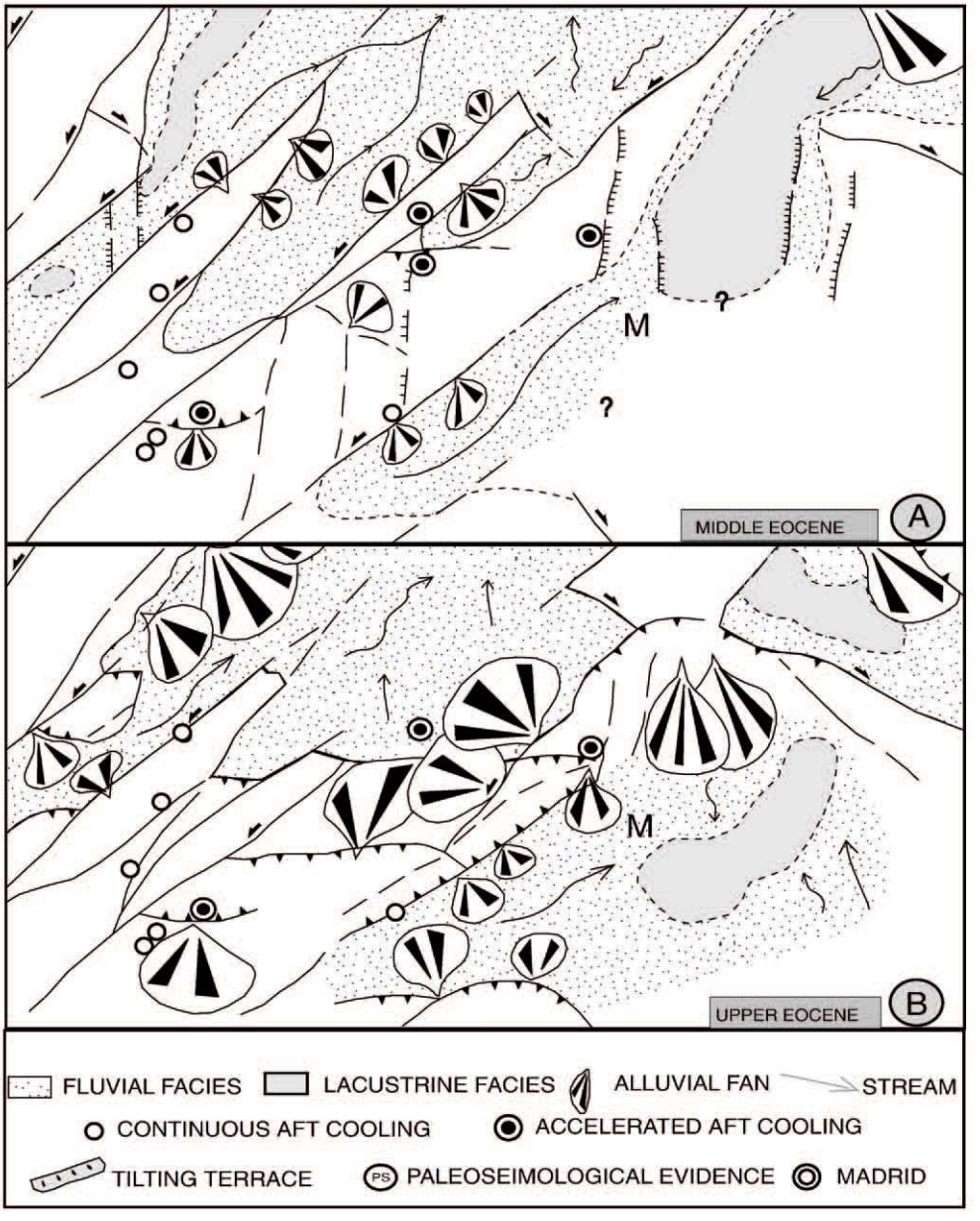

Fig. 25. Tectonic and topographic evolution of the Central System and surrounding Duero and Tagus Basins during the Cenozoic. Note the normal sequence of backthrusts towards the NW (Duero Basin) from the Southern Border Thrust during Upper Eocene–Lower Miocene (see also Fig. 26). Change in drainage pattern (from Easternward to Westernward) occurs during Pliocene to Quaternary times (Fig. 27). A) Middle Eocene. B) Upper Eocene.

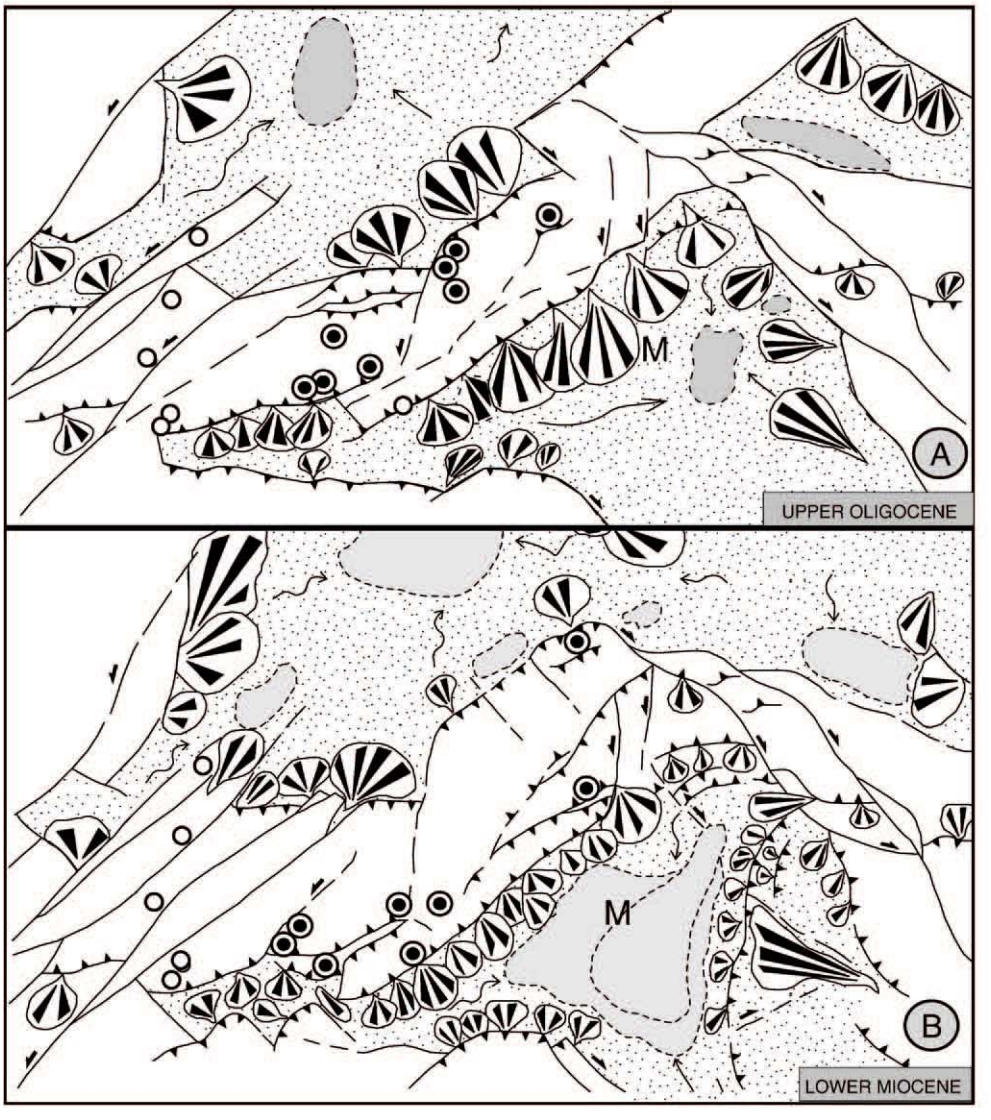

Fig. 26. Legend, see Fig. 25. A) Upper Oligocene. B) Lower Miocene.

If one assumes that the bulk lithosphere deformation is caused by *plane strain*, the Central System can be described as a result of *buckling* of the entire crust. In this perspective, shortening in the brittle upper crust may cause the development of a *crustal-scale thrust*, at one border of the lithospheric anticline, which explains the positive arching of the topography and the accommodation of the upper-crust shortening (e.g. Sokoutis et al., 2005). In contrast, the more ductile lower crust assumes the accommodation of shortening in the center of the crustal anticline in a *pure-shear* manner, perhaps due to a space problem. This can indeed explain the relative thickening of the lower crust and the negative topography of the *moho* (Fig. 5C).

8.3. The history of deformations in the Central System as a guide to the interpretation of the deep chain structure

Although, as previously mentioned, good seismic data showing the deeper structure of the Central System is not available, the integration of gravimetric data (Fig. 7) with patterns of sedimentary filling and the AFT throughout the Cenozoic (Figs. 25–28) shows a clear difference, both in time and space, in accommodation of the deformation between the northern and southern borders of the range. While the thrust fault of the southern border appears to have concentrated the deformation and has been active throughout practically

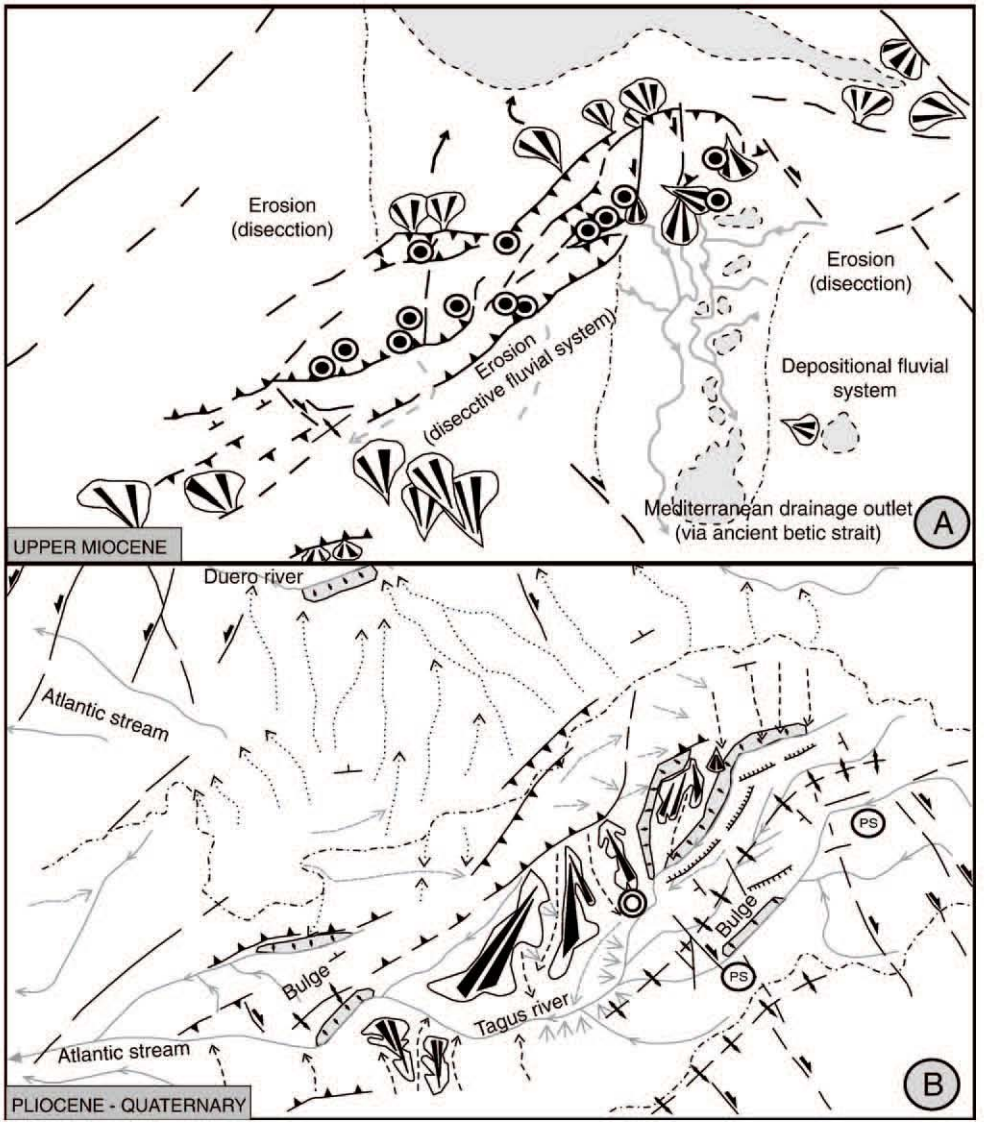

Fig. 27. Legend, see Fig. 25. A) Upper Miocene. B) Pliocene–Quaternary.

all the Cenozoic, the northern deformation appears more dispersed and with a normal sequence of thrusts towards the relative foreland (the Duero Basin) (Figs. 25 and 26).

This model is valid up to the Lower Miocene so we can therefore consider the Central System, together with the Iberian Chain, as the main range of the Pyrenean foreland.

This asymmetry in the deformation is also evident in tectonic cartography (Figs. 2, 3, 8) and structural observations in the field. Along the entire trace of the S thrust, the structure lying immediately to the north is a backthrust. In the eastern and western sectors this pattern is established by the construction of an extensive narrow pop-up, while in the transition zone, where imbricated thrust systems are more common, a number of retrovergent thrusts appear with tectonic transport in the opposite direction to the S thrust (in the Tortuero zone) (Figs. 8 and 11).

8.4. Asymmetry in the Central System crustal structure

At shallow depths the structure of the Central System is clearly marked by asymmetry in uplift. Along the southern border, reverse displacements up to several kilometres magnitude are localized on faults with a high angle dip (>45°). At the northern border, north vergent shallow dipping thrusts are distributed in a wider zone and marked by less vertical displacement to the order of several hundred meters.

SCS
M.B.
PLIOCENE
5.4
MIOCENE
UPPER
MEDIUM
LOWER
16.8
23.2
OLIGOCENE
UPPER
LOW
35.4
EOCENE
UPPER
MEDIUM
LOWER
56.5
R
0 1
0 1
σ1
σ2
σ3
Rejuvenation
Constrictiom
General uplift
Fission track
actvity (%)
10 50 80
0 10
Convergence vel
?
Sea Level
0 200
Dry/
Hot
Wet/
Cold
Climate

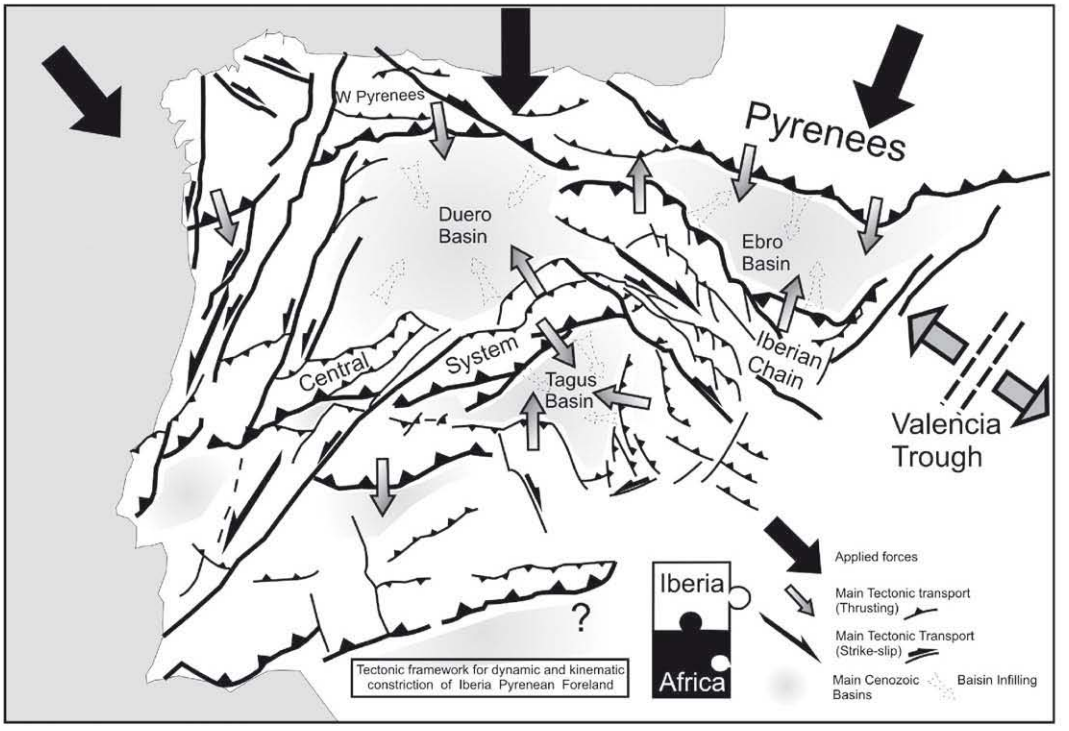

Fig. 29. Tectonic model of the building up of the Iberia Pyrenean foreland Ranges and Basins during Oligocene–Lower Miocene.

This feature corresponds exactly to the concentration of strain at the southern border of the upper-crust primary anticline and to the subsequent main rupture that reaches the Moho (Fig. 5C). Alternatively it may represent the strain localization at a pre-existing main crustal fault. Whatever the origin, the overall configuration of the crust resembles the models described for some *interplate* mountain chains (Fig. 7, Profile A) (e. g. Beaumont et al., 2000). However, the surface asymmetry of the interplate collisional chains, showing the classical distribution of forward- and back-thrusts (e.g. Alps and Pyrenees), is clearly related to the lithospheric subduction at depth. In these mountain belts, geodynamic and analogue models indicate that the asymmetry in surface deformation is caused by the dynamics of lithospheric convergence at greater depth (e.g. Beaumont et al., 2002). In this context the observed convergence at depth can be interpreted as a southward dipping imbricate thrust system below the southern border, resulting in localized "back thrusting" at the southern border fault, and more distributed forward thrusting at the northern side. This model has been adopted in the gravity profiles (Fig. 7).

In this context, the Southern Border results in a structural model that represents a zone of strain localization along which deep "back" thrusts develop, whereas the northern border is made up of shallow "forward" thrusts. It should be remembered that this crustal configuration fits to the large-scale topography of this intraplate mountain chain.

8.5. Paleo-topography evolution

The gravity models show a clear difference between profiles A and B (Fig. 7), in terms of average Moho thickness and the thickness of (mainly Tertiary) sediments bordering the Central System. In the Western profile (B) the average Moho depth is larger than in the Eastern profile (A) (Fig. 7). Comparison of the gravity maps indicate that this transition can be traced and is oriented NNW–SSE parallel to the Variscan macrostructure, corresponding more or less to the border between the

Fig. 28. Tectonic evolution of the Central System during the Cenozoic. From left to right: Sedimentary infilling of the Madrid Basin (SCS: S Central System Border. M.B: Central Madrid Basin). Main sedimentary ruptures are also shown. Age (My). Global stress regime: R value (Normal, Strike–slip, reverse) and principal horizontal axes stress orientations. Fission tracks accelerated cooling episodes (arrows). The curve shows the percentage of samples with clear activity (after De Bruijne and Andriessen, 2002). Convergence velocity (mm/yr) between Iberia–Eurasia up to Middle Miocene and Iberia–Africa since Upper Miocene. Sea level (m). Climate.

western sector (Gredos zone) and eastern-transition sectors (Somosierra–Guadarrama zone) (Fig. 3). The transition is overprinted by the border fault activity, erosion and sedimentation in the Tagus and Duero Basins. Conspicuously, the Tagus and Duero Basins flanking Gredos (profile B) are marked by much shallower infilling of sediments compared to the Tagus and Duero Basins flanking the Guadarrama (profile A). It is tempting to argue that erosion and sediment infilling are fully controlled by varying degrees of border fault activity. However, we will show below that the transition of Tertiary sediment thickness must be largely attributed to significant pre-existing topography (Mesozoic) in the Variscan massif, which plays a key role in the distribution of sediments eroded from the Central System.

There is very little evidence of regional features in the peneplained post-Variscan surface, apart from some "local" irregularities, mainly due to the different resistance of rocks to erosional processes (e.g. Martin Serrano, 2000). Nevertheless, on a *peninsular* scale and prior to the main Tertiary mountain building in the interior of the Iberian Variscan Massif, an area emerging appears to have existed during Mesozoic times between the Atlantic Portuguese margin and the arrested rift that later became the Iberian Chain. The main divide, the culminant "highs", ought to be placed somewhere in this intermediate emerged "Variscan" area. This inherited pre-Tertiary landscape prefigured an ancestral Atlantic drainage that was truncated by the emergence of Tertiary mountains, resulting in tectonic activity along the Vilariça–Bragança fault corridors (Cunha et al., 2000; De Vicente and Álvarez, 2005).

Geological studies show that west of the aforementioned east–west gravity transition, no sedimentation occurred during the Mesozoic, whereas east of this transition the Tagus and Duero Basins and Central System were covered by sediments related to Iberian Chain rifting (Van Wees et al., 1998). As reflected by the westward termination of Upper Cretaceous sediments, which are widely present in the east, the paleotopography was high enough to remain elevated during the Cretaceous sea-level high, rising at least 100 m higher than the lowest Tertiary level. Assuming local isostasy, we can estimate the paleotopography above 100 m from the "residual topography" which accounts for the amount of topography that cannot be explained by local isostasy (c.f. Gaspar-Escribano et al., 2001). The residual topography is calculated from observed Tertiary sediment thickness and observed topography in the Tagus and Duero Basins, assuming that no crustal deformation (thickening) occurred in the Cenozoic basins during deposition (cf. Gaspar-Escribano et al., 2001). In a local isostasy assumption:

$$\mathrm{Topo}_r = h - \mathrm{sed}\frac{\rho_{\mathrm{mantle}} - \rho_{\mathrm{sed}}}{\rho_{\mathrm{mantle}}} \quad (2)$$

Where Topo_r is residual topography, sed is cenozoic sediment thickness, ρ_{sed} is sediment density (2300 kg m^{-3}), ρ_{mantle} is mantle density (3300 kg m^{-3}). Values for residual topography are consistently positive in the western part (Fig. 15), whereas they are close to zero in the east, and would be negative close to the border faults (due to downward flexure (see also Van Wees et al., 1996)).

From the interpretation of positive values of residual topography as Mesozoic paleo-topography it is clear that there is a residual topography of ca 200–300 m in the western part of the Tagus Basin, and higher magnitude paleo-topography, up to 800 m, in the western part of the Duero Basin. The interpreted paleo-topography is consistent with increased regional crustal thickness (excluding sediments) interpreted in the gravity profiles (Fig. 7) measuring up to ca 33 km in the west versus ca 30 km in the east. The existence of this amount of paleo-topography may very well explain the remarkable features of the distribution of eroded sediments through time. During the Early Tertiary, when the Central System was uplifted, sediments were transported from the westward topographic highs to the lows in the east (Figs. 25–27). As the Tagus and Duero Basins became disconnected from the Mediterranean and Atlantic, the eastern parts gradually overfilled causing a levelling of the topography in the western and eastern basins. At a later stage, caused either by more intensive tectonics in the east (most likely), or more intensive drainage in the west (less likely), a reversal of the topography took place, finally giving way to Atlantic drainage of the Tagus and Duero Basins (Fig. 27).

Nevertheless, the roles of inherited Mesozoic topography and the Moho paleodepth controlling the crustal Central System structure are not yet fully understood. As mentioned earlier active crustal thickening is not fully limited to the Central System (especially towards the west) and may influence the results.

8.6. Quaternary and active tectonics

There is abundant evidence of large-scale folding, tilting and widespread faulting within the Miocene, Pliocene and Quaternary deposits filling the Madrid Basin (Fig. 24), but very little in the northern Duero Basin (e.g. Gracia et al., 1991). Miocene to Quaternary tectonics to the south of the Central System are mostly

related to the amplification and propagation of the "forebulge" from the Middle Miocene (i.e. Vallesian, c.a. 10 Ma ago), which implies the occurrence of brittle tectonics along the NE–SW trending forebulge edge. Forebulge initiation triggered surface upwarping on the lacustrine–palustrine paleosurfaces of the Middle and (later) the Upper Miocene units of the Madrid Basin. Large-scale surface upwarping led to the occurrence of: (a) the generation of a intrabasinal paleotopography controlling the Upper Miocene to Pliocene depositional systems (Fig. 27); and (b) the elevation of ground surface and Middle to Middle Miocene evaporite facies above the regional paleo-watertable leading to the occurrence of karstification, multicollapse events and, eventually the generalized dissection of the basin along the surface NE–SW trending faults above the forebulge. This process continued during Pliocene and Quaternary times influencing the pattern of fluvial dissection within the basins. During the Plio-Pleistocene the Central System forebulge reached the most central basin locations, where thicker evaporite facies were deposited, facilitating linear collapse and faulting along both flanks of the forebulge (i.e. present Tajuña Anticline). In fact, the main dissectional fluvial systems of the basin are accommodated north (Henares–Jarama valleys) and south (Tagus valley) of the present anticline and their junction is situated in the presumed periclinal termination of the Tajuña anticline at the southern basin location. Valley subsidence was enhanced by episodic feedback processes of faulting and karstification leading to the occurrence of Plio-Pleistecene and Pleistocene thickening of fluvial sequences of more than 40 m in some places, but also to the general SE shifting of fluvial deposits north of the forebulge axis. Simultaneously, sedimentary input from the Central System became limited to relatively thin piedmont systems: Arkosic ramps (Glacis-type) from the granitic sector of Guadarrama (Vaudour, 1979; Silva, 1988) and large alluvial fans ("Rañas") from the metamorphic sectors of Somosierra and Gredos (Pérez Gonzalez, 1994). These piedmont systems merged distally to the initial fluvial system bordering the northern margin of the forebulge (Henares–Jarama–Tagus edge).

Ongoing Quaternary activity along the forebulge margins is highlighted by the record of normal faulting, backtilting and soft-sediment deformations (some of a paleoseismic nature) within the fluvial archives of the Jarama, Tagus and Manzanares rivers at basin centre locations (Giner et al., 1995, 1996; Silva et al., 1997; Silva, 2003), as well as by the generation of anomalous U-Shaped linear valleys flanked by relevant gypsum escarpments more than 40–60 m high and c.a. 7–10 km length, especially from the Middle Pleistocene (Giner et al., 1996; Silva et al., 2003). Cliff sections of many rivers expose hanged (c.a. +100 to +60 m) fluvial deposits of Late–Middle Pleistocene age. During the Middle Pleistocene the development of gypsum escarpments promoted the reorganization of the intrabasinal valley network, leading to the occurrence of relevant fluvial captures and the formation of large-scale abandoned valleys (Silva et al., 1988a; Pérez Gonzaléz, 1994). It was at this time that the Tajuña river valley (a tributary of the Jarama) eventually developed (Silva et al., 1988b) as a fluvial line dissecting the up-warped axis of the Tajuña Anticline, facilitated by brittle deformation structures which originated along the forebulge edge (in fact, an anticline valley) (Fig. 27). The Holocene situation is similar and nowadays seismicity occurs along the forebulge margins (Fig. 23) supporting the ongoing activity of this structure. However, the southern thrust of the Central System and the Iberian Chain border (East) also displays seismic activity revealing on-going continuous deformation at both basin margins.

This paper emphasizes the utility of intraplate deformation concepts in order to explain the building up of a relatively well-studied mountain chain situated amid a broad intracontinental plate boundary. In this context, the described tectonic features permit a coherent scenario for the recent topographic evolution, as well as for the onset and evolution of the drainage system, in the central part of the Iberian Peninsula. Moreover, the tectonic model here presented represents a contribution to the understanding of the complex landscape that characterize the broad region, comprised between the Pyrenees and the Atlas System, pertinent to the Africa–Europe complex zone of plate interaction.

We consider also that this integration of independent tectonic and geomorphic studies can contribute in a great extent to the knowledge of the recent evolution of other intraplate areas.

Acknowledgements

This work was mainly funded by the PRIOR project (UCM-CSN-ENRESA-IGN) and the HIDROBAP I–II projects (UPM-UCM-CSN-ENRESA). Current funding is provided by "Emanometría y simulación estocástica para sistemas hidrogeológicos complejos" N°C02062502 Project. Juan Álvarez thanks the 'Consejería de Educación de la Comunidad de Madrid y Fondo Social Europeo' for his pre-doctoral grant.

We particularly appreciate the very detailed and elaborate comments of Dr. Vrabec and an anonymous reviewer, which help to focus and enrich the manuscript.

The study was supported by consolider Ingenio 2006 "Topo Iberia" CSD2006-00041 and Spanish National Research Program CGL2006-13926-C02-01-02 "Topo Iberia Foreland".

References

Alonso-Gavilán, G., 1989. Relleno de canales abandonados en la formación Areniscas de Cabrerizos, Eoceno, Salamanca. Geogaceta 6, 58–60.

Alonso-Gavilán, G., Armenteros, I. (coord.), Carballeira, J., Corrochano, A., Huerta, P., Rodríguez, J.M., 2004. Cuenca del Duero. In: Geología de España (J.A. Vera, Ed.), SGE-IGME, Madrid. pp.550–556.

Alonso-Zarza, A.M., Calvo, J.P., Garcia del Cura, M.A., 1993. Palaeogeomorphological controls on the distribution and sedimentary styles of alluvial systems, Neogene of the NE of the Madrid Basin (central Spain). Spec. Publ. Int. Assoc. Sedimentol. 17, 277–292.

Alonso-Zarza, A.M. (coord.), Calvo, J.P., Silva, P.G., Torres, T., 2004. Cuenca del Tajo. In: Geología de España (J.A. Vera, Ed.), SGE-IGME, Madrid. pp 556–561.

Álvarez, J., Muñoz-Martín, A., Carbó, A., De Vicente, G., Llanes, P., 2002. Mapa de anomalías isostáticas residuales de la Peninsula Ibérica. Proc. 3ª Asamblea Hispano-Portuguesa de Geodesia y Geofísica, Valencia, Spain, pp. 221–224.

Álvarez, J., Muñoz-Martín, A., De Vicente, G., Vegas, R., 2004. Reactivación intraplaca de un relieve apalachiano: Las Sierras de Guadalupe y Montánchez. Geotemas 6 (5), 221–225.

Andeweg, B., De Vicente, G., Cloething, S., Giner, J.L., Muñoz Martín, A., 1999. Local stress fields and intraplate deformation of Iberia: variations in spatial and temporal interplay of regional stress sources. Tectonophysics 305, 153–164.

Antón, L., 2003. Análisis de la fracturación en un área granítica intraplaca: El Domo de Tormes. Ph.D.Thesis. Univ. Complutense de Madrid, Spain.

Arribas, J., Arribas, M.E., 1991. Petrographic evidence of different provenance in two alluvial fan sysytems (Palaeogene of the northern Tajo Basin, Spain). Geol. Soc. (Lond.), Sp. Publ. 57, 263–271.

Beaumont, C., Muñoz, J.A., Hamilton, J., Fullsack, P., 2000. Factors controlling the Alpine evolution of the central Pyrenees inferred from a comparison of observations and geodynamical models. J. Geophys. Res. 105 (B4).

Bergamín, J.F., Carbó, A., 1986. Discusión de modelos para la corteza y manto superior en la zona sur del área Centroibérica, basados en anomalías gravimétricas. Estud. Geol. 42, 143–146.

Birot, P., Solé-Sabaris, L., 1954. Recherches morphologiques dans le nord-ouest de la peninsule iberique. Mem. Doc. Centre Rech. et Docum. Cartogr. et Geograph., vol. 4, pp. 7–61.

Bond, J., 1996. Tectono-sedimentary evolution of the Almazan basin, NE Spain. In: Friend, P.F., Dabrio, C.J. (Eds.), Tertiary Basins of Spain, vol. 6. Cambridge Univ. Press, pp. 203–213.

Brown, R.W., Summerfield, M.A., Gleadow, A.J.W., 1994. Apatite fission track analysis: its potential for the estimation of denudation rates and implications of long-term landscape development. In: Kirkby, M.J. (Ed.), Process Models and Theoretical Geomorphology. Wiley, New York, pp. 23–53.

Cabral, J., Ribeiro, A., 1989. Incipient subduction along West-Iberia continental margin. Inter. Geol. Congr., 28, vol. 1, p. 223.

Cabral, J., Ribeiro, A., 1990. Neotectonic studies in Portugal—the neotectonic map. Bull. INQUA Neotectonics Comm. 13, 6–8.

Cañaveras, J.C., Calco, J.P., Hoyos, M., Ordoñez, S., 1996. Paleomorphologic features o fan intra-vallesian paleokarst, Tertiary Madrid Basin: significance of paleokarstic surface in continental basin analysis. In: Friend, P.F., Dabrio, C.J. (Eds.), Tertiary Basin of Spain. Cambridge Univ. Press, pp. 278–284.

Cañaveras, J.C., Sánchez del Moral, S., Ordoñez, S., Calvo, J.P., 2003. Perfiles paleokársticos en el techo de la Unidad Intermedia del Mioceno de la Cuenca de Madrid. Estud. Geol. 67–82.

Capote, R., Carro, C., 1968. Existencia de una red fluvial intramiocena en la Depresión del Tajo. Estud. Geol. 24, 91–95.

Capote, R., De Vicente, G., González-Casado, J.M., 1990. Evolución de las deformaciones alpinas en el sistema central Español. Geogaceta 7, 20–21.

Capote, R., Villamar, P., Tsige, M., 1996. La tectónica alpina de la Falla de Alentejo-Plasencia (Macizo Hespérico). Geogaceta 20 (4), 921–924.

Cloetingh, S., Burov, B.E., 1996. Thermomechanical structure of European continental lithosphere. Tectonophysics 136, 27–63.

Cloetingh, S., Burov, E., Beekman, F., Andeweg, B., Andriessen, P.A.M., Garcia-Castellanos, D., De Vicente, G., Vegas, R., 2002. Lithospheric folding in Iberia. Tectonics 21 (5), 1041–1067.

Corrochano, A., 1980. Los sistemas de abanicos aluviales del Paleógeno de Zamora. Temas Geol.-Min. 6, 802–804.

Corrochano, A., 1989. Facies del Cretácico terminal y arquitectura secuencial de los abanicos terciarios del norte de la depresión del Duero. Studia Geológica Salamanticensia, Volumen Especial 5. Univ. De Salamanca, pp. 89–106.

CSN, 1998. Proyecto SIGMA: Análisis del estado de esfuerzos tectónicos reciente y actual en la Península Ibérica. Consejo de Seguridad Nuclear. Colección Otros Documentos, Madrid, Spain.

CSN, in press. Proyecto PRIOR: Análisis de Fallas de Primer Orden. Consejo de Seguridad Nuclear. Colección Otros Documentos. Madrid, Spain.

De Bruijne, C.H., 2001. Denudation, intraplate tectonics and far fields effects in central Spain. Ph.D Thesis , Free University. Amsterdam, The Netherlands.

De Vicente, G., (ed.) 2004. Estructura alpine del Antepaís Ibérico. In: Geología de España (J.A. Vera, Ed.), SGE-IGME, Madrid, pp.587–634.

De Vicente, G., Álvarez, J., 2005. Rheological constraints on the Cenozoic strike–slip corridors of Iberia. Proceedings Tectonics of Strike–slip Restraining and Releasing Bends in Continental and Oceanic Setting, London.

De Vicente, G., Giner, J.L., Muñoz-Martín, A., González-Casado, J.M., Lindo, R., 1996. Determination of present-day stress tensor and neotectonic interval in the Spanish Central System and Madrid Basin, central Spain. Tectonophysics 266, 405–424.

De Vicente, G., Muñoz Martín, A., Vegas, R., Cloetingh, S., Casas, A., González Casado, J.M., Álvarez, J., 2005a. Neutral points and constrictive deformation in paleostresses analysis: the Cenozoic contraction of Iberia. Geophys. Res. Abstr. 7, 04272.

De Vicente, G., Elorza, F.J., Olaiz, A., García-Castellanos, D., Muñoz-Martín, A., Vegas, R., Álvarez, J., 2005b. Number-size distribution invariante of Iberian cenozoic basins. Geophys. Res. Abstr. 7, 04296.

Elorza, F.J., Florez, F., Paredes, C., Calle, O., Mazadiego, L., Llamas, F.J., Pérez, E., Vela, A., Vives, L., Carrera, J., Muñoz Martín, A., De Vicente, G., Casquet, C., Bajos, C., 1999. Hydrogeological simulation for the Berrocal Granitic Batholit. Int. Mine Water Assoc. 1575–1595.

Fernández Casals, M.J., 1976. Estudio meso y microtectónico de la zona de transito paleozoico-metamórfica de Somosierra (Sistema Central, España). Ph.D.Thesis Univ. Compultense de Madrid.

Fernández, P., Garzón-Heydth, G., 1994. Ajustes en la red de drenaje y morfoestructura de los ríos del Centro-Sur de la Cuenca del Duero. In: Arnáez, J., García-Ruíz, J.M., Gómez-Villar, A. (Eds.), Geomorfología en España. SEG, Logroño, Spain, pp. 471–484.

Fernández-Casals, M.J., Capote, R., 1970. La tectónica paleozoica del Guadarrama en la región de Buitrago del Lozoya. Bol. Geol. Min. 81 (6), 562–568.

Fitzgerald, P.G., Stump, E., 1997. Cretaceous and Cenozoic episodic denudation of the Transantarctic Mountains, Antarctica: new constraints from apatite fission track thermochronology in the Scott Glacier region. J. Geophys. Res. 102, 7747–7765.

Fleischer, R.L., Price, P.B., Walker, R.M., 1975. Nuclear tracks in solids. In: Fleischer, R.L., Price, P.B., Walker, R.M. (Eds.), Principles and Applications, pp. 159–211.

Gallagher, K., Sambridge, M., 1994. Genetic Algorithms: a powerful method for large-scale non-linear optimisation problems. Comput. Geosci. 20, 1229–1236.

Gallagher, K., Brown, R., Johnson, C., 1998. Fission track analysis and its applications to geological problems. Annu. Rev. Earth Planet. Sci. 26, 519–572.

Garrido-Megías, A., 1982. Introducción al análisis tectonosedimentario: aplicación al estudio dinámico de cuencas. V Congr. Lationamer. Geol., Argentina. Actas, pp. 385–402.

Gaspar-Escribano, J.M., van Wees, J.D., ter Voorde, M., Cloetingh, S., Roca, E., Cabrera, L., Muñoz, J.A., Ziegler, P.A., Garcia-Castellanos, D., 2001. Three-dimensional flexural modelling of the Ebro Basin (NE Iberia). Geophys. J. Int. 145, 349–367.

Gil Toja, A., Jiménez Ontiveros, P., Seara Valero, J.R., 1985. Cuarta fase de deformación Hercínica en la zona centroibérica del macizo Hespérico. Cuad. Lab. Xeol. Laxe 9, 91–103.

Giner, J.L., 1996. Análisis neotectónico y sismotectónico en el sector centro-oriental de la cuenca del Tajo. PhD. Thesis Univ. Complutense de Madrid, Spain.

Giner, J.L., De Vicente, G., González-Casado, J.M., 1994. Geotectónica del Borde Oriental de la Cuenca de Madrid. Cuad. Lab. Xeol. Laxe 19, 191–202.

Giner, J.L., De Vicente, G., Pérez González, A., Sánchez Cabañero, J., Pinilla, L., 1996. Crisis tectónicas cuaternarias en la Cuenca de Madrid. Geogaceta 20 (4), 842–845.

Gleadow, A.J.W., Duddy, I.R., Green, P.F., Lovering, J.F., 1986. Confined fission track lengths in apatite: a diagnostic tool for thermal history analysis. Contrib. Mineral. Petrol. 94, 405–415.

Gómez-Ortíz, D., Tejero, R., Babín-Vich, R., Rivas, A., 2005. Crustal density structure in the Spanish Central System derived from gravity data analysis (Central Spain). Tectonophysics 403 (1–4), 131–149.

Green, P.F., Duddy, I.R., Gleadow, A.J.W., Tingate, P.R., 1985. Fission-track annealing in apatite: track length measurements and the form of the Arrhenius plot. Nucl. Tracks 10, 323–328.

Guimerá, J., 2004. La Unidad de Cameros. In: Vera, J.A. (Ed.), Geología de España. SGE-IGME, Madrid, pp. 606–608.

Gutiérrez Elorza, M., 2005. Geomorfología climática. Ed. Rueda, Madrid, Spain.

Hayford, J.F., Bowie, W., 1912. The effect of topography and isostatic compensation upon the intensity of gravity. U.S. Coast Geod. Surv. Sp. Publ., vol. 10. 132 pp.

Heiskanen, W.A., Moritz, H., 1967. Physical Geodesy. W.H. Freeman, New York.

Herraiz, M., De Vicente, G., Lindo, R., Giner, J.L., Simón, J.L., González-Casado, J.M., Vadillo, O., Rodríguez-Pascua, M.A., Cicuendez, J.I., Casas, A., Cabanas, L., Rincón, P., Cortes, A.L., Ramírez, M., Lucini, M., 2000. The Recent (Upper Miocene to Quaternary) and present tectonic stress distributions in the Iberian Peninsula. Tectonics 19, 762–786.

Hoyos, M., Junco, F., Plaza, J.M., Ramírez, A., Sánchez-Porro, J., 1986. El Mioceno de Madrid. In: Alberdi, M. (Ed.), Geología y Paleontología del Terciario Continental de la Provincia de Madrid. CSIC-MNCN, Madrid, Spain, pp. 9–16.

IGME, 1990. Mapa del Cuaternario de España Escala 1:1.000.000 (A. Pérez González Ed.). IGME, Madrid, Spain, 279 pp.

ILIHA DSS Group, 1993. A deep seismic sounding investigation of the lithospheric heterogeneity beneath the Iberian Peninsula. Tectonophysics 221, 35–51.

Jachens, R.C., Simpson, R.W., Blakely, R.J., Saltus, R.W., 1989. Isostatic residual gravity and crustal geology of the United States. Geol. Soc. Amer. Mem. 172, 405–424.

Lazaro-Ochaitia, I., Asensio-Amor, 1980. Síntesis geomorfológica del borde meridional de la Sierra de Guadarrama. Bol. R. Soc. Esp. Hist. Nat. (Geol.) 78, 113–131.

Martín Serrano, A., 1991. La definición y el encajamiento de la red fluvial actual sobre el Macizo Hepérico en el marco de su geodinámica Alpina. Rev. Soc. Geo. Esp. 4 (3–4), 337–351.

Martín-Serrano, A., Santiesteban, J.J., Mediavilla, R., 1996. Tertiary of Central System Basins. In: Friend, P.F., Dabrio, C.J. (Eds.), Tertiary Basin of Spain. Cambridge Univ. Press, pp. 255–260.

Mediavilla, R., Dabrio, C.J., Martín-Serrano, A., Santiesteban, J.L., 1996. Lacustrine neogene systems of the Duero Basin: evolution and controls. In: Friend, P.F., Dabrio, C.J. (Eds.), Tertiary Basin of Spain. Cambridge Univ. Press, pp. 228–236.

Mezcua, J., Gil, A., Benarroch, R., 1996. Estudio gravimétrico de la Península Ibérica e Islas Baleares. Inst. Geogr. Nac.

Molina, E., Armenteros, I., 1986. Los arrasamientos Pliocenos y Plio-Pleistoceno en el sector suroriental de la cuenca del Duero. Stud. Geol. Salmant., Univ. Salamanca 22, 293–307.

Montes, M., Silva, P.G., in press. Cartografía y memoria geológica de la hoja de Getafe (19–23). Mapa Geológico de España escala 1:50.000 3ª Edición (MAGNA). IGME., Madrid. Serv. Pub. M° Industria, Madrid. 37 pp.

Muñoz Martín, A., Cloetingh, S., De Vicente, G., 1996. Modelos de elementos finitos sobre los campos de paleoesfuerzos terciarios en el borde oriental de la cuenca del Tajo (España central). Geogaceta 20 (3), 838–841.

Muñoz Martín, A., Cloetingh, S., De Vicente, G., Andeweg, B., 1998. Finite element modelling of tertiary paleostress fields in the eastern border of the Tajo basin (central Spain). Tectonophysics 300, 47–62.

Muñoz-Martín, A., Álvarez, J., Carbó, A., De Vicente, R., Cloethingh, S., 2004. La estructura de la corteza del Antepaís Ibérico. In: Vera, J.A. (Ed.), Geología de España. SGE IGME, Madrid, pp. 592–597.

Naeser, C.W., 1979. Thermal history of sedimentary basins: fission trackdating of subsurface rocks. In: Scholle, P.A., Schluger, P.R. (Eds.), Aspects of diagenesis. Sot. Econ. Paleontol. Mineral. Spec. Publ., pp. 109–112.

Olaiz, A., De Vicente, G., Vegas, R., González-Casado, J.M., Muñoz-Martín, A., Álvarez, J., 2004. El cabalgamiento de Valdesotos: consecuencias de la acomodación del acortamiento cenozoico en el zócalo del Sistema Central. Geotemas 5 (6), 237–240.

Parker, R.L., 1973. The rapid calculation of potential anomalies. Geophys. J. R. Astron. Soc. 31, 447–455.

Pérez-Estaún, A., Carbonell, R., Martí, D., Flecha, I., Jurado, M.J., Fernández, M., Marzán, I., Escuder-Viruete, J., 2002. Estudios geológicos-estructurales y geofísicos en Mina Ratones (plutón de Albalá). V Jornadas de I+D de Enresa, 229 pp.

Pérez-González, A., 1982. Neógeno y Cuaternario de la llanura manchega y sus relaciones con la Cuenca del Tajo. PhD Thesis. Univ. Complutense. Madrid.

Pérez-González, A., Gallardo, J., 1987. La Raña al Sur de Somosierra y Sierra de Ayllón: un piedemonte escalonado del Villafarnquiense medio. Geogaceta 2, 29–32.

Pérez-Gonzalez, A., Silva, P.G., Roquero, E., Gallardo, J., Morales, J., Calvo, J.P., Pozo, M., Peláez Campomanes, P., Santonja, M., 2004. Geomorfología fluvial y edafología del Sector Centro-Meridional de la Cuenca de Madrid. In: Benito, G., Díez Herrero, A. (Eds.), Itinerarios Geomorfológicos por Castilla - La Mnacha. SEG, Toledo, Spain, pp. 15–48.

Pozo, M., Calvo, J.P., Silva, P.G., Morales, J., Peláez-Campomanes, P., Nieto, M., 2004. Geología del sistema de yacimientos de mamíferos miocenos del Cerro de los Batallones, Cuenca de Madrid. Geogaceta 35, 143–146.

Proença-Cunha, P., Antunes-Martins, A., Daveau, S., Friend, P.F., 2004. Tectonic control of the Tejo river fluvial incision during the Late Cenozoic, in Ródao-central Portugal (Atlantic Iberian border). Geomorphology 64 (3–4), 17, 271–17, 298.

Querol, R., 1989. Geología del Subsuelo de la Cuenca del Tajo. Instituto Tecnológico Geominero de España, Madrid.

Racero, A., 1988. Consideraciones acerca de la evolución geológica del margen NW de la Cuenca del Tajo durante el Teciario a partir de datos del subsuelo. Congreso Geológico de España, Granada, pp. 213–221.

Reches, Z., Baer, G., Hatzor, Y., 1992. Constrains on the strength of the upper crust from stress inversion of fault slip data. J. Geophys. Res. 97 (B9), 12481–12493.

Ribeiro, A., Kullberg, M.C., Kullberg, J.C., Manupella, G., Phipps, S., 1990. A review of Alpine tectonics in Portugal foreland detachment in basement and cover rocks. Tectonophyscis 184, 357–366.

Rodríguez Pascua, M.A., De Vicente, G., 1998. Análisis de paleoesfuerzos en cantos de depósitos conglomeráticos terciarios de la Cuenca de Zaorejas (Rama Castellana de la Cordillera Ibérica). Rev. Soc. Geol. Esp. 11 (1–2), 169–180.

Rodríguez-Fernandez, L.R., 1990. Estudio de los procesos de deformación en la zona de cizalla de Hiendelaencína (Sistema Central Español). PhD. Thesis, Univ. Complutense Madrid, Spain.

Rodríguez-Vidal, J., Díaz del Olmo, F., 1994. Macizo Hespérico Meridional. In: Gutiérrez-Elorza, M. (Ed.), Geomorfología de España. Rueda, Madrid, pp. 101–122.

Rueda, J., Mezcua, J., 2005. Near-real-time Seismic Moment-tensor determination in Spain. Seismol. Res. Lett. 76 (4), 455–465.

Salas, R., Casas, A., 1993. Mesozoic extensional tectonics, stratigraphy and crustal evolution during the Alpine cycle of the eastern Iberian Basin. Tectonophysics 228, 33–55.

Sanz, M.E., 1996. Sedimentología de las Formaciones Neógenas del sur de la Cuenca de Madrid. Cedex, Madrid.

Silva, P.G., 1988. El Cuaternario del sector centro-meridional de la Cuenca de Madrid: Aspectos geomorfológicos y neotectónicos. PhD. Thesis Univ. Complutense de Madrid, Spain.

Silva, P.G., 2003. El Cuaternario del Valle inferior del Manzanares (Cuenca de madrid, España). Estud. Geol. 107–132.

Silva, P., Cañaveras, J.C., Sanchez-Moral, S., Lario, J., Sanz, E., 1997. 3D soft sediment deformation structures, evidence for quaternary seismicity in the Madrid Basin, Spain. Terra Nova 9 (5–9), 208–212.

Silva, P., Goy, J.L., Zazo, C., 1988a. Neotectónica del sector centro-meridional de la cuenca de Madrid. Estud. Geol. 4 (5–6), 415–427.

Silva, P.G., Goy, J.L., Zazo, C., 1988b. Evolución geomorfológica de la confluencia de los ríos Jarama y Tajuña durante el Cuaternario (Cuenca de Madrid, España). Cuatern. Geomorfol. 2, 125–133.

Silva, P.G., Palomares, M., Rubio, F., Goy, J.L., Hoyos, M., Martín-Serrano, A., Zazo, C., Alberdi, M.T., 1999. Geomorfología, Estratigrafía, Paleontología y Procedencia de los depósitos arcósicos cuaternarios de la Depresión Prados-Guatén (SW Madrid). Cuatern. Geomorfol. 13 (1–2).

Silva, P.G., Goy, J.L., Zazo, C., Bardaji, T., 2003. Fault-generated mountain fronts in southeast Spain; geomorphologic assessment of tectonic and seismic activity. Geomorphology 50 (1–3), 203–225.

Simón-Gómez, J.L., 1989. Recent stress field and brittle tectonics in the Iberian Chain and Ebro Basin (Spain). J. Struct. Geol. 11 (3), 285–294.

Simpson, R.W., Jachens, R.C., Blakely, R.J., Saltus, R.W., 1986. A new isostatic residual gravity map of the conterminous United States with a discussion on the significance of isostatic residual anomalies. J. Geophys. Res. 91 (B), 8348–8372.

Sokoutis, D., Burg, J.P., Bonini, M., Corti, G., Cloetingh, S., 2005. Lithospheric-scale structures from the perspective of analogue continental collision. Tectonophysics 406 (1–2), 1–15.

Sopeña, A., 1979. Estratigrafía del Pérmico y Triásico del noroeste de la Provincia de Guadalajara. Semin. Estratigr. 5, 1–329.

Stapel, G., 1999. The nature of isostasy in West Iberia. And its bearing on mesozoic and cenozoic regional tectonics. PhD. Thesis, Free University, Amsterdam, The Netherlands.

Stich, D., Ammon, C.J., Morales, J., 2003. Moment tensor solutions for small and moderate earthquakes in the Ibero–Maghreb region. J. Geophys. Res. 108 (2002JB002057).

Suriñach, E., Vegas, R., 1988. Lateral inhomogeneities of the Hercynian crust in central Spain. Phys. Earth Planet. Inter. 51, 226–234.

Talwani, M., Heirtzler, J.R., 1964. Computation for magnetic anomalies caused by two-dimensional bodies of arbitrary shape. In: Parks, G.A. (Ed.), Computers in the Mineral Industries, Part 1. Stanford Univ. Publ. Geological Sciences, vol. 9, pp. 464–480.

Tejero, R., Ruiz, J., 2002. Thermal and mechanical structure of the central Iberian Peninsula lithosphere. Tectonophysics 350, 49–62.

Tejero, R., Perucha, M.A., Rivas, A., Bergamin, J.F., 1996. Modelos gravimétrico y estructural del Sistema Central. Geogaceta 20, 947–950.

Van Wees, J.D., Cloetingh, S., De Vicente, G., 1996. The role of pre-existing weak-zones in basin evolution: contraints from 2D finite element and 3D flexure models. In: Buchanan, P.G., Nieuwland, D.A. (Eds.), Modern Developments in Structural Interpretation, Validation and Modelling. Geol. Soc. (London), Sp. Publ., vol. 99, pp. 297–320.

Van Wees, J.D., Arche, A., Beijdorff, C.G., Lopez-Gomez, J., Cloetingh, S., 1998. Temporal and spatial variations in tectonic subsidence in the Iberian Basin (E Spain). Tectonophysics 300, 285–310.

Vaudour, J., 1979. La Región de Madrid, alterations, sols et paléosols. Ed. Ophrys, París.

Vegas, R., 2004. Cadenas sin cobertera. In: Vera, J.A. (Ed.), Geología de España. SGE-IGME, Madrid, pp. 617–631.

Vegas, R., Banda, E., 1982. Tectonic framework and evolution of the Iberian Peninsula. Earth Evol. Sci. 2 (4), 320–343.

Vegas, R., Pérez-González, A., Miguez, F., 1975. Cartografía y memoria geológica de la hoja de Getafe (19–23). Mapa Geológico de España escala 1:50.000 2ª Serie (MAGNA). IGME. Serv. Pub. M° Industria, Madrid.

Vegas, R., Vázquez, J.T., Suriñach, E., Marcos, A., 1990. Model of distributed deformation, block rotations and cristal thickening for the formation of the Spanish Central System. Tectonophysics 184, 367–378.

Vegas, R., De Vicente, G., Muñoz Martín, A., Palomino, R., 2004. Los corredores de fallas de regua-Verín y Vilariça: zonas de

transferencia de la deformación intraplaca en la península ibérica. Geotemas 6 (5), 245–249.
Vegas, R., De Vicente, G., Muñoz Martín, A., Olaiz, A., Palencia, A., Osete, M.L., 2005. Was the Iberian Plate moored to Africa during the Tertiary? Geophys. Res. Abstr. 7, 06769.
Vening Meinesz, F.A., 1939. Tables fondamentales pour la réduction isostatique régionale. Bull. Geod. 63, 711–776.
Vera, J.A. (Ed.), 2004. Geología de España. SGE-IGME, Madrid.
Wagner, G.A., Miller, D.S., Jäeger, E., 1979. Fission-track ages on apatite of Bergell rocks from Central Alps and Bergell boulders in Oligocene sediments. Earth Planet. Sci. Lett. 45, 355–360.
Won, I.J., Bevis, M., 1987. Computing the gravitational and magnetic anomalies due to a polygon: algorithms and fortran subroutines. Geophysics 52, 232–238.